

การเตรียมแผ่นเส้นใยนาโนจากการผสมไหมไฟโบรอิน/ เจลาติน/ ไซโตซาน เพื่อใช้เป็น
แผ่นเยื่อวางกัน



นางสาวพรเพ็ญ ศิริดำรง

จุฬาลงกรณ์มหาวิทยาลัย

CHULALONGKORN UNIVERSITY

บทคัดย่อและแฟ้มข้อมูลฉบับเต็มของวิทยานิพนธ์ตั้งแต่ปีการศึกษา 2554 ที่ให้บริการในคลังปัญญาจุฬาฯ (CUIR)
เป็นแฟ้มข้อมูลของนิสิตเจ้าของวิทยานิพนธ์ ที่ส่งผ่านทางบัณฑิตวิทยาลัย

The abstract and full text of theses from the academic year 2011 in Chulalongkorn University Intellectual Repository (CUIR)
are the thesis authors' files submitted through the University Graduate School.

วิทยานิพนธ์นี้เป็นส่วนหนึ่งของการศึกษาตามหลักสูตรปริญญาวิทยาศาสตรดุษฎีบัณฑิต

สาขาวิชาทันตชีววัสดุศาสตร์ (สหสาขาวิชา)

บัณฑิตวิทยาลัย จุฬาลงกรณ์มหาวิทยาลัย

ปีการศึกษา 2558

ลิขสิทธิ์ของจุฬาลงกรณ์มหาวิทยาลัย

PREPARATION OF SILK FIBROIN/ GELATIN/ CHITOSAN BLENDED
NANOFIBROUS MEMBRANES TO BE USED AS BARRIER MEMBRANES

Miss Pornpen Siridamrong



A Dissertation Submitted in Partial Fulfillment of the Requirements
for the Degree of Doctor of Philosophy Program in Dental Biomaterials Science
(Interdisciplinary Program)

Graduate School

Chulalongkorn University

Academic Year 2015

Copyright of Chulalongkorn University

Thesis Title	PREPARATION OF SILK FIBROIN/ GELATIN/ CHITOSAN BLENDED NANOFIBROUS MEMBRANES TO BE USED AS BARRIER MEMBRANES
By	Miss Pornpen Siridamrong
Field of Study	Dental Biomaterials Science
Thesis Advisor	Assistant Professor Niyom Thamrongananskul, D.D.S., Ph.D.
Thesis Co-Advisor	Professor Somporn Swasdison, D.D.S., Ph.D.

Accepted by the Graduate School, Chulalongkorn University in Partial
Fulfillment of the Requirements for the Doctoral Degree

..... Dean of the Graduate School
(Associate Professor Sunait Chutintaranond, Ph.D.)

THESIS COMMITTEE

..... Chairman
(Professor Pasutha Thunyakitpibal, D.D.S., Ph.D.)

..... Thesis Advisor
(Assistant Professor Niyom Thamrongananskul, D.D.S., Ph.D.)

..... Thesis Co-Advisor
(Professor Somporn Swasdison, D.D.S., Ph.D.)

..... Examiner
(Assistant Professor Usa Sangwatanaroj, Ph.D.)

..... Examiner
(Narong Lumbikananda, D.D.S., Ph.D.)

..... External Examiner
(Assistant Professor Piyaporn Kampeerapapun, Ph.D.)

พรเพ็ญ ศิริดำรง : การเตรียมแผ่นเส้นใยนาโนจากการผสมไหมไฟโบรอิน/ เจลลาติน/ ไคโตซาน เพื่อใช้เป็นแผ่นเยื่อขวางกั้น (PREPARATION OF SILK FIBROIN/ GELATIN/ CHITOSAN BLENDED NANOFIBROUS MEMBRANES TO BE USED AS BARRIER MEMBRANES) อ.ที่ปรึกษาวิทยานิพนธ์หลัก: ผศ. ทพ. ดร. นิยม ชำรงค์อนันต์สกุล, อ.ที่ปรึกษาวิทยานิพนธ์ร่วม: ศ. ทพ. ดร. สมพร สวัสดิ์ศิริทรัพย์, 95 หน้า.

งานวิจัยนี้ ได้ทำการศึกษา อัตราส่วนต่างๆ ของไหมไฟโบรอิน เจลลาติน ไคโตซาน ใน สารละลาย กรดฟอร์มิก ถูกปั่นเป็นเส้นใยขนาดนาโนเมตรด้วยไฟฟ้าสถิต อัตราส่วนของการผสมของไหมไฟโบรอิน เจลลาติน ไคโตซาน ที่ 10:20:0, 10:20:0.5, 10:20: 1, 10:20:1.5, 10:20:2 และ 20:10:1 โดย เฟอร์เซ็นน้ำหนัก จะพบว่า เมื่อปริมาณไคโตซานในสารละลายผสม เพิ่มขึ้น ขนาดเส้นใยโดยเฉลี่ยลดลง 280 ถึง 100 นาโนเมตร และมีการกระจายตัวของขนาดเส้นใยอยู่ในช่วงแคบ กรดฟอร์มิก ที่ใช้เป็นตัวทำละลาย ไม่มีผลต่อความสามารถในการปั่นเส้นใยด้วยไฟฟ้าสถิต และลักษณะสัณฐานวิทยาของเส้นใยนาโนผสมของไหมไฟโบรอิน เจลลาติน ไคโตซาน จะพบว่าเมื่อใช้ความเข้มข้นของสารละลายไหมไฟโบรอิน เจลลาติน ไคโตซานที่ 10:20:1 และ 20:10:1 และค่าศักย์ไฟฟ้าที่ 20 กิโลโวลต์ สามารถผลิตเส้นใยผสมของไหมไฟโบรอิน เจลลาติน ไคโตซาน จะพบว่าขนาดนาโนเมตรที่ได้มีความสม่ำเสมอโดยไม่มีปมปมเกิดขึ้น ค่าความแข็งแรงของแผ่นเส้นใยนาโนผสมของไหมไฟโบรอิน เจลลาติน ไคโตซาน จะมีค่าความแข็งแรงลดลงเมื่อปริมาณของไหมไฟโบรอินมีปริมาณมากขึ้น แผ่นเส้นใยไหมไฟโบรอิน เจลลาติน ไคโตซานถูกเชื่อมขวางด้วย แอลกอฮอล์ เอทิล ไดเมทิลอะมิโนโพรพิล คาร์โบไดอิมายด์ ไฮโดรคลอไรด์/ เอ็น ไฮดรอกซีซัลซานาไมด์ เป็นเวลา 72 ชั่วโมง ล้างด้วยน้ำกลั่นเป็นเวลา 30 นาที และทำให้แห้งในโถดูดความชื้นที่อุณหภูมิห้อง จะพบว่า แผ่นเส้นใยไหมไฟโบรอิน เจลลาติน ไคโตซานถูกเชื่อมขวางด้วย เอทิล ไดเมทิลอะมิโนโพรพิล คาร์โบไดอิมายด์ ไฮโดรคลอไรด์/ เอ็น ไฮดรอกซีซัลซานาไมด์ สามารถคงรูปของเส้นใยได้หลังจากการจุ่มลงสารเชื่อมขวาง และผลที่ได้ยังพบว่า แผ่นเส้นใยไหมไฟโบรอิน เจลลาติน ไคโตซาน 20:10:1 จะบวมตัวต่ำกว่า 10:20:1 ทั้งนี้เนื่องจากปริมาณเจลลาตินมีผลต่อการบวมตัว แผ่นเส้นใยไหมไฟโบรอิน เจลลาติน ไคโตซาน 20:10:1ถูกเชื่อมขวางด้วย เอทิล ไดเมทิลอะมิโนโพรพิล คาร์โบไดอิมายด์ ไฮโดรคลอไรด์/ เอ็น ไฮดรอกซีซัลซานาไมด์ ได้ถูกเลือกเพื่อการทดสอบสมบัติทางชีวภาพ โดยผลการทดสอบในห้องปฏิบัติการด้วยเซลล์เหงือก จะพบว่า เซลล์มีการยึดเกาะได้ดี และ มีการแผ่กระจายตัวได้ดีบนแผ่นเส้นใยไหมไฟโบรอิน เจลลาติน ไคโตซาน จากผลการทดลองที่ได้นี้ ได้บ่งชี้ให้เห็น สามารถผลิตแผ่นเส้นใยนาโนจากไหมไฟโบรอิน เจลลาติน ไคโตซานด้วยการปั่นขึ้นรูปด้วยไฟฟ้าสถิต และสามารถนำไปพัฒนาใช้เป็นแผ่นเยื่อขวางกั้นได้

สาขาวิชา ทันตชีววัสดุศาสตร์

ปีการศึกษา 2558

ลายมือชื่อนิติกร

ลายมือชื่อ อ.ที่ปรึกษาหลัก

ลายมือชื่อ อ.ที่ปรึกษาร่วม

5487789720 : MAJOR DENTAL BIOMATERIALS SCIENCE

KEYWORDS: SILK FIBROIN / GELATIN / CHITOSAN / ELECTROSPINNING / MEMBRANE

PORNPEN SIRIDAMRONG: PREPARATION OF SILK FIBROIN/ GELATIN/ CHITOSAN BLENDED NANOFIBROUS MEMBRANES TO BE USED AS BARRIER MEMBRANES. ADVISOR: ASST. PROF. NIYOM THAMRONGANANSKUL, D.D.S., Ph.D., CO-ADVISOR: PROF. SOMPORN SWASDISON, D.D.S., Ph.D., 95 pp.

In this study, various compositions of silk fibroin (SF)/ gelatin (G)/ chitosan (C) in formic acid solutions were electrospun into nanofiber mats. The blending ratios ranged of 10:20:0, 10:20:0.5, 10:20:1, 10:20:1.5, 10:20:2, and 20:10:1(wt%: wt%: wt%). When the chitosan content in blended solution increased, the average diameter decreased from 280 to 100 nm and fiber sizes distribution was narrow. The formic acid as solvent did not affect the electrospinnability and morphology of SF: G: C blended nanofiber. The appropriate condition of electrospinning process of SF: G: C of 10:20:1 and 20:10:1 blended solution at 20 kV could generate the uniform nanofibers without beads. Tensile strength of SF: G: C (10:20:1) blended nanofiber was decreased with increasing of silk fibroin content, SF: G: C (20:10:1). The nanofiber mats were crosslinked with the vapor of ethanol, 1-ethyl-3-(3-dimethylaminopropyl) carbodiimide hydrochloride (EDC) /N-hydroxysuccinimide (NHS) (EDC/NHS), and glutaraldehyde (GA) for 72 hours, rinsed in distilled water for 30 minutes and then drying in a desiccator at room temperature. It was found that EDC/NHS was able to maintain the original nanofiber morphology after water exposure. It was observed that the SF: G: C at 20:10:1 swelled lower than SF: G: C at 10:20:1. The gelatin effected to swelling of nanofiber mats. The results showed that the EDC/NHS- crosslinked SF: G C (20:10:1) nanofiber mats was selected for the biological testing. *In vitro* testing of gingival tissues showed good cell adhesion and proliferation. The results indicated that SF: G: C electrospun nanofiber mats could be prepared and have a potential to be applied in barrier membrane application.

Field of Study: Dental Biomaterials Science

Academic Year: 2015

Student's Signature

Advisor's Signature

Co-Advisor's Signature

ACKNOWLEDGEMENTS

Firstly, I would like to thank my advisor, Associate Professor Dr. Niyom Tharongananskul for his essential support and guidance for the last five years. He is not only my teacher, but he is a big brother. He never let me stand alone, but he stood by me all the time, when I got the problem. Not only myself, he has always helped my family. Thank you, my big brother.

Furthermore, I would also like to thank my minor advisor, Professor Somporn swasdison. She has not only a great support for advice, assistance and generous encouragement, but also for kindly reviewing throughout this thesis. She always points me, how to be a professional person. My Professor, I try to be as fast as you want. I want you to forgive me many things. One day, I will be a great person that you want me to be. Thank you, my Professor from my heart.

I would like to express deep appreciation to Professor Dr. Pasutha Thunyakitpisal, Dr. Narong Lumbikananda, Associate Professor Dr. Usa Sawatanaroj, and Associate Professor Dr. Piyaporn Kampeerapappun for serving as the chairman and members of my thesis committee, respectively, including valuable suggestions and comments.

I would like to gratefully acknowledge a grant from Faculty Research Grant (DRE 58004), Faculty of Dentistry, Chulalongkorn University, Thailand. The authors thank the DRE project for financial support.

Special thanks should go out the financially supported by a grant from Faculty of Dentistry, Chulalongkorn University. I also have to thank the Thailand institute of scientific and technological research (TISTR) for paying salary to me for paying fees.

Moreover, I would like to thank all friends to encourage me. Especially, the official of graduate school has kindness for me, Mr. Banglung and Ms. Region Phatipsan from Scientific and Technological research equipment center, Chulalongkorn University.

Finally, I would like to special thanks to my family for support me all by without conditions.

CONTENTS

	Page
THAI ABSTRACT	iv
ENGLISH ABSTRACT.....	v
ACKNOWLEDGEMENTS	vi
CONTENTS.....	vii
LIST OF FIGURES	ix
LIST OF TABLES	xii
CHAPTER I INTRODUCTION.....	1
CHAPTER II THEORY AND LITERATURE REVIEW.....	5
2.1. Theory.....	5
2.1.1. Barrier membrane.....	5
2.1.1.1 Type of barrier membranes	5
2.1.2 Biomaterials.....	8
2.1.2.1. Chitosan.....	8
2.1.2.2. Silk fibroin.....	9
2.1.2.3. Gelatin	12
2.1.3 Electrospinning process.....	13
2.1.4 Crosslinking methods	15
2.2 Literature review.....	17
2.2.1 Electrospinning of chitosan blend	17
2.2.2 Electrospinning of silk fibroin blend.....	21
2.2.3 Electrospinning of gelatin blend.....	23
2.2.4. The other techniques of silk fibroin, chitosan and gelatin blend.....	24
2.2.5 Crosslinking of silk fibroin, gelatin, and chitosan.....	27
CHAPTER III MATERIAL AND METHODS.....	30
3.1 Materials and reagents	30
3.2 Apparatus	31
3.3 Experimental procedures	31
3.3.1 Part I: Preparation of silk fibroin from fresh silk cocoon.....	31

	Page
3.3.2 Part II: Fabrication of nanofiber membranes from gelatin, chitosan, and silk fibroin by electrospinning technique	32
3.3.4 Part IV: Physical and biological characterization of the nanofiber membranes.....	34
3.3.4.1 Physical characterization of the membrane.....	34
3.3.4.2 Mechanical properties	34
3.3.4.3 Biological characterization of membranes	36
CHAPTER IV RESULTS AND DISCUSSIONS	39
4.1 Prepared silk fibroin sponge	39
4.2 Effect of formic acid on morphology of nanofibers mats.....	43
4.3 Effect of polymer concentration on morphology of nanofibers	45
4.4 Effect of electrical field and spinning distance.....	49
4.5 Morphological appearance of nanofiber mats before and after crosslinking	54
4.6 Morphology of nanofibers crosslinked with EDC/NHS.....	63
4.7 Air permeability.....	66
4.8 X-Ray Diffraction (XRD) analysis	67
4.9 Mechanical property analysis	70
4.10 In vitro studies: cellular response to the nanofiber barrier membranes.....	71
4.11 The membrane permeability study	75
4.12 Cost of materials and membranes.....	78
CHAPTER V CONCLUSIONS AND SUGGESTIONS	80
5.1 Conclusions.....	80
5.2 Suggestions	81
REFERENCES	82
APPENDIXS.....	90
Appendix A.....	91
Appendix B.....	94
VITA.....	95

LIST OF FIGURES

	Page
Figure 1 Chemical structures of chitin and chitosan[49]	9
Figure 2 Structure of silk fiber [51]	10
Figure 3 The structure of fibroin [51]	11
Figure 4 Schematic structure of Bombyx Mori silk fiber, protein [52]	12
Figure 5 Molecular structure of gelatin[53]	13
Figure 6 Conventional electrospinning	14
Figure 7 SEM images magnification X 10,000 of the chitosan and PVA blended electrospun fiber. The volume ratio of chitosan 10: PVA = 90:10 (a), 70:30 (b), 50:50 (c), 30:70 (d) and 0:100 (e) chitosan 100 was dissolved in formic acid (or 0.2 M acetic acid) at 2 wt.% and the solution was mixed with 9 wt.% PVA in a volume ratio of 50:50, then the mixed solution was electrospun (f)	18
Figure 8 SEM images of collagen-chitosan-TPU nanofibers and diameter distribution: (A) random oriented nanofiber; (B) and (C) aligned nanofiber with 5000 and 10,000 magnification.....	19
Figure 9 SEM images of electrospun gelatin-chitosan nanofibers in different mass ratio (gelatin/chitosan). (a) 0/100; (b) 25/75; (c) 50/50; (d) 75/25; (e) 100/0. The insets showed the fiber size distributions.....	20
Figure 10 SEM images of electrospun PCL-chitosan nanofibers in different mass ratio (gelatin/chitosan) (a) 100/0; (b) 75/25; (c) 50/50; (d) 25/75; (e) 0/100.....	21
Figure 11 The morphology of various nanofibers (a)CECS/PVA; (b) CECS/PVA/SF 4%; (c) CECS/PVA/SF 8%	21
Figure 12 Electrospinning process	32
Figure 13 Dumbbell of DIN 53504-S2	34
Figure 14. The membrane permeability study	38
Figure 15 Digital photographs of (a) silk fibroin fiber and (b) silk fibroin sponge	39
Figure 16 FTIR-ATR spectrum of silk fibroin sponges.....	40
Figure 17 FTIR-ATR spectrum of (a) gelatin film, (b) silk fibroin film, and (c) chitosan film.....	41

Figure 18 SEM images of electrospun SF: G: C (10:20:1) nanofiber by fixing the spinning distance at 15 cm under electric field at 20 kV and flow rate at 0.2 ml/h with storage time; (a) 0 hour and (b) 24 hours (Magnification x2, 000)	44
Figure 19 SEM images of electrospun nanofiber SF:G:C at various ratios (wt%:wt%:wt%) of 20:0:0, 0:24:0, 10:20:0, 10:20:0.5, 10:20:1,10:20:1.5 , 10:20:2, and 20:10:1respectively, with electric field of 10 kV , spinning distance of 10 cm and feeding rate of 0.2ml/h (Magnification x 2,000 and x 7,500).....	47
Figure 20 Diameter distributions of nanofibers at different compositions of SF: G: C in formic acid solution (SF: G: C, wt%: wt%: wt %) for (a) 10:20:0.5, (b) 10:20:1, (c) 10:20:1.5, (d) 10:20:2, and (e) 20: 10: 1	49
Figure 21 SEM images of electrospun SF: G: C blends (10wt%/20wt%/1wt %) at a spinning distance of 10 cm. and electrical fields of (a) 10 kV. (b) 15 kV. (c) 20 kV. (Magnification X2, 000 and X7, 500).....	50
Figure 22 SEM images of electrospun SF: G: C (10wt%/20wt%/1wt%) at a spinning distance of 15 cm.and electrical fields of (a) 10 kV. (b) 15 kV. (c) 20 kV. (Magnification x2, 000 and x7, 500).....	51
Figure 23 SEM images of electrospun SF: G: C (10:20:1) and (10:20:1) nanofiber by fixing the spinning distance at 10 and 15 cm and electrical fields at 15 and 20 kV, (Magnification x7, 500)	53
Figure 24 Digital photographs of nanofiber mats before and after crosslinking with ethanol.....	54
Figure 25 Digital photographs of (a) gelatin nanofiber mats of morphologies after dipping in distilled water, (b) SF: G: C nanofiber mats at (10:20:1), and (c) (20:10:1) after ethanol crosslinking	55
Figure 26 Weight loss and swelling of SF, G, and SF: G: C at 10:20:1 and 20:10:1 nanofiber mats after crosslinking with ethanol.....	56
Figure 27 Digital photographs of nanofiber mats before and after crosslinking with GA.....	57
Figure 28 Weight loss and swelling of SF, G, and SF: G: C at 10:20:1 and 20:10:1 nanofiber mats after crosslinking with GA.....	58
Figure 29 Digital photographs of the nanofiber mats of morphologies before and after crosslinking with EDC/NHS	60
Figure 30 Weight loss and swelling of SF, G, and SF: G: C at 10:20:1 and 20:10:1 nanofiber mats after crosslinking with EDC/NHS.....	61

Figure 31 SEM images of electrospun SF, G, SF: G: C (10:20:1) and (20:10:1) nanofiber mats before crosslinking (Magnification x7,500) and after crosslinking with EDC/NHS (Magnification x10,000)	64
Figure 32 SEM images of nanofiber mats SF: G: C (wt%:wt%:wt%) 10:20:1 and 20:10:1 before and after crosslinking with various crosslinkers	65
Figure 33 Air permeability of nanofiber mats (a) SF: G: C (10:20:1) before crosslinking, (b) SF: G: C (10:20:1) after crosslinking, (c) SF: G: C (20:10:1) before crosslinking, and (d) SF: G: C (20:10:1) after crosslinking with EDC/NHS ...	66
Figure 34 XRD of (a) gelatin nanofiber mats and (b) silk fibroin nanofiber mats	67
Figure 35 XRD of electrospun nanofiber mats of (a) silk fibroin nanofiber mats, (b) SF: G: C (20:10:1), and (c) SF: G: C (10:20:1) before crosslinking	68
Figure 36 XRD diffraction peaks of SF: G: C of (a) 20:10:1 before crosslinking and (b) after crosslinking with EDC/NHS	69
Figure 37 Normal human gingival fibroblasts of three patients by the inverted microscope	73
Figure 38 SEM images of HGF on EDC/NHS- crosslinked nanofiber mats at SF: G: C (20:10:1) (Magnification x500 and x5, 000).....	74
Figure 39 SEM images of HGF on commercial membrane (Collprotect ® membrane) (Magnification x200, x500 and x5,000)	75
Figure 40 SEM images of HGF 1st, 2nd, and 3th on EDC/NHS- crosslinked nanofiber mats at SF: G: C (20:10:1) (Magnification x 200, x500 and x5,000).....	77

LIST OF TABLES

	Page
Table 1 Planner for research.....	4
Table 2 Overview of the types of membranes available with some commercial brands [47, 48].	7
Table 3 Parameters of electrospinning[59]	15
Table 4 Methods of crosslinking [39-42].....	16
Table 5 Microscopic computerized tomographic (μ -CT) analysis	26
Table 6 Histomorphometric analysis.....	26
Table 7 Summary specific spectrum band of silk fibroin film, gelatin film, and chitosan film from FTIR analysis	42
Table 8 Crystallinity index obtained for SF, G, and SF: G: C nanofiber mats	69
Table 9 Tensile strength and elongation at break of the nanofiber electrospun membranes from SF, G and SF: G: C blends solution at different concentrations.....	70
Table 10 Cost of collagen, silk, gelatin, and chitosan.....	78
Table 11 Cost of SF, G and C in membrane fabrication by the electrospinning technique (15x20 mm) ²	78

CHAPTER I

INTRODUCTION

Guided bone regeneration (GBR) is an important therapy to repair mandible and alveolar bone defects affected by periodontal diseases. In this technique, a barrier membrane is adapted to help prevention of ridge resorption after extraction, augmentation of alveolar ridge defects and improvement of bone healing around dental implants [1].

The barrier membranes are categorized into 2 types based on their resorbability as non-resorbable and resorbable membranes. Commercial non-resorbable membranes are made from synthetic polymer such as expanded- polytetrafluoroethylene (ePTFE: Gore-Tex®), cellulose acetate (Millipore filter), and polytetrafluoroethylene (PTFE: TefGen-FD®). Whereas the resorbable membranes are made from either synthetic polymers such as polylactic acid (Guidor®), polylactic/ polyglycolic acid (Vocryl®) or natural materials such as collagen (Bio-Gide®, BioMend®)[2].

Materials for membrane fabrications have been extensively developed over the years in clinical field as the utilization of membrane based techniques tends to increasing. These materials should also be safe, efficient, cost effective, and easy to use. Moreover, the materials must stay intact as physical barriers with the ability to take out unwanted cells until regeneration is complete, yet not interfere with the growth of newly formed tissue. Each material has its advantage and disadvantage inherent for the application in which it is insuring success. The biological and physical characteristics of biomaterials used to manufacture membranes can significantly influence barrier function as well as host tissue reaction.

Physical characters of the barrier membrane including pore size, tri-dimensional topography and method of membrane fabrication play an important role in GBR. The pore size of the barrier membrane can affect the prevention of excessive fibrous tissue penetration into the bone defect therefore allow neovascularization and bone formation [3] . Pores membrane are necessary for cell migration.[4]. It can change the cell occlusion properties and the biological reaction of different cell types to the membrane.

Electrospinning is a novel membrane fabrication method which can produce ultrafine fiber in a level of microns to nanometers and produce the tri- dimensional structure[5]. Electrospinning technique can fabricate nanofiber from various types of polymers such as silk fibroin (SF)[6-8], collagen[9], gelatin (G)[10], chitosan(C)[11], polycaprolactone (PCL)[12], and poly lactic acid (PLA)[13, 14], etc. However, the natural polymers for example SF, G, and C have been commonly used in medicine because they are inexpensive, biocompatible and biodegradable [15-17].

Recently, silk, gelatin, and chitosan are a bunch of natural material in Thailand that can be constructed and utilized in medical treatments.

Nang noi Srisaket 1, silk fiber from one of silk races, is a natural and an economical fiber in Thailand. Structurally, each silk consists of two main proteins, silk sericin and silk fibroin (SF). SF possesses potential properties as a resource of biomaterials because it is non-toxic, good biocompatible and biodegradable [8, 15]. It has been widely used in medical application for sutures, skin tissue and artificial ligaments [15, 18].

Gelatin (G) is a natural polymer, which can be generally found in animal tissues such as skin, muscle, and bone. Because it has biocompatibility and biodegradability properties, gelatin has been commonly used in biomedical applications [19]. In addition, gelatin is a promising choice to be used for nanofiber production as it is cheap and available [9].

Chitosan (C) can be prepared from chitin mostly found in crustacean shell. It is ranked number two being found in natural materials. Chitosan has a unique property of antimicrobial activity that is useful in medical fields. It is biocompatible and biodegradable. Furthermore, it can be applied for wound healing [17], periodontal treatment[20], and tissue engineering [21].

The above mentioned materials have been studied as sole material preparation or in combination with others. Currently the properties of different biopolymer blends and their applications have been widely studied for the improvement of the biomaterial properties. Previously, there were several reports on preparation of polymers using these natural materials such as collagen/chitosan blends [22] , chitosan/silk fibroin

blends [15, 23, 24] , silk fibroin/gelatin blends [25] and also blends of natural polymer with synthetic polymer [11, 26, 27] .

A solvent selection for a preparation of natural polymer especially in electrospinning technique, a choice of solvent is a key parameter. In this case, a solvent providing electric charges is considered. Several researchers have been studied to find suitable solvents for their raw materials. 85% formic acid [24, 28, 29], and 1, 1, 1, 3, 3, 3 hexafluoro-2-propanol [6, 30], have been used to dissolve silk fibroin. Formic acid[31], 2,2,2-trifluoroethanol [30, 32, 33], 1,1,1,3,3,3 hexafluoro-2- propanol [34] and N,N- dimethylformamide [21] can be applied with gelatin. Solvents that have been used with chitosan were trifluoroethanol [25], formic acid [35], acetic acid [36], and dichloromethane [37]. However, chitosan is difficult to create by electrospinning because it has three-dimensional networks of strong hydrogen bonds [38]. Some researches tried to produce fiber from chitosan by solvent mixing and blending with other materials [25, 36].

Unfortunately, the electrospun membrane of natural polymer exhibited unstable structure in water and poor mechanical property. So a crosslinking process was required to chemically join two or more molecules by a covalent in order to improve their properties by using techniques such as chemical [39], dehydrothermal [40], ultraviolet [41], and irradiation crosslinking[42]. Glutaraldehyde (GA) [30], triethylene glycol dimethacrylate (TEGDMA)[27], *N*-hydroxysuccinimide[43], genipin[44], and 1-ethyl-3-(3-dimethylaminopropyl)-carbodiimide(EDC)[43] are chemicals agents for crosslinking.

Due to the advantage properties of silk fibroin, gelatin, and chitosan are very interesting thus, this study aimed to prepare nanofiber mats from SF: G: C by using formic acid as a solvent. The morphology and physical properties of the SF: G: C blended fiber mats were investigated. The effects of chemicals on crosslinking of nanofiber of SF: G: C blended fiber mats and biological properties of the nanofiber mats were also studied.

Hypothesis of research: The electrospun silk fibroin/ gelatin/ chitosan blended nanofiber mats can be applied as a barrier membrane for Guided bone regeneration or Guided tissue regeneration.

CHAPTER II

THEORY AND LITERATURE REVIEW

2.1. Theory

Wong et al, 2016 [45] referred to the 1st introduction of guided tissue regeneration (GTR) by Hurley in 1950s, in spine surgery using barrier membrane to separated soft tissue from active areas of bone formation. However, until 1980s, the GTR technique was clinically applied for periodontal tissue regeneration. Since, major goals of periodontal treatment are to preserve the teeth in relatively function and comfortable, good health, and at the same time to maintain the esthetic expectations of the patient.

Principle on GTR treatment, a barrier membrane plays major role to prevent epithelial or soft tissue migration into the infective area and it allows hard tissue such as bone, cementum, and periodontal ligament regeneration to growing in the prevention areas. Currently, guided bone regeneration (GBR) is the most using for the treatment of bone defects or insufficient bone volume in the jaws at oral implant sites or to preserve alveolar sockets after tooth extraction[46]. These barrier membranes have been used to encourage appropriate progenitor cell populations at the wound site.

2.1.1. Barrier membrane

In guided bone regeneration (GBR) technique, a major role of barrier membrane is to prevent epithelial or undesirable tissues migration into bone defect which allows sufficient time for bone, cementum, and periodontal ligament regeneration. In the field of oral surgery and periodontal surgery, a barrier membrane is used to prevent gingival epithelium, which regenerates relatively quickly more than bone.

2.1.1.1 Type of barrier membranes

Barrier membranes are among the most widely studied as biomaterial scaffolds for tissue regeneration. The choice of membrane type depends largely on the required duration of function of the membrane and use membrane-based techniques. Several studies have shown that biological and physical characteristics of biomaterials used in manufacture of membranes can significantly influence barrier function as well as host

tissue response. The properties of the biomaterials used in regenerative procedure should involve biocompatibility, space-making ability to achieve tissue integration or attachment and clinical manageability. These materials also should be safe, efficient, cost effective, and easy to use. Generally, there are two types of membranes used in GTR and GBR which are resorbable and non-resorbable membranes (Table 2)

The first developed membranes were non-resorbable which required a second surgery for membrane removal after achieving tissue formation. This second procedure hindered the utilization of the original barrier membranes and led to later development of resorbable membranes. However research reveals no statistically significant difference in surgical success between the two types of membranes[47].



Table 2 Overview of the types of membranes available with some commercial brands [47, 48].

Non-resorbable	Resorbable
- PTFE (polytetrafluoroethylene) <ul style="list-style-type: none"> • TefGen-FD • BioBarrier NP 	- Collagen <ul style="list-style-type: none"> • Bio-Gide • Ossix • BioMend
- ePTFE (expanded polytetrafluoroethylene) <ul style="list-style-type: none"> • Gore Tex 	- Polylactic acid <ul style="list-style-type: none"> • Guider
- Cellulose <ul style="list-style-type: none"> • Millipore 	- Polylactic/ polyglycolic acid <ul style="list-style-type: none"> • Ethisorb • Vicryl • Inion
- Rubber dam	- Polylactic acid (PLA), Polyglycolide (PG) & Trimethylcarbonate (TMC) <ul style="list-style-type: none"> • Gore Resolut
	- Acellular Dermal Allograft <ul style="list-style-type: none"> • Alloderm
	- Polyethylene glycol <ul style="list-style-type: none"> • Membragel
	- PG & TMC <ul style="list-style-type: none"> • Gore Resolut Adapt
	Polyethylene glycol <ul style="list-style-type: none"> • Membragel

Note: Commercial available membranes are in “Bold ”

The first non-resorbable membranes were produced from cellulose (Millipore) and expanded polytetrafluoroethylene (ePTFE) (Gore-Tex Regenerative material, W.L. Gore and Associates, Inc., Flagstaff, AZ) and used in the GTR experiments. These materials were chosen as barrier materials because of their biocompatibility. Moreover, their porosity allows infiltration of biological fluids while excluding certain cell types.

However, they were generally difficult to manipulate and must be sutured around the necks of teeth to hold them in place. Besides requirement of second surgery for removal, many complications were reported, especially premature exposure, which were related to poorer defect filling[48].

Resorbable membranes have been developed to avoid the second surgery, primarily using polyglycolide, polylactide (PLA) and/or a combination of polylactide/ polyglycolide/ trimethylcarbonate (WL Gore, Flagstaff, AR, USA) (Table 2). After that collagen membrane has been dramatically used. The market leader of collagen production is Bio-Gide (Geistlich, Wolhusen, Switzerland)[47].

Over last decades, synthetic materials such as aliphatic polyesters (polylactide, polyglycolic acid or polyethylene glycol) have been used as materials for membrane in medical application. Meanwhile, natural materials such as collagen, gelatin, chitosan or silk have been increasingly materials of interest in research and development of barrier membranes [47].

2.1.2 Biomaterials

A selection of biomaterials for design and development of tissue engineering product is important thus interacting with tissue to repair or replacement application such as vascular grafts, skin tissue, and bone and so on. Natural materials such as chitosan, gelatin, and silk fibroin are potential in medical application.

2.1.2.1. Chitosan

Chitin is a natural substance found in crab and shrimp shells. Chitin is a natural polysaccharide of poly (β -(1-4) -N-acetyl-D-Glucosamine) and can be extracted from crab shells by dissolving calcium carbonate in acid. Subsequently proteins are eliminated using alkaline. The alkaline condition is a partial deacetylation to obtain chitosan[21]. The deacetylation degree (DD) of chitosan is calculated by the ratio of D-Glucosamine to the sum of D-Glucosamine and N-acetyl D-Glucosamine. DD is an indication of the number of amino groups in the molecules. As the degree of deacetylation of chitin is higher than 50%, it is called chitosan.

Chemical structure of chitosan is a linear, semi-crystalline polysaccharide consisting of 2-acetamido-2-deoxy- β -D-glucan (*N*-acetyl D-Glucosamine) and 2-amino-2-deoxy- β -D-glucan (*N*-acetyl D-Glucosamine) as repeating units. The structure of this polymer is depicted in Figure 2.

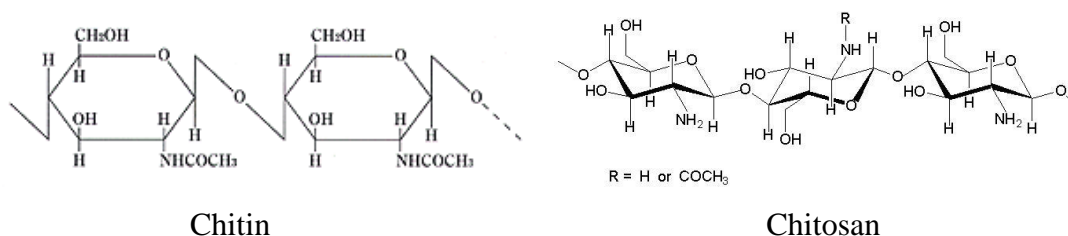


Figure 1 Chemical structures of chitin and chitosan[49]

Chitosan is soluble in acids. Chitosan in acid aqueous solution becomes gel because chitosan can form weak intermolecular link at H-bone through hydrophobic interactions between residual acetyl groups. The amino groups of the D-Glucosamine residues might be patented providing soluble in diluted acidic aqueous solutions (pH<6). The amino groups of chitosan becomes polycation that can subsequently form ionic complexes with a wide variety of natural or synthetic anionic species such as lipids, proteins, DNA and some negatively charged synthetic polymers as poly(acrylic acid). In fact, chitosan is the only positively charged, naturally occurring polysaccharide[49]. As a polyelectrolyte, chitosan can notably be employed for the preparation of multilayered films, using layer-by-layer deposition technique [50]. Chitosan has a unique property of antimicrobial activity that is useful in medical fields. It is biocompatible and biodegradable. Furthermore, it can be applied for wound healing[17], periodontal treatment[20], and tissue engineering[21].

2.1.2.2. Silk fibroin

Silk has been investigated as biomaterials due to the successful use as suture material since the end of the 19th century. Silk is a natural protein fiber from silkworms, *Brobryx mori* containing about 70-75% of actual fiber fibroin secreted from two salivary glands at the head of the silkworm larva, and about 25-30% sericin as shown in Figure 3.

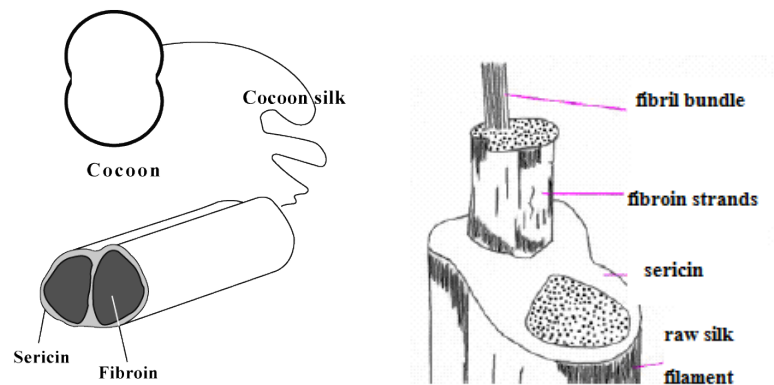


Figure 2 Structure of silk fiber [51]

Sericin, hydrophilic protein, is the group of gummy protein that binds the fibroin filaments. It is a yellow, brittle, and inelastic substance. Sericin is insoluble in cold water. However, it can be hydrolyzed, into smaller fractions of molecules, which are easily solubilized in hot water. It is called De-gumming process[8].

The structure of silk is generally β -sheet due to the dominance of hydrophobic domains of short side chain amino acids in the primary sequence and the spun. Silk fibroin fibers are about 10 – 25 μm in diameter and consist of two proteins: light chain (~26k Da) and heavy chain (~390k Da), linked by a single disulfide bond. This structure permits tight packing of stacked sheets of hydrogen bonded anti-parallel chains of the protein (Figure 4). Large hydrophobic domains interspaced with smaller hydrophilic domains foster the assembly of silk and the strength and resiliency of silk fiber [28].

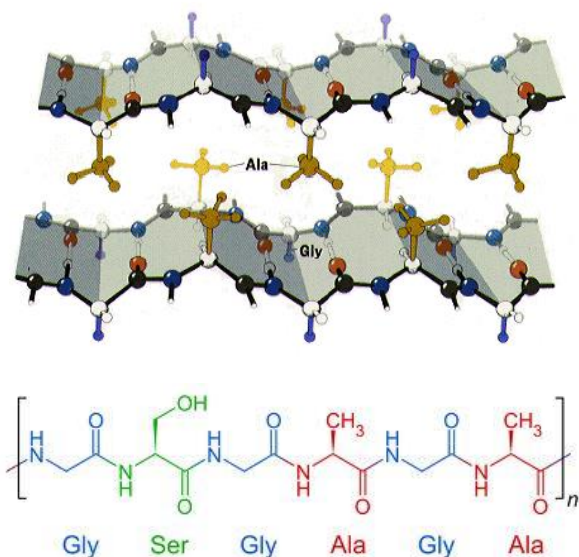


Figure 3 The structure of fibroin [51]

The heavy chain forms the crystalline regions in silk fibers and makes up 94% of the sequence. Glycine-X functional group bonds with other repeating units Alanine, Serine, Threonine and Valine. Each domain consists of sub-domain hexapeptides including: GAGAGS, GAGAGY, GAGAGA or GAGYGA where G is Glycine, A is Alanine, S is Serine and Y is Tyrosine (Figure 5). The repeat GAGAGS has been the most frequently (70%) occurring hexapeptide repeating sequence. These sub-domains end with tetrapeptides such as GAAS or GAGS is the less crystalline forming regions of the fibroin heavy chain known as linkers. All the linkers have non-repetitive sequence, which is composed of charge amino acids. However, it is not found in the crystalline region.

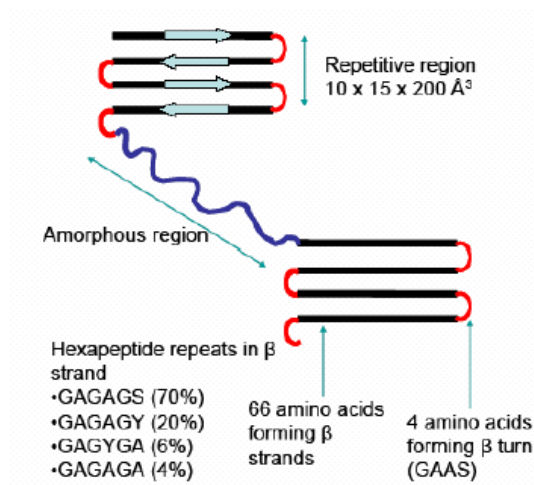


Figure 4 Schematic structure of Bombyx Mori silk fiber, protein [52]

Generally, silk fibroin is insoluble in several solvents, including water, dilute acid or dilute alkaline solutions. It is thermally stable up to 250°C, allowing processing over a high range of temperature. It is a poor conductor of electricity. Silk fibroin possesses potential properties to produce biomaterials because it is non-toxic, good biocompatible and biodegradable [8, 15]. It has been widely used in medical application for sutures, skin tissue and artificial ligaments [15, 18].

2.1.2.3. Gelatin

Gelatin is a soluble protein compound obtained by partial hydrolysis of collagen, a main component found in connective tissue, skin and bone of human and animals. Gelatin is nearly tasteless and odorless. It is colorless or slightly yellow, transparent and brittle. It is soluble in hot water, glycerol, and acid, and insoluble in organic solvents. Gelatin has a unique protein structure that provides a wide range of functional properties. Gelatin is amphoteric, meaning that it is neither acidic nor alkali, depending on the nature of the solution. It is a polypeptide, a series of amino acids joined together by peptide bonds as shown in Figure 5. Its properties are biodegradable, biocompatible, non-toxic and non-carcinogenic biopolymer. Gelatin has biological properties similar to collagen but it is cheaper and easier to prepare into solution than collagen.

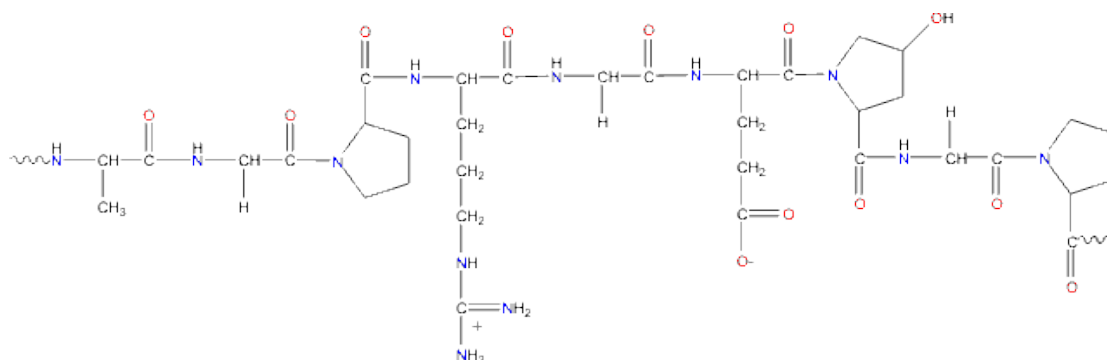


Figure 5 Molecular structure of gelatin[53]

Gelatin is a high molecular weight water-soluble protein. On a dry weight basis, gelatin consists of 98% to 99% of protein. The molecular weight between 20,000 and 250,000 are the large protein structures[54]. Coils of amino acids are joined together by peptide bonds. The predominant amino acid sequence is Glycine-Proline-Hydroxyproline (Gly-Pro-Hyd). The properties of gelatin from various sources can be different. For example, fish gelatin is distinguished from bovine or porcine gelatin by its low melting point, low gelation temperature, and high solution viscosity[55].

2.1.3 Electrospinning process

Key factor of the barrier membrane is tissue integration and permeability of blood vessel[45]. The pore size of the barrier membrane can affect the prevention of excessive fibrous tissue penetration into the bone defect and allowing neovascularization and bone formation. The tri-dimensional topography of the membrane with interconnecting pores and canals is considered, as it can change the cell occlusion properties and the biologic reaction of different cell types to the membrane[5]. Electrospinning is a new technique to production the high porosity by creating ultra-fiber. Electrospinning have been recognized as an efficient technique for the fabrication of submicron-sized polymer nanofibers ranging from nanometers to micrometers[56]. Various macromolecules have been successfully electrospun into ultrafine fibers as thin as several nanometers. Conventional electrospinning (Figure 6) involves drawing a polymer solution droplet from a capillary dispensed by a syringe pump. The solution undergoes extensional flow and deposits into a collector by the application of an external electrostatic field. The formation of nanofibers through electrospinning is based on the uniaxial stretching of a viscoelastic solution. The

electric field is applied between the needle capillary and the collector so that surface charge is induced on a polymer fluid deforming a spherical pendant droplet to a conical shape. As the electric field surpasses a threshold value where the electrostatic repulsion force of the surface charges overcomes surface tension, the charged fluid jet is ejected from the tip of the conical protrusion commonly known as Taylor cone[5]. The charge density on the jet interacts with the external field to produce instability. Before reaching the collector, the solvent partially evaporates. The jet of solution is subjected to intensive extensional strain, leading to the deposition of long and thin fibers, eventually at the nanoscale. The most typical morphology of obtained corresponds to a randomly aligned and porous non-woven mats[57].

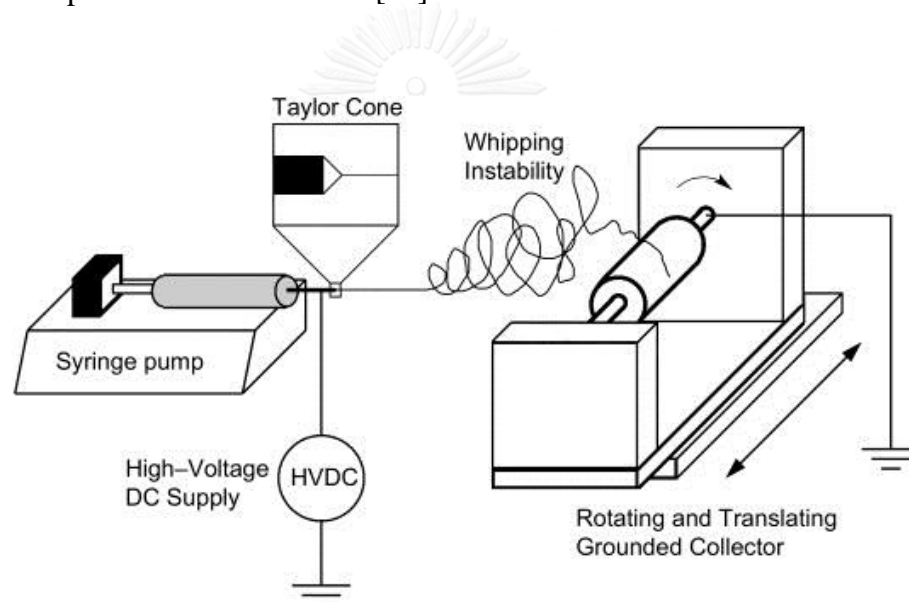


Figure 6 Conventional electrospinning

The properties of the obtained mats depend on various parameters such as molecular weight, viscosity, conductivity and surface tension of polymer and solution properties. Moreover the electrospinning conditions such as applied electric voltage, tip-to collector distance, feeding rate, etc. are important parameters[58].

Table 3 Parameters of electrospinning[59]

Parameter	Effect on fiber diameter
Flow rate	Decreasing flow rate tends to decrease fiber diameter
Distance from nozzle to collector	Average fiber diameters tend to decrease with increase in spinning distance
Polymer concentration/viscosity	Average fiber diameters increase when increasing polymer concentration
Applied voltage	Generally, increasing applied voltage results in a larger fiber diameter. However, an initial decrease in diameter with increasing applied voltage was also reported.
Vapor diffusivity	Lower evaporating solvent tends to decrease fiber diameter
Surface tension	The effect of surface tension on fiber diameter is negligibly small.
Solution conductivity	Increasing solution conductivity tends to decrease fiber diameter.
Solvent	Electrospinnability at rate of solidification of the jet on evaporation of the solvent depend on with dipole moment and conductivity of solution.

2.1.4 Crosslinking methods

Unfortunately, the electrospun nanofiber mats of natural polymer had unstable structure in water and poor mechanical property. Crosslinking is a technique that can be used to improve structures stabilities and mechanical properties of nanofiber mats. Crosslinking divided into 2 methods as physical crosslinking (dehydrothermal, ultraviolet, and electrobeam irradiation) and chemical crosslinking [40, 41]. Crosslinking technique is the process of chemically joining of molecules via covalent bond[21, 39].

Table 4 Methods of crosslinking [39-42]

Methods of Crosslinking	Effect and reaction
Physical crosslinking	
<ul style="list-style-type: none"> • Dehydrothermal crosslinking 	<p>Treatment in a vacuum oven at temperature above 100 °C. The amino and carboxyl groups of molecules are bonded due to thermal dehydration. However, the dehydrothermal treatment is less crosslinking than chemical treatment.</p>
<ul style="list-style-type: none"> • Ultraviolet irradiation (UV) 	<p>UV irradiation generates radicals at the aromatic residues of amino acids. However, it is possible that irradiation for longer time preferably acts on the chain scission of gelatin molecules. A balance of the crosslinking and chain scission will result in an unchanged density of crosslinking.</p>
<ul style="list-style-type: none"> • Electron beam irradiation 	<p>Electron beam processing is used to improve mechanical, thermal, chemical and other properties as sterilization of medical and pharmaceutical goods. Electron beam irradiation is one of crosslinking of polymer at chain scission by making the polymer chain shorter by changing the polymer structure to be crystallinity.</p>
Chemical crosslinking	<p>The disadvantage of some chemical crosslinking is toxic to cells. For examples, chemical crosslinking agents as glutaraldehyde and formaldehyde are toxic to cells and sometimes change the color of scaffolds. The formaldehyde and 1-ethyl-3-(3-dimethyl aminopropyl) carbodiimide (EDC) are mostly found as the crosslinking agents.</p>

.2 Literature review

2.2.1 Electrospinning of chitosan blend

Chitosan is natural polymers with a huge potential use in numerous fields such as biomedical, biological, and industrial applications. Both chitin and chitosan were found to be hard for electrospinning because they have three –dimensional networks of strong hydrogen bonds [60]. However, many researchers tried to produce nanofiber using special solvents such as Trifluoroacetic acid (TFA) [38], 1,1,1,3,3,3, -hexafluoro-2-propanol (HFIP) [39], and acetic acid [40].

Ohkawa et al, (2004)[11] mixed chitosan with poly vinyl alcohol (PVA). PVA is known to be non-toxic, water-soluble, biocompatible, and biodegradable synthetic polymer, which is widely used in the biomedical field and has excellent fiber forming ability and highly hydrophilic properties, it is to be expected that a membrane composed of nanofibers of PVA/Chitosan blend produced by electrospinning could have an important role in the biomedical field [41]. PVA was chosen because it strongly interacts with chitosan through hydrogen bonding on a molecular level and it can be conveniently electrospun from an aqueous medium. Two chitosan samples were used. The first was chitosan 10 (viscosity average molecular weight, $M_v = 2.1 \times 10^5$) and the second was chitosan 100 ($M_v = 1.3 \times 10^6$; degree of deacetylation, 0.77). The electrospinning experiments were performed at room temperature. The electrospinning was conducted by dissolving the PVA in distilled water at a concentration of 9 wt%, and chitosan was dissolved in neat formic acid at 7 wt%. When a small portion of the PVA was mixed with chitosan (chitosan: PVA= 90:10), beads were deposited in the collector. As the ratio of chitosan in the solution decreased (chitosan: PVA = 70:30), the size of the beads became smaller and thin fibers coexisted among the beads. When equal volumes of the chitosan and PVA (50:50) solutions were blended, homogenous fiber with an average diameter of 120 nm could be spun (Figure 7c, diameter distribution, 83-170 nm). At a chitosan: PVA ratio of 30:70 the fibers was thicker (Figure 7d, average diameter, 170 nm diameter distribution, 110-220 nm) than those prepared in 50:50. Chitosan 100 was dissolved in formic acid (or 0.2 M acetic acid) at 2 wt.% and the solution was mixed with 9 wt.% PVA in a volume ratio of 50:50, then

the mixed solution was electrospun (Figure 7f, average diameter, 170 nm; diameter distribution, 120-220 nm)[11].

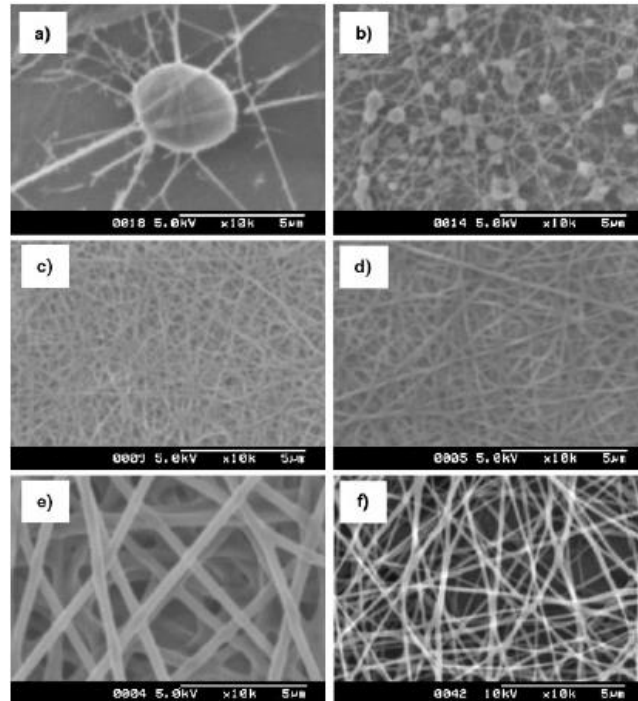


Figure 7 SEM images magnification X 10,000 of the chitosan and PVA blended electrospun fiber. The volume ratio of chitosan 10: PVA = 90:10 (a), 70:30 (b), 50:50 (c), 30:70 (d) and 0:100 (e) chitosan 100 was dissolved in formic acid (or 0.2 M acetic acid) at 2 wt.% and the solution was mixed with 9 wt.% PVA in a volume ratio of 50:50, then the mixed solution was electrospun (f)

Huang et al, (2011) [22] studied a novel kind of scaffolds for blood vessel and nerve repairs from collagen-chitosan-thermoplastic polyurethane (TPU) blended by electrospinning. Collagen (8 wt%) and TPU (6wt%) were dissolved in 1,1,1,3,3,3-hexafluoroisopropanol (HFP) while chitosan (8wt%) was dissolved in HFP/TFA mixture (v/v, 90/10). Before electrospinning, the three solutions were blended at a weight ratio of collagen/chitosan/TPU = 60%/15%/25% with sufficient stirring at room temperature for 1 hour. The collagen- chitosan-TPU nanofibrous membrane was crosslinked in 25% glutaraldehyde aqueous solution and kept in a desiccator at room temperature for 2 days. Figure 8 showed the randomly oriented and aligned collagen-chitosan- TPU nanofibrous scaffolds with fiber diameter in the range of 360 ± 220 and 256 ± 145 nm, respectively. The mechanical properties of the scaffolds were good flexibility with a high tensile strength. Cell viability studies using endothelial cells and

Schwann cells were shown biocompatibility and aligned fibers could regulate cell morphology by inducing cell orientation. Vascular grafts and nerve conduits were electrospun or sutured based on the nanofibrous scaffolds. The results revealed that collagen- chitosan- TPU blended nanofibrous scaffolds might be a potential candidate for vascular repair and nerve regeneration [22].

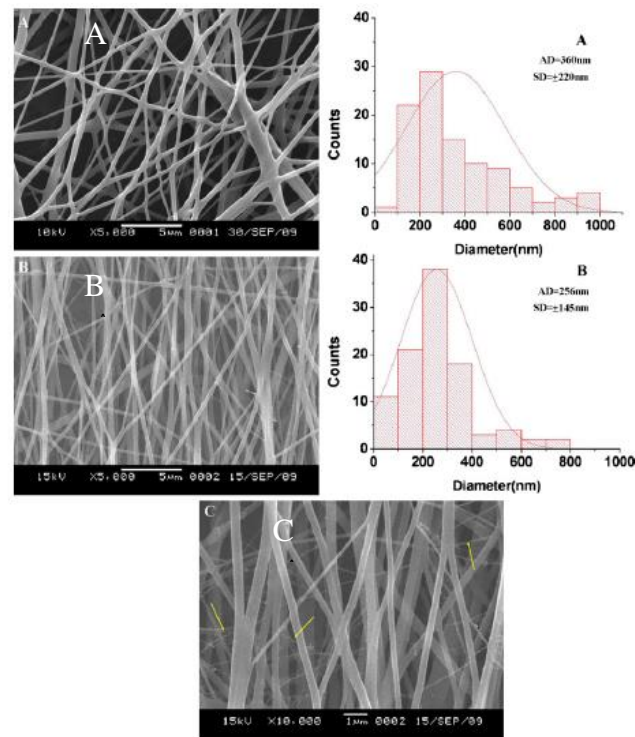


Figure 8 SEM images of collagen-chitosan-TPU nanofibers and diameter distribution: (A) random oriented nanofiber; (B) and (C) aligned nanofiber with 5000 and 10,000 magnification

Wang and Zhao, (2012) [25] prepared gelatin- chitosan nanofiber by electrospinning. Gelatin (isoelectric point: 6; Mw: 60 kDa) and chitosan (75-85% deacetylated; Mv: 50 kDa- 190 kDa) were dissolved in trifluoroacetic acid (TFA)/ dichloromethane (DCM) (v/v, 70/30) to make 30% gelatin and 7% chitosan solution with different mass ratios (gelatin/chitosan: 0/100, 25/75, 50/50, 75/25, 100/0). Figure 9 showed the gelatin-chitosan nanofiber between 250 nm to 470 nm. The gelatin-chitosan nanofibers possessed more uniform morphologies (Figure 9 b to d) than the pure gelatin and chitosan nanofiber.

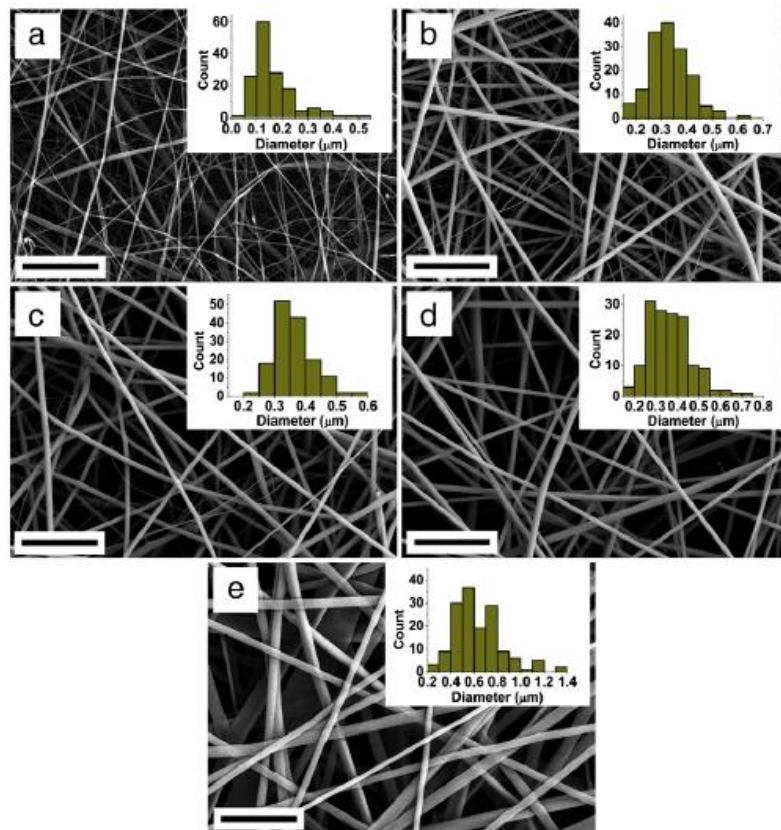


Figure 9 SEM images of electrospun gelatin-chitosan nanofibers in different mass ratio (gelatin/chitosan). (a) 0/100; (b) 25/75; (c) 50/50; (d) 75/25; (e) 100/0. The insets showed the fiber size distributions

Cooper et al, (2013) [61] mixed chitosan with poly (ϵ -caprolactone) (PCL). PCL is commonly found in tissue engineering application due to its structural and mechanical stability [45]. Chitosan with 85% deacetylated was used and dissolved in 5 and 7 wt% with trifluoroacetic acid and refluxed at 70% for 3h. PCL (10 and 12 wt%) was dissolved in 2,2,2- trifluoroethanol. The electrospinning experiments were performed at room temperature. Figure 10 (a-d) shown in the SEM images uniform nanofibrous membranes from all PCL and chitosan-PCL solution with fiber diameter of 200-400 nm.

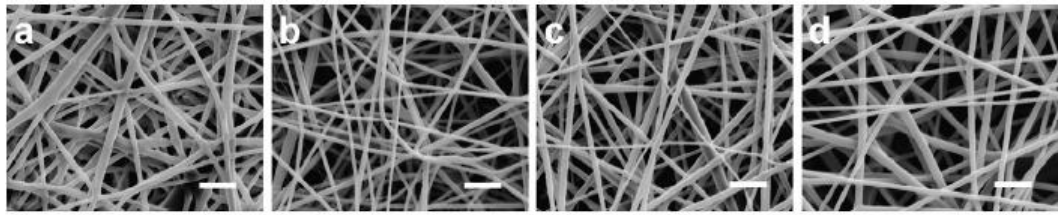


Figure 10 SEM images of electrospun PCL-chitosan nanofibers in different mass ratio (gelatin/chitosan) (a) 100/0; (b) 75/25; (c) 50/50; (d) 25/75; (e) 0/100

Zhou et al, (2013) [27] fabricated composite nanofibrous membranes from water-soluble N- carboxyethyl chitosan (CECS) / poly (vinyl alcohol) (PVA) / silk fibroin nanoparticles (SF) using electrospinning for wound dressings. Figure 11 illustrated SEM images of CECS/PVA nanofiber and CECS/PVA/SF with different SF content. It was found that CECS/PVA (40/60) were smooth and homogeneous fibers. When the SF nanoparticles were added into CECS/PVA solution, fiber morphology with beads or several particles was produced, indicating that SF nanoparticles were partially embedded in the composite for all SF nanoparticles concentration. The electrospun of CECS/PVA/SF had good in vitro biocompatibility with mouse fibroblasts (L929). These novel electrospun matrices have the potential to be used as materials for wound dressing for skin regeneration.

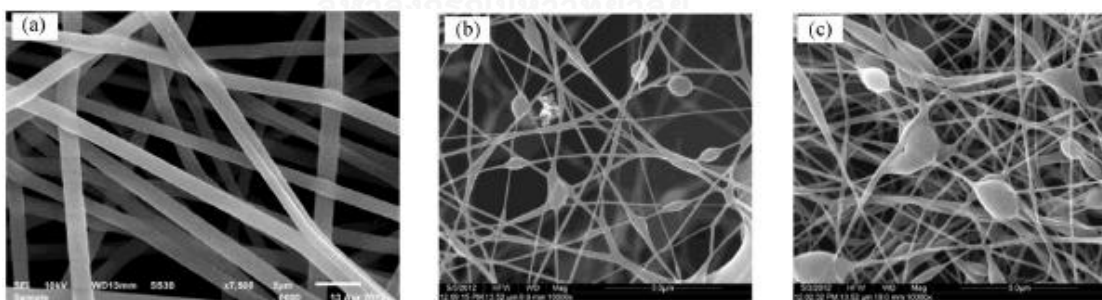


Figure 11 The morphology of various nanofibers (a)CECS/PVA; (b) CECS/PVA/SF 4%; (c) CECS/PVA/SF 8%

2.2.2 Electrospinning of silk fibroin blend

Park et al, (2004)[38] studied the effect of chitosan on morphology and the conformation of electrospun silk fibroin nanofibers. The electrospinning of silk fibroin (SF) /chitosan (CS) blends with different composition ratio was performed with formic

acid as a spinning solution. The SF/CS blends containing up to the CS content of 30% could be electrospun into the continuous fibrous structure, although pure CS was not able to be electrospun into the fibrous structure. The as-spun SF/CS blend nanofibers had smaller diameters and narrower diameter distributions than pure SF nanofibers, and their diameter gradually decreased up to ~ 100 nm with the addition of CS. Comparing with the pure SF nanofibers, the conformational change of the as-spun SF/CS blend nanofibers into β -sheet was fast because the CS with a rigid backbone synergistically might promote the conformational transition of SF by an intermolecular interaction.

Studies of Kim et al, (2005)[15] evaluated the biocompatibility of the silk fibroin (SF) nanofiber membrane, and examined its effect on bone regeneration in a rabbit calvarial model. The results found that the cell numbers and osteocalcin production labels were significantly increased in accordance with culture period. In in vivo tests, a complete bony union across the defects was observed after 8 weeks. At 12 weeks, the defect had completely healed with new bone. The SF nanofiber membrane was shown to possess good biocompatibility with enhanced bone regeneration without evidence of any inflammatory reaction. Their results strongly suggested that the SF membrane should be useful as a tool for guided bone regeneration.

Meechaisue et al, (2007)[24] prepared a preliminary study of electrospun silk fibroin fiber mats as bone scaffolds. Silk fibroin from cocoons of indigenous Thai silkworms (Nang-Lai) and Chinese/Japanese hybrid silkworms (DOAE7) was fabricated into ultra-fine fibers by electrospinning. The effects of solution concentration at 10-40% (w/v) in 85% (v/v) formic acid and applied electrostatic field strength at 10 to 20 kV/10 cm on morphology and size of the electrospun silk fibroin products were investigated. At lower concentrations, the SF solutions produced discrete beads or beaded fiber, while, at high solution concentrations, $\geq 30\%$ w/v, only smooth fiber was observed. The average diameter of Nang Lai SF fiber was 217-610 nm and DOAE7 was 183-810 nm. The potential for using of the electrospun fiber mats as bone scaffolds was assessed with mouse osteoblast-like cells (MC3T3-E1) that were either seeded or cultured on the surface of SF fiber mats prepared from 35% (w/v) Mang-Lai SF solution. The electrospun SF fiber mats could be used as scaffolding materials for bone cell culture, as the cell adhered and proliferated well on their

surfaces. Okhawili et al, (2010)[62] studied the effect of preparations for electrospun fiber mats of Thai silk fibroin/Type B gelatin (SF/GB) for controlling release applications. The blended solution of SF/GB at weight blending ratios of 10/90, 20/80, 30/70, 40/60 and 50/50 could be produced fibers. The results on in vitro biodegradation test showed that SF/GB 10/90 electrospun fiber mats was rapidly degraded in collagenase solution due to direct biodegradation of gelatin by collagenase. From in vitro controlled release of two active agents (azo-casein and methylene blue) from SF/GB blended fiber mats, it was suggested that methylene blue could be adsorbed on the blended fiber mats, possibly due to attractive interaction between the positively charged molecules of methylene blue and negatively charged SF/GB fiber mats. In contrast, the same charge of blended fiber mats and azo-casein would result in the repulsive force, resulting in continuous diffusion of azo-casein from blended fiber mate within 72 hours. SF/GB electrospun fiber mats had high potential to be applied in controlled release applications.

2.2.3 Electrospinning of gelatin blend

Huang et al, (2004)[10] investigated mechanical properties and the mass concentration of electrospun nanofiber from gelatin. 2, 2, 2-trifluoroethanol (TFE) had been found to be suitable for gelatin at 5-12.5% concentration that can be successfully electrospun into nanofibers of a diameter in the range from 100 to 340 nm. The study showed that both the fiber diameter and the beads on to fiber surface could influence the mechanical performance of the electrospun nanofiber membranes.

Ki et al, (2005)[31] tried to develop the novel dope solution of gelatin for electrospinning for producing gelatin nanofibers. Gelatin was dissolved in formic acid. Gelatin nanofiber was successfully prepared using gelatin-formic acid dope solution. After keeping the dope solution of gelatin at 5 hours, the stability of dope solution was not affected to the spinability and morphology of gelatin nanofiber. In this result, formic acid dissolved the gelatin at room temperature and used as a solution for the electrospinning of gelatin.

Vaz et al, (2005)[63] developed a scaffold architecture mimicking both morphological and mechanical what that of a blood vessel by applying a sequential

multi-layering electrospinning on a rotating mandrel-type collector. The polycaprolactone (PCL) inner layer was a porous bead-like fibrous structure with interconnected pores (~ 15µm average pore size) composed of randomly oriented microfibers with diameters ranging from 1.5 to 6 µm and percentage of nano-fibrils (600± 400 nm diameter). The PLA outer layer consisted of uniform fibers with diameters ranging from 800 nm to 3µm and interconnected pores with size smaller than 10µm. The PLA/PCL bi-layered scaffolds were also proved to be capable of supporting the attachment, spreading and growing of mouse fibroblasts and human fibroblasts.

Ghasemi et al, (2008) [34] investigated the properties of PCL/gelatin nanofibrous scaffolds for nerve tissue engineering. PCL/gelatin at the ratio of 70:30 was found to exhibit the most balanced properties to meet all the required specifications for nerve issue. In addition it was used for in vitro culture of nerve stem cell (C17.2 cells). MTT assay and SEM results showed that the biocomposites of PCL/gelatin 70:30 nanofibrous scaffolds enhanced the nerve differentiation and proliferation compared to PCL nanofibrous scaffolds and acted as a positive cue to support neurite outgrowth.

Wang and Zhao,(2012)[25] prepared the gelatin-chitosan nanofibers by electrospinning. Gelatin and chitosan were dissolved in trifluoroacetic acid (TFA) and dichloromethane (DCM) (TFA/DCM, v/v, 70/30) at different mass ratios (gelatin/chitosan: 0/100, 25/75, 50/50, 75/25, 100/0). The electrospun gelatin-chitosan nanofibers possessed more uniform morphologies than the pure gelatin or chitosan nanofibers. Atomic force microscopy (AFM)–Harmoni X mode indicated the existence of intermolecular interaction within the electrospun gelatin-chitosan nanofibers.

2.2.4. The other techniques of silk fibroin, chitosan and gelatin blend

S. Putthanarat et al, (2002)[64] studied the effect of processing temperature on the morphology of silk membranes. The liquid silk from the middle section of the Middle Division of the silk gland of *Bombyx mori* was prepared by casting onto glass plates at 20, 40, 60 and 80°C. Silk from the anterior and posterior sections was cast at 20°C. Samples cast at 20°C exhibit particles, grains, nanofibrils and an irregular morphology. Samples cast above 50°C exhibited larger grains and high densely packed

nanofibrils. All these changes might result from conversion of the amorphous structure to the β -pleated structure (Silk II). The nanofibrils were appeared to be self-assembled bio-nanofibrils. Membranes of regenerated fibroin treated with an aqueous methanol solution exhibited grains and apparent nanofibrils.

Kim et al, (2005)[18] developed a new strategy for silk fibroin processing for biomaterials that avoided the use of organic solvents or harsh chemicals by using the particle size of granular NaCl. Three-dimensional porous scaffolds were generated by salt leaching, gas forming or freeze-drying. The results of this process were scaffolds with controllable porosity and pore size that fully degrade in the presence of proteases.

A mechanism for this novel process imparted physical stability via hydrophobic interactions. Adjusting the concentration of silk fibroin in water, and the particle size of granular NaCl used in the process, leads to the control of morphological and functional properties of the scaffolds. The aqueous-derived scaffolds had highly homogeneous and interconnected pores with pore sizes ranging from 470 to 940 μm , depending on the mode of preparation. The scaffolds had porosities $> 90\%$, compressive strength and modulus up to 320 ± 10 and 330 ± 500 KPa, respectively, when formed from 10% aqueous solutions of silk fibroin. The scaffolds fully degraded upon exposure to protease during 21 days, unlike the scaffolds prepared from organic solvent processing.

She et al, (2008)[65] studied the blending of silk fibroin and chitosan into three-dimensional silk fibroin/chitosan scaffolds (SFCS) by freeze-drying method. In vitro degradation behaviors of SFCS scaffolds were systematically investigated up to 8 weeks in phosphate buffer saline (PBS) solution at 37°C . SFCS scaffolds maintained its porous structure till 6 weeks of degradation. During the first 2 weeks, the pH value fluctuated in a narrow range from 6.53 to 6.93. SFCS scaffold degraded much more quickly during the first 2 weeks, and the weight loss reached 19 wt% after 8 weeks of degradation. The degradation process insignificantly affected SFCS scaffolds' swelling properties.

Mandal et al, (2009)[66] prepared multilayer films based on silk fibroin protein and gelatin in aqueous solution for controlled drug release. In this study, release of molecules from silk fibroin multilayer was modulated by controlling the crystalline

structure and by addition of self-degradable polymer to provide more delicate and programmable control. Multilayered fibroin/ gelatin film of different ratios (1:1, 2:1, and 4:1) was fabricated by treating each layer with methanol. Methanol treatment induced transition from random coil to β -sheets, which provide physical crosslink between fibroin/gelatin, giving rise to the structural stability to the layers. The film was tested for in vitro release using three different molecular weight model compounds. It depended on multilayer film degradation for sustained release. The highly versatile and tunable properties of fibroin/gelatin multilayer films making them exciting candidates for the controlled release of a wide spectrum of bioactive molecules.

Song et al, (2011) [67] studied silk fibroin membrane (SFM) that could be used for guided bone regeneration (GBR). In this study, 3 different types of SFM were used for the GBR technique by casting SF solution on polystyrene dish to make transparent SFM. The results of the microscopic computerized tomographic (μ -CT) analysis were presented in Table 6. The average values of the 2 measured variables higher in the SFM group than in the control group at 4 and 8 weeks were reported.

Table 5 Microscopic computerized tomographic (μ -CT) analysis

	4 weeks			8 weeks		
	Control	Silk membrane	P value	Control	Silk membrane	P value
Bone volume (mm ³)	6.89 ± 4.94	13.44 ± 6.81	0.041	22.31± 9.07	36.79 ± 10.30	0.017
Bone mineral density (mg/mm ³)	0.36 ± 0.13	0.39 ± 0.07	NS	0.43 ± 0.11	0.47 ± 0.16	NS

Table 6 Histomorphometric analysis

	4 weeks			8 weeks		
	Control	Silk membrane	P value	Control	Silk membrane	P value
Total new bone (%)	4.68± 4.13	34.16±4.42	0.001	35.42±14.58	67.02±5.50	0.007

The histomorphometric analyses (Table 6) were also in good agreement with the μ -CT (Table 7) results. The total formation of new bone was $4.68 \pm 4.13\%$ in the control group and $34.16 \pm 4.42\%$ in the experimental group at 4 weeks after surgery.

Sionkowska and Planecka, (2013)[68] prepared and characterized the three-dimensional silk/chitosan (SF/CS) composite sponges with an interconnected porous structure, proper swelling and mechanical properties. Sponges were prepared by means of freezing and lyophilization of corresponding composite solutions. The pore size in SF/CS sponge was from 20 to 150 μm and was suitable for cell growth. SF/CS sponges have sufficient mechanical integrity to resist handling during implantation and in vivo loading in both dry state and PBS solution. The compressive modulus and compressive strength of the sponge depended on the silk content in the blend. SF/CS sponges were biocompatible for the fibroblast 3T3. Three- dimension sponges made of SF/CS mixtures can be interesting materials for scaffolds preparation that temporary supports the formation of new tissue and organs.

2.2.5 Crosslinking of silk fibroin, gelatin, and chitosan

Zhang et al, (2006)[30] improved the water-resistant ability and thermo-mechanical property of electrospun gelatin nanofiber. Glutaraldehyde (GA) was used for crosslinking agent. GA vapor was crosslinked at room temperature for 3 days after that it was soaked in 37°C warm water for 6 days. It was found that the crosslinkings improved thermo- stability and substantial enhancement in mechanical properties. The cytotoxicity was investigated by culturing human dermal fibroblasts. The crosslinking gelatin fibrous scaffold for 1, 3, 5 and 7 days found cell expansion and proliferation of human dermal fibroblasts.

Ratanavaraporn et al, (2010)[69] has investigated the factors of crosslinking on electrospun type A and type B gelatin fiber mats. The optimize concentration of 20-40 % of gelatin solution was fabricated to produce the gelatin fibers with smooth surface throughout the fiber length. The dehydrothermal treatment (DHT) and plasma treatment on gelatin fiber mats provided a low crosslinking degree, but kept the original structure of fiber mats. By using DHT followed by spaying/immersion in the EDC / NHS in

water or ethanol and glutaraldehyde (GA) vapor, high crosslinking degrees of swollen fiber mats was obtained.

Marin et al, (2011)[70] produced a novel blend film of N-(2-hydroxy) propyl-3-trimethylammonium chitosan chloride (HTCC)/ poly (vinyl alcohol) by crosslinking with glutaraldehyde. The increasing content of HTCC was affected by increasing of the equilibrium degree of swelling. The content of GA has negligibly affected the swelling rate and time reached swelling equilibrium. GA has effected on chitosan derivative.

Bigi et al, (2001)[44] studied the effect of glutaraldehyde concentration on the mechanical, thermal, swelling and release properties of gelatin films. 1 wt% of GA have effect to degree of crosslinking next to 100%. The young's modulus was increased up to 20 times of uncrosslinking. The thermal stability and swelling were increased.

Zhang et al, (2008)[30] fabricated gelatin nanofibrous by electrosinning for GTR. The EDC/NHS was chosen for the chemical crosslinking. Using 50mM EDC and 20mM NHS showed the optimum crosslinking degree. As The EDC/NHS concentration was increased, the degree of swelling was declined.

Liu et al, (2012)[16] prepared the tusssah silk fibroin (TSF) nanofibers by crosslinking with 1-(3-Dimethyl-aminopropyl-3-ethylcarbodiimide/ N-hydroxysuccinimide/Ethanol (EDC/NHS/ethanol) solution. Fibroblast L373 and BMSCs were seeded onto the crosslinked TSF nanofiber. The TSF diameters of nanofiber increased from 611 to 787 in ethanol treatment and 611 to 841 nm in EDC/NHS/Ethanol treatment. The fibroblast L373 and BMSCs were spread on the crosslinked TSF nanofibers.

Jeong et al, (1996)[71] investigated the effects of 1-(3-dimethyl-aminopropyl-3-ethylcarbodiimide (EDC) / N-hydroxysuccinimide (NHS) and glutaraldehyde (GA) on the hydrothermal and biochemical of bovine pericardium. The ratio of ECD/HNS was achieved up to 2:1 but the increasing ratio of 4:1 was no significant consequence. EDC/NHS and GA were very similarly increased resistance to collagenase. EDC/HNS were more extensible and more elastic than GA.

For literature reviews, they showed many techniques to fabricate biomaterials (Scaffold, film or sponge) from gelatin, silk fibroin or chitosan for medical and other applications. Over last decades, electrospinning technique is a process to produce nanofiber fibers and has high porous sheet. The effects of electrospinning process have solvent, concentration or electrical field, etc. Several solvents and the mix-solvents for electrospinning used for dissolve silk fibroin, gelatin and chitosan such as trifluoroacetic acid (TFA) and 85% (v/v) formic acid [24, 31], 2,2,2-trifluoroethanol (TFE)[10], 1,1,1,3,3,3- hexafluoroisopropanol (HFIP) and HFIP/TFA mixture (v/v, 90/10) etc. The most crosslinking reagent used EDC/NHS and GA of natural polymer from protein structure [44, 72, 73].

In this study, we were interested in the advantage of silk fibroin, gelatin, and chitosan, thus two objectives of this study were as follows, firstly to prepare nanofiber mats by electrospinning from SF: G: C by using formic acid as a solvent. The morphology and physical properties of the SF: G: C blended fiber mats were investigated. Another objective was studying the effect of chemical for crosslinking on nanofiber of SF: G: C blended fiber mats from ethanol, EDC/NHS and GA and biological properties of the SF: G: C nanofiber mats



CHAPTER III

MATERIAL AND METHODS

This research project was divided into 4 parts.

Part I: Preparation of silk fibroin.

Part II: Fabrication of nanofiber membranes from gelatin, chitosan, and silk fibroin by electrospinning technique.

Part III: Crosslinking of nanofiber mats.

Part IV: Physical and biological characterizations of membranes.

3.1 Materials and reagents

Materials and reagents used for preparation and fabrication of nanofiber mats.

1. *Bombyx Mori cocoon*, Nangnoi Srisaket (The Queen Sirikit Department of Sericulture, Ministry of Agriculture and Cooperatives)
2. Gelatin from porcine skin, lot# BCBF0852V (Fluka-Aldrich, Germany)
3. Chitosan, Mw. 300,000 (Biolife, Thailand)
4. Sodium carbonate (Na_2CO_3) (Sigma-Aldrich, Germany)
5. Calcium chloride (CaCl_2) (Ajax Finechem, Australia)
6. Formic acid (98%), Sigma-Aldrich, Germany
7. 1-ethyl-3-(3-dimethylaminopropyl) carbodiimide (EDC) (Sigma-Aldrich, Germany)
8. N-hydroxysuccinimide (NHS) (Sigma-Aldrich, Germany)
9. 3.5% Glutaraldehyde (Sigma-Aldrich, Germany)
10. 95% ethanol (Sigma-Aldrich, Germany)

Materials and reagents used for biological characterization of nanofiber mats.

1. Dulbecco's Modified Eagle Medium (DMEM) (GIBCO BRL, USA)

2. DMEM without phenol red (GIBCO BRL, USA)
3. Antibiotic- antimycotic solution (GIBCO BRL, USA)
4. L-glutamine (GIBCO BRL, USA)
5. Fetal bovine serum (GIBCO BRL, USA)
6. Glutaraldehyde
7. Osmium tetroxide

3.2 Apparatus

1. Dialysis (MW cut off 12,000) (Spectra/ Pro®6 Dialysis Membrane, Lot# 3225902)
2. High-Voltage power supply (Spellman SL300, USA)
3. Scanning Electron Microscope (JEOL, JSM-5410 LV, Japan)
4. Lyophilizer (Heto, Power Dry LL, USA)
5. CO₂ incubator (Shel Lab, USA)
6. Biohazard Hood (MDH, UK)
7. Spectrophotometer (Ultrospec 3000, UK)
8. Inverted phase contrast microscope (Olympus ck2, Japan)

3.3 Experimental procedures

3.3.1 Part I: Preparation of silk fibroin from fresh silk cocoon

1. Fresh silk cocoon was immersed in 0.02M Na₂CO₃ at 100°C for 1 hour, then rinse with distilled water. This process was repeated twice to remove sericin which is the glue-like proteins. It is called degumming. Then the degummed silk was dried at room temperature.
2. The degummed silk fibroin were dissolved in co-solvent composed of CaCl₂: CH₃CH₂OH: H₂O (1:2:8 in molar ratio) at 80 °C for 6 hours.
3. The mixture was dialyzed with dialysis tube (Mw cut off 12,000) in distilled water for 3 days at room temperature.

4. The silk fibroin solution was centrifuged at 4,000 rpm, 4 °C for 20 min to remove impurities.
5. The silk fibroin solution was lyophilized to obtain the silk fibroin sponges which were used as the source of silk fibroin.

3.3.2 Part II: Fabrication of nanofiber membranes from gelatin, chitosan, and silk fibroin by electrospinning technique

1. 1 wt% chitosan was dissolved in a 90 % formic acid.
2. Silk fibroin sponges, gelatin and chitosan solution were dissolved in 98% formic acid with various concentrations and the mixtures were stirred for 1-2 hours at room temperature.
3. Each mixture was loaded in a 5 ml syringe equipped with stainless steel needle.
4. The syringe was connected to syringe pump for accurately to control the solution flow rate of 0.2 ml/h.
5. The syringe needle was connected to a power supply. A stainless rolling drum was used as a collector for nanofiber mats collection.
6. The electrical potential was set at 10 - 20 kV and the distance between the needle and the collector was between 5 to 20 cm for proper electrospinning conditions.
7. The nanofiber mats from electrospinning collector were dried overnight in a vacuum oven to remove moisture before measurements.

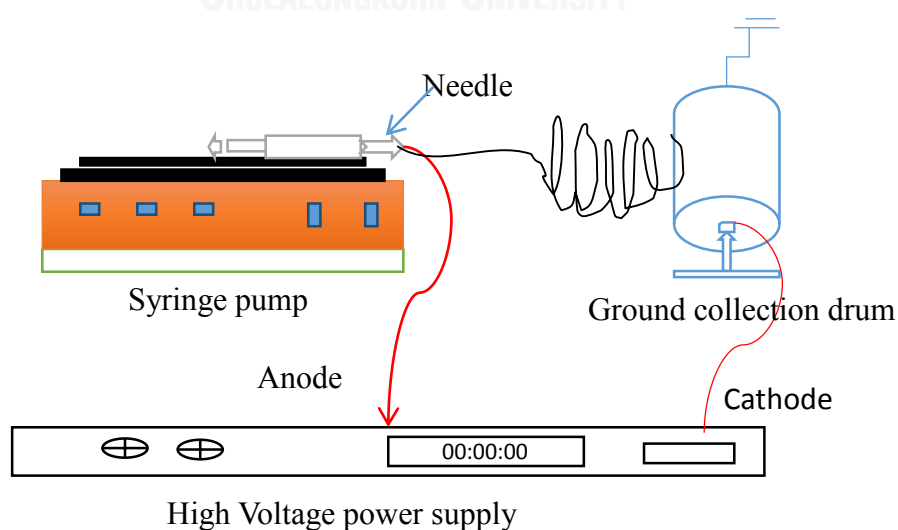


Figure 12 Electrospinning process

3.3.3 Part III: Crosslinking of nanofiber mats

All the dry electrospun nanofiber mats were cut into small pieces of 5 X 5 cm² and were divided into three groups for different crosslinking methods. 95% Ethanol, 35% glutaraldehyde (GA), and 1-ethyl-3-(3-dimethylaminopropyl) carbodiimide (EDC) / *N*-hydroxysuccinimide (NHS) (EDC/NHS) were used as crosslinking agents. EDC/NHS solution with wt/wt ratios at 2/1 was added into 95% ethanol. All samples were treated in such agents by fumigation for 72 hours followed by dipping for 10 minutes. Then those samples were washed in distilled water for 30 minutes and dried in desiccator at room temperature.

Method	Chemical crosslinker	Experimental process
A	Ethanol	Dry in a chamber with ethanol and leave for 72 hours, after that dipping in ethanol 10 min, washing with PBS pH 7.4 to remove ethanol. Finally, dry in desiccator.
B	GA	Dry in a chamber with GA and leave for 72 hours, after that dipping in GA 10 for min, washing with PBS pH 7.4 to remove GA. Finally, dry in desiccator.
C	EDC/NHS	Dry in a chamber with EDC/NHS and leave for 72 hours, after that dipping in EDC/NHS 10 min, washing with PBS pH 7.4 to remove EDC/NHS. Finally, dry in desiccator.

3.3.4 Part IV: Physical and biological characterization of the nanofiber membranes

3.3.4.1 Physical characterization of the membrane

- **Morphology of nanofiber mats before and after crosslinking**

The dry nanofiber mats were cut into small pieces. The specimens were fixed on the stubs and coated with gold particles before investigation under the scanning electron microscope (SEM). The average diameter of electrospun nanofiber mats was determined by measuring the diameter of the nanofiber in the SEM images by Image J program. The fiber diameters were presented as the average standard deviation.

- **Functional group of reactionaries**

Fourier Transform Infrared Spectroscopy (FTIR) was used to identify the chemical structure of the nanofiber mats before and after crosslinking. FTIR spectroscopy was applied to confirm the presence of silk fibroin/gelatin/chitosan in blended nanofiber mats and films. The nanofiber mats and films were crushed and mixed with potassium bromide (KBr) and made into pellets. Then each pellet was placed in a sample holder. The measurements were measured between 400 to 4,000 cm^{-1} , recorded with an accumulation of 40 scans and a resolution of 2 cm^{-1} .

3.3.4.2 Mechanical properties

- **Tensile Strength**

Each nanofiber mats were cut into dumbbell shape as shown in Figure 13, according to DIN 53504-S2.

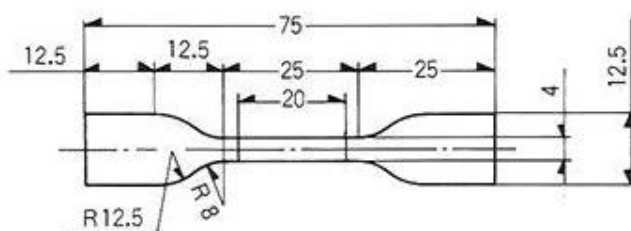


Figure 13 Dumbbell of DIN 53504-S2

The mechanical properties of the non-crosslinked membrane were tested at a crosshead speed of 1 mm/min under an ambient condition. The reported data were average from five repeated measurements.

- **Weight loss and Degree of swelling from crosslinking**

The efficiency of crosslinked nanofiber mats with ethanol, GA, and EDC/NHS was investigated by weight loss. The crosslinked- nanofiber membrane was kept in desiccator 24 hours (W_b) at room temperature. After 24 hours, the samples were submerged in distilled water for 2 hours and removed from the distilled water, placed between two pieces of tissue paper under metal sheet for removing excess water (W_s). The samples were dried in desiccator for 72 hours (W_d). The weight loss (%) and the degree of swelling (%) of each sample were calculated according to the following equation.

$$\text{Weight loss (\%)} = \frac{(W_b - W_d) \times 100}{W_d}$$

$$\text{Degree of swelling (\%)} = \frac{(W_s - W_d) \times 100}{W_d}$$

- **Crystallinity**

The crystallinity of nanofiber mats of non-crosslinked and crosslinked were investigated by using X-ray diffraction (XRD) analysis (Lab XRD-6000, Shimadzu, Japan). Each nanofiber mats were cut into a circular shape with 6 mm in diameter and was attached into a holder. The membrane was investigated by using Cu $K\alpha$ radiation. Irradiation conditions were 40 kV and 40mA at 2θ scanning from 5 to 40° with a scan speed of $0.02^\circ \text{ sec}^{-1}$. Crystallinity index CrI_{100} was determined according to using the equation of Focher [74].

$$CrI = [(I - I_{am})/I] \times 100$$

Where,

CrI = Crystallinity index

I = Maximum intensity at around 20°

I_{am} = Amorphous diffraction at around 9°

- **Air permeability**

Air permeability of the membrane was measured using Oxygen Permeability tester, (Illinois 8000, Germany). Each nanofiber mats was cut into a circular shape with 6 mm in diameter and was placed into a sample holder. The membrane was measured at 25 °C, 100% RH. At least 3 samples were tested and averaged results were recorded.

- **Statistical analysis**

All data were reported as mean ± standard deviation.

3.3.4.3 Biological characterization of membranes

The samples of non-crosslinked and crosslinked nanofiber mats were cut into a rectangular shape, size 0.7 x 0.5 cm², soaked in PBS for 10 minutes, then immersed in DMEM with 5% antibiotics-antimycotics solution for 1 hour and washed with simple DMEM twice before testing.

In vitro studies: cellular response to the nanofiber barrier membranes [75]

Normal human gingival fibroblasts were prepared from healthy gingival tissues. Briefly, the tissue samples from gingivectomy were cut into small pieces and transferred to 35 mm culture plates (Falcon, Germany). The tissue samples were cultivated in Dulbecco's Modified Eagle Medium (DMEM) supplemented with 10% fetal calf serum, 1% L-glutamine, 100 units/ml penicillin and 1% antibiotic antimycotic solution (Gibco BRL, USA) and maintained at 37 °C in a humidified atmosphere of

95% air and 5% CO₂. The medium was changed every day. The explants were observed under the inverted microscope daily. On day 3 to 10 after tissue explant, a lot of cells migrated out of the tissue. The subculture of the cell clusters were performed in order to reduce the density of cell population and evenly distribute the cells in the new culture plates.

The method of the subculture was described below:

1. Remove the culture medium and wash twice with simple DMEM.
2. Detach the cell with trypsin-EDTA for 5 minutes.
3. Stop the trypsin-EDTA reaction with trypsin inhibitor.
4. The cell suspension was filtered with lens paper, and then centrifuged at 2,000rpm. The supernatant was discarded. The pellet was re-suspended in the fresh medium.
5. The cells were plated at the cell density of 4×10^4 per ml in culture medium. The culture plate was kept at the 37 °C in a humidified atmosphere of 95% air, 5% CO₂.
6. After leaving the cells to attach the plate for 1 hour, the old culture medium with unattached cells were replaced with a fresh one.

The medium was changed every 2 days. When the populations of cells reach high density, the subculture was repeated as described above. With this method of selective attachment of the cells, clone of fibroblasts could establish approximately at the 5th passage. In this study, cells from the fifth passage were used in the study of the of fibroblasts response to the membrane.

Membrane permeability study

Each aseptic nanofiber mats was cut into a circular shape with 13 mm in diameter and was placed in the culture chamber as shown in Figure 14. The cells were plated onto the membranes in the culture chamber at the concentration of 10⁵ cells/ml. The culture chambers were maintained at 37°C in a humidified atmosphere of 95% air, 5% CO₂ for 24 hours. After 24 hours, the culture chamber in the experimental group was turned upside down and the cells were facing the bottom of the plates. The culture

medium was added in the upper parts of the culture chamber. Therefore the cells were separated from the medium by the membranes while the cells in the control group were in the culture medium. The culture medium was changed every day. The culture was maintained for 72 hours, then membranes were investigated with scanning electron microscopy.

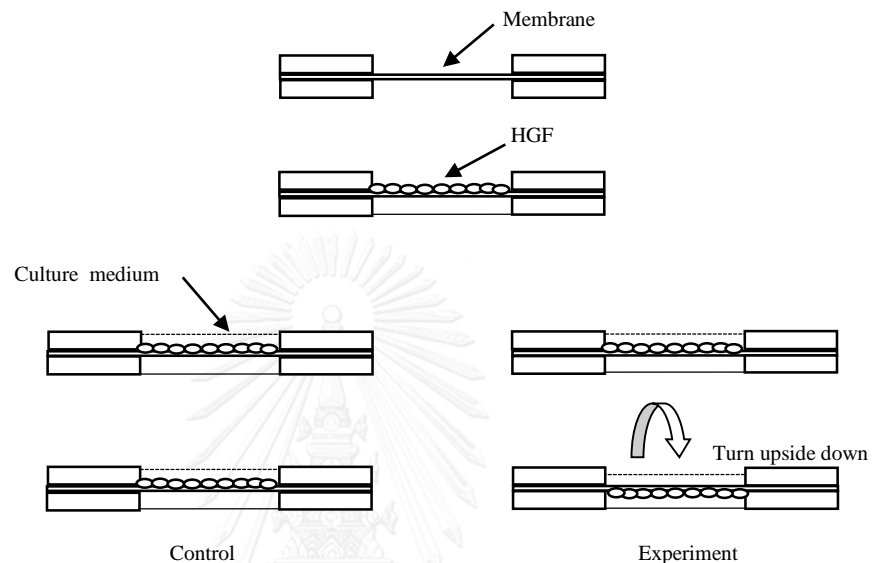


Figure 14. The membrane permeability study

Morphology of HGF after biology testing

Briefly, the small pieces of crosslinked nanofiber membranes were washed with 0.1 M PBS at pH 7.4 for 3 times and fixed with 2% glutaraldehyde in 0.1 M phosphate buffer (PB), pH 7.2 at 4 °C for 1 hour and 1% osmium tetroxide for 1 hour. After fixation, the specimens were dehydrated with graded ethanol each condition 35%, 50%, 75%, 95%, and 100% of concentration respectively for 15 minutes. The specimens were then dried at a critical point drying with liquid nitrogen, fixed on the stubs and coated with gold particles before investigation under the scanning electron

CHAPTER IV

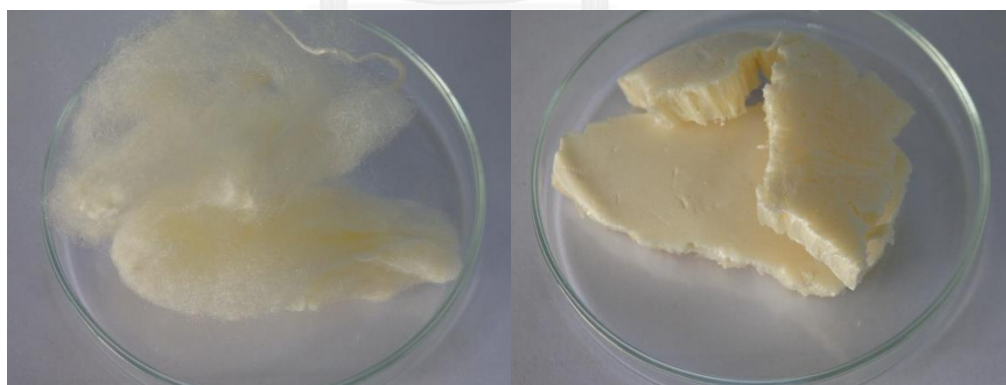
RESULTS AND DISCUSSIONS

Results and discussion shown in this chapter are presented in 4 parts as follows.

Part I: Preparation of silk fibroin sponge, gelatin, and chitosan solution

4.1 Prepared silk fibroin sponge

Fresh silk cocoon has two kinds of proteins containing, fibroin and sericin. Sericin as the glue-like proteins can dissolve in hot water but as well as in soda ash. In this work, silk fibroin fiber (Figure 15 (a)) was found to be dissolved in a co-solvent composed of CaCl_2 : $\text{CH}_3\text{CH}_2\text{OH}$: H_2O (1:2:8 in molar ratio) at 80°C . The resultant silk fibroin solution was dialyzed in a cellulose membrane tube (Molecular Weight Cut Off, MWCO 12,000) in distilled water for 3 days at room temperature. The distilled water was changed every 6 hours to prevent a bacterium could decompose the proteins of silk fibroin solution. The silk fibroin solution was centrifuged at 4,000 rpm, 4°C for 20 min to get rid of impurities and then it was poured in an Erlenmeyer flask, after that it was dipped in liquid nitrogen before lyophilized process at -80°C for 2 days. The silk fibroin sponges were used as the source of silk fibroin as showed in Figure 15(b).



(a) Silk fibroin fiber

(b) Silk fibroin sponge

Figure 15 Digital photographs of (a) silk fibroin fiber and (b) silk fibroin sponge

The structure of silk fibroin composes of amino acids repeating unit : glycine, alanine, and serine, (Gly-Ser-Gly-Ala-Gly-Ala) n . Normally, silk fibroin has two structure forms, silk I and silk II. Silk I and Silk II types of molecular conformation are the secondary structure of silk fibroin. Silk I is non-crystalline; random coil, and α -helix conformation that it is soluble in water. Silk II has a very stable and organized structure; β - sheet conformation that it is not insoluble in water[76, 77]. Our prepared silk fibroin sponge has two structures. The absorption bands were found to be at $1,651\text{ cm}^{-1}$ and $1,638\text{ cm}^{-1}$ (amide I) and $1,511\text{ cm}^{-1}$ (amide II), corresponding to the SF silk II structural conformation (β -sheet). Furthermore, the absorption bands at $1,541\text{ cm}^{-1}$ (amide II) and $1,240\text{ cm}^{-1}$ (amide III) were found to represent silk I conformation (random coil and α -helix). FTIR-ATR spectra of silk fibroin sponge also confirmed the presence of silk I and silk II structures. However, silk fibroin sponge showed high water solubility and the main structure was silk I (Figure 16).

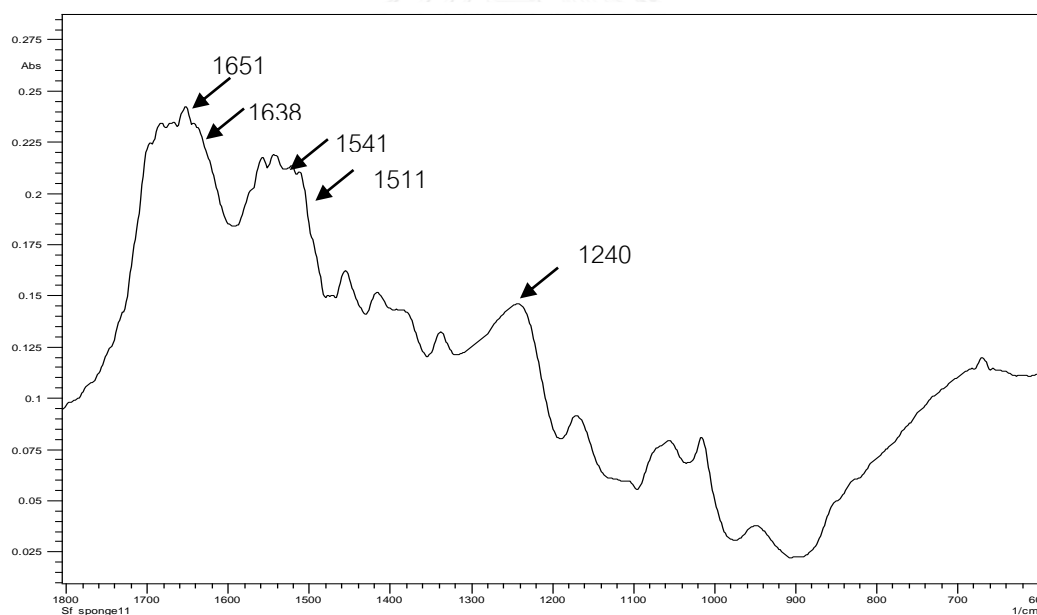


Figure 16 FTIR-ATR spectrum of silk fibroin sponges

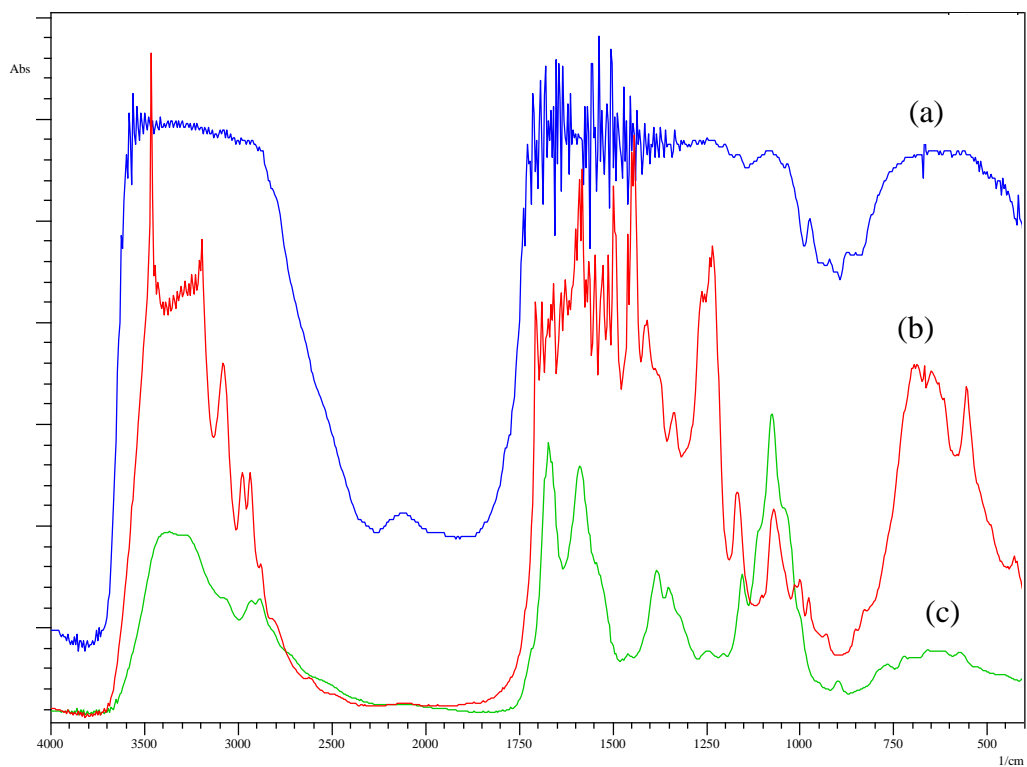


Figure 17 FTIR-ATR spectrum of (a) gelatin film, (b) silk fibroin film, and (c) chitosan film

Table 7 Summary specific spectrum band of silk fibroin film, gelatin film, and chitosan film from FTIR analysis

Frequency (cm ⁻¹)	Groups	silk fibroin film	gelatin film	chitosan film
3100-3600	ν_{OH} ν_{NH} amide A and free water, ν_{OH} amide B(ν_{CH} aromatic)	3288	3302	3247
2850-2960	ν_{CH} Symm/Asymm (alkane)	2935	2956	2936
1630-1660	ν_{CO} amide I(C=O)	1647	1649	1654
1540-1470	ν_{NH} amide II(- NH ₂)	1539	1541	1558
1446	CO ₃ ⁻² , pyrrolidine ring, ν_{CH} , CO ₃ ⁻²	1448	1450	1457
1325-1410	δ_{OH} , δ_{NH} , δ_{CH3}	1409	1406	1381
1204-1310	δ_{CH} , δ_{NH} amide III	1238	1242	1246
1167-1033	Pyranose cycle bone	1068/1103	1082/1165	1153
900-1150	Pyranose ring and amino groups	948	920/974	920
	= CO skeleton stretch			1072

Silk fibroin sponge and gelatin powder were dissolved in 98% formic acid and chitosan powder were dissolved in 90% formic acid and fabricated film for FTIR analysis. Figure 17 and Table7 showed FITR spectra of silk fibroin film, gelatin film, and chitosan film. A broad peak at 3100-3600 cm⁻¹ was assigned to the stretching vibration of N=H and O-H bond vibrations. The peaks at 1630-1660 cm⁻¹ and 1540-1470cm⁻¹ indicate C=O (amide I) and, NH₂ (amide II) stretching. Peaks 900 -1150 cm⁻¹ were assigned to the C₂ position of pyranose rings and amino groups, The position of

relevant peaks in the spectrum of chitosan film, silk fibroin film, and gelatin film were similar to those described by other authors [78, 79].because of the same protein structure compositions.

Part II: Fabrication of nanofiber barrier membranes from gelatin, chitosan, and silk fibroin by electrospinning technique

4.2 Effect of formic acid on morphology of nanofibers mats

Choice of solvent is a key factor for fabrication of electrospinning technique. Silk fibroin fiber does not dissolved in water, but silk fibroin sponge could dissolve in water after modifying with in co-solvent composed of CaCl_2 : $\text{CH}_3\text{CH}_2\text{OH}$: H_2O (1:2:8 in molar ratio) at 80°C . Gelatin dissolves in hot water. Chitosan dissolves in a mild acid solution such as 1-2% acetic acid[76]. Solvents, water and acetic acid, are not suitable for electrospun of silk fibroin, gelatin and chitosan.

In our study, we used formic acid to dissolve silk fibroin, gelation and chitosan to avoid phase separation. We found that 90% formic acid could dissolve chitosan. An addition of water in 98% formic acid had the potential to dissolve chitosan. Therefore, formic acid at 90% concentration was chosen to dissolve chitosan in this experiment. Silk fibroin/gelatin and chitosan dissolve in the same solvent to avoid phase separation. It could produce nanofiber by electrospinning. In the electrospinning process, an evaporation of solvent is necessary for fiber formation during ejection. Formic acid is a volatile organic solvent with high evaporation rate when it was ejected by electric force. During ejection, the polymer blend solution could rearrange its structure to form fiber. In this result, we found that formic acid could not degrade the structure of polymer blended solution. The stability of SF: G: C blended solution in formic acid was examined by SEM at different spinning time in Figure 18.

From Figure 18 (a) and (b), they showed that the SF: G: C (10:20:1) nanofiber could be generated uniformly in both storage times. The mean diameter of the electrospun nanofiber was (a) 39 ± 6.00 and (b) 36 ± 1.82 nanometers at 0 and 24 hours respectively. It can be observed that the fiber diameter is not significantly different after

prolonged storage time. As a consequence, it can be concluded that the morphology of SF: G: C blended fiber does not depend on storage times.

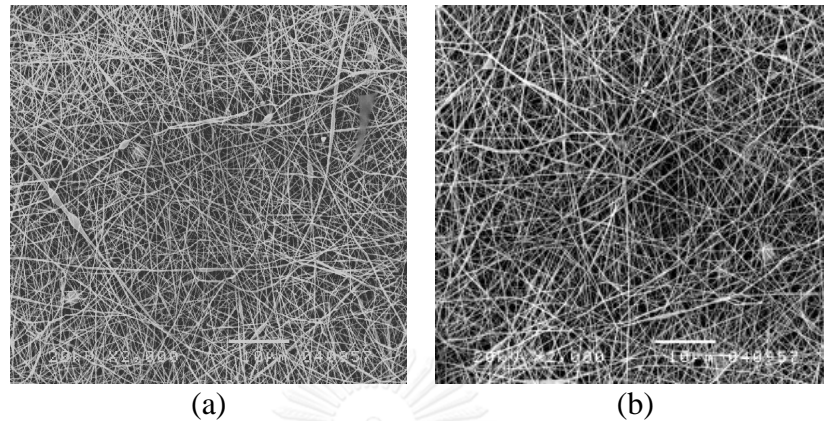


Figure 18 SEM images of electrospun SF: G: C (10:20:1) nanofiber by fixing the spinning distance at 15 cm under electric field at 20 kV and flow rate at 0.2 ml/h with storage time; (a) 0 hour and (b) 24 hours (Magnification x2, 000)

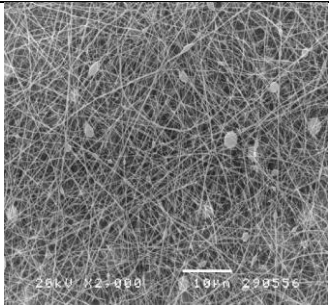
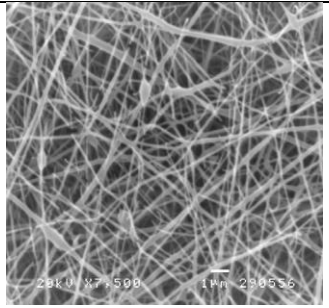
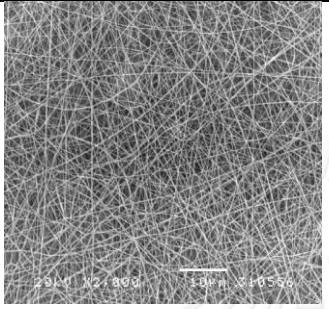
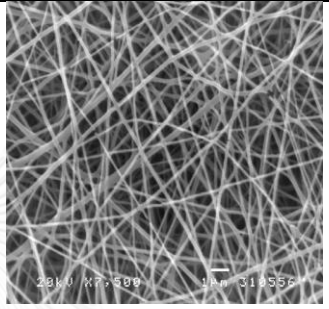
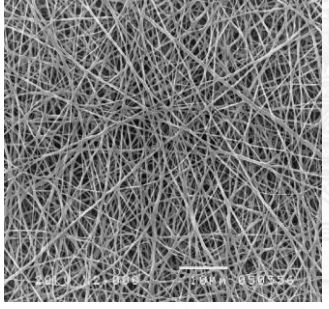
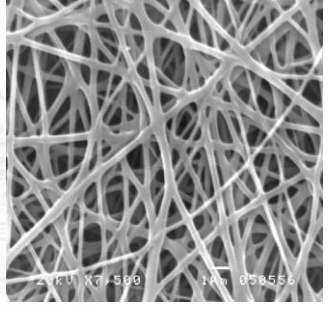
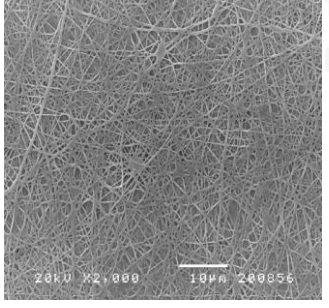
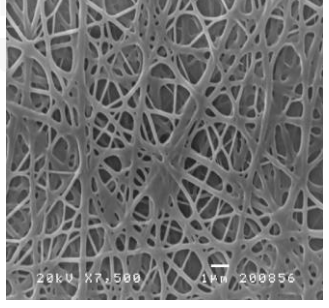
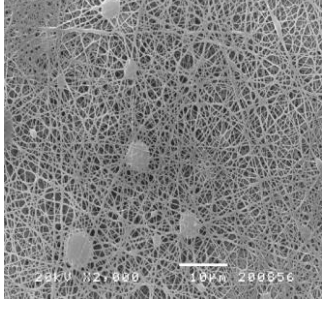
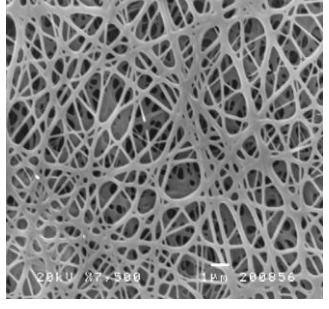
K-H. Kim et al (2005)[15] reported that formic acid at a concentration of 85%-98% could successfully dissolve silk fibroin sponges and the solution could be spun by an electrospinning process. Furthermore, gelatin could be dissolved in formic acid and obviously prepared nanofiber mats by electrospinning[32]. But chitosan could not be electrospun with a common solvent because it had three-dimensional networks of strong hydrogen bonds [65, 76]. Some researchers tried to produce fiber from chitosan by solvent mixing and blending with other materials [25, 80]. C.S Ki et al (2005) [31] found that gelatin could be used to produce gelatin nanofiber using formic acid as a solvent. Formic acid did not affect the structure of gelatin. Okhawili et al (2010)[62] studied silk fibroin/gelatin blended nanofiber mats by using formic acid. 98% formic acid could dissolve silk fibroin/gelatin blends 10/90, 20/80, 30/70, 40/60, 50/50, 60/40, 70/30, and 80/20 to nanofiber mats. The sizes of silk fibroin/gelatin fiber at various applied voltages were between 117-557 nanometers. Silk fibroin solution and chitosan in 2% acetic acid solution could not successfully blend because silk fibroin solution has a pH of 7, while chitosan solution had a pH of 4. Chitosan solution precipitated at near isoelectric pH because of the same quantity of the equivalent charges. When the pH of silk fibroin solution was adjusted to lower than 5, the phase separation did not appear

because silk fibroin solution formed gelation with a highly organized molecular structure. Under this condition, the pH values of silk fibroin/ chitosan solution were adjusted to avoid phase separation and to allow interactions between silk fibroin/chitosan structure with the carboxyl groups of silk fibroin[81]

4.3 Effect of polymer concentration on morphology of nanofibers

Polymer concentration is a key factor in improving to control the diameter of nanofiber produced from electrospinning. The SF: G: C blended solutions at ratio of (wt%:wt%:wt%) 20:0:0, 0:24:0, 10:20:0, 10:20:0.5, 10:20:1, 10:20:1.5, 10:20:2, and 20:10:1 were spun at electrical field of 10 kV and spinning distance of 10 cm at feeding rate 0.2ml/h, respectively. The morphology and fiber diameters of SF: G: C blends were displayed in Figure 19



SF: G: C (wt%:wt%:wt%)	Magnification		Fiber diameter
Concentration	2,000X	7,500X	(nm)
20:0:0			109±23.29
0:24:0			148±48.10
10:20:0			286±18.63
10:20:0.5			202±77.9
10:20:1			223± 84.7

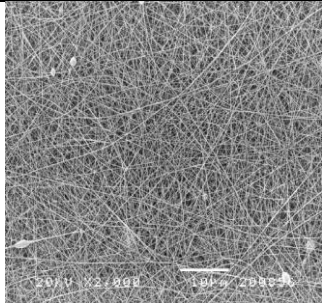
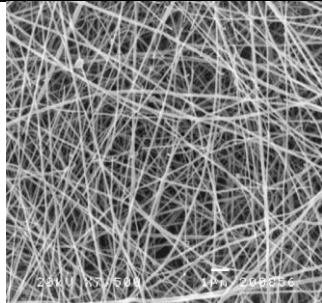
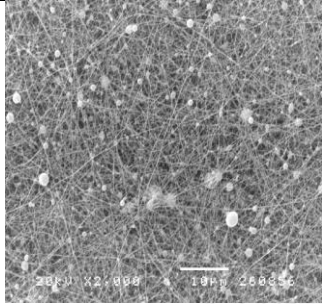
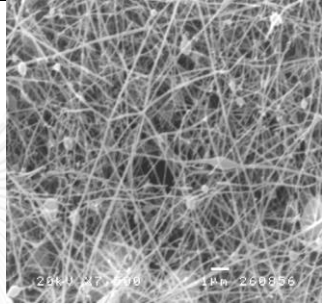
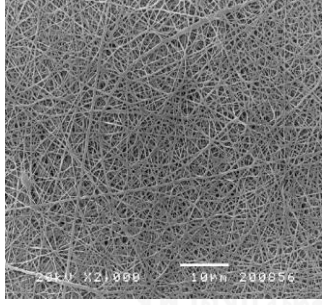
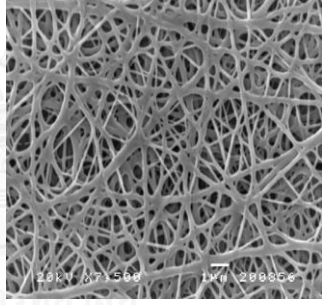
SF: G: C (wt%:wt%:ml)	Magnification		Fiber diameter (nm)
	2,000X	7,500X	
10:20:1.5			245 ± 102
10:20:2			102 ± 76.5
20:10:1			208 ± 81.40

Figure 19 SEM images of electrospun nanofiber SF:G:C at various ratios (wt%:wt%:wt%) of 20:0:0, 0:24:0, 10:20:0, 10:20:0.5, 10:20:1, 10:20:1.5, 10:20:2, and 20:10:1 respectively, with electric field of 10 kV, spinning distance of 10 cm and feeding rate of 0.2ml/h (Magnification x 2,000 and x 7,500)

Figure 19 shows the morphology and fiber diameter of SF: G: C blended nanofiber with different chitosan contents. In this work, the electrospinning process conditions was at electrical field of 10 kV, a spinning distance of 10 cm and feeding rate of 0.2ml/h. It was found that 20%w of SF and 20%w of G with 98% formic acid could be spun. On the other hand, chitosan could not be fabricate into nanofiber because of the three –dimensional networks of strong hydrogen bonds in the structure of chitosan. The blend solution of SF: G: C at a ratio of 10:20:0 was fabricated into

nanofiber at an electrical field of 10 kV, a spinning distance of 10 cm and a feeding rate of 0.2ml/h. The morphology of SF: G: C (10:20:0) nanofiber arranged randomly with 286 ± 18.63 nanometer diameter size. This result is in agreement with Okhawilai et al, 2010)[62]. They reported that the SF: G electrospun fiber was able to fabricate at the ratio 10:90 (162 ± 24 nm), 20:80 (280 ± 66 nm), 30:70 (258 ± 60 nm) and 40:60 (304 ± 65 nm) with an electrical field of 15 KV and a spinning distance of 20 cm. The results showed that SF: G in formic acid could be easy to fabricate nanofiber by electrospinning technique. However, 0.5, 1, 1.5, and 2 ml of chitosan solution was added into SF: G and the solution was electrospun into the average diameter of SF: G: C (10: 20: 0.5, 10: 20: 1, 10: 20: 1.5, and 10: 20: 2) were 202 ± 77.9 , 223 ± 84.7 , 245 ± 102 , and 102 ± 76.5 nm, respectively. The chitosan solution at 0.5, 1, 1.5 and 2 %w at were showed different the morphology. When 0.5 and 1 %w of chitosan solution were used, the fibers fused together because the electrical field and the distance were not appropriated for spinning condition. But when chitosan solution at 1.5 and 2 %w was used, the fibers did not fuse and short fiber appeared. It was successfully to fabricate the silk fibroin, gelatin and chitosan blend with formic acid by electrospinning technique.

In addition, the distributions of nanofiber diameter became narrow as exhibited in Figure 20. Because an ionizable amino group in chitosan resulted in the conductivity of the electrospun blended solution[38]. The aqueous solution of formic acid provided an electric charge, thus giving repulsion in SF: G: C blended solution during electrospinning. It is possible that a single jet of polymer blend solution might produce multiple filaments during charge repulsion. It appears that an increase in the amount of chitosan gives rise to the formation of short fiber and a reduction of fiber diameter[82].

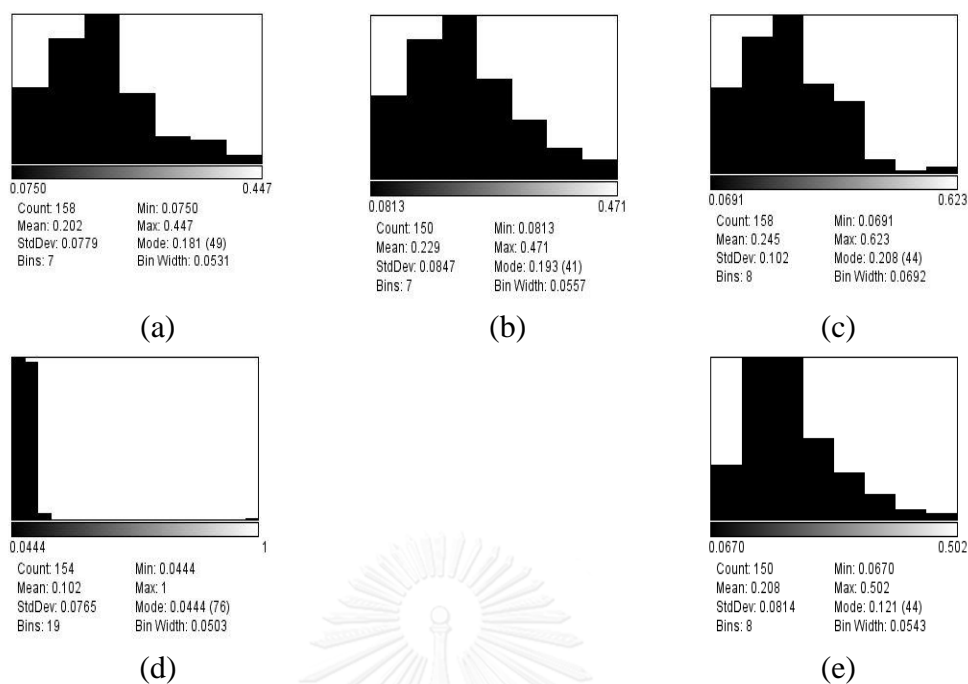


Figure 20 Diameter distributions of nanofibers at different compositions of SF: G: C in formic acid solution (SF: G: C, wt%: wt%: wt %) for (a) 10:20:0.5, (b) 10:20:1, (c) 10:20:1.5, (d) 10:20:2, and (e) 20: 10: 1

4.4 Effect of electrical field and spinning distance

10:20:1 of SF: G: C (wt%: wt%: wt%) blend solution of were used for spinning at spinning distances of 10 and 15 cm under electrical fields at 10, 15, and 20 kV and the morphology and fiber diameter of SF: G: C blended was shown in Figure 21 and Figure 22.

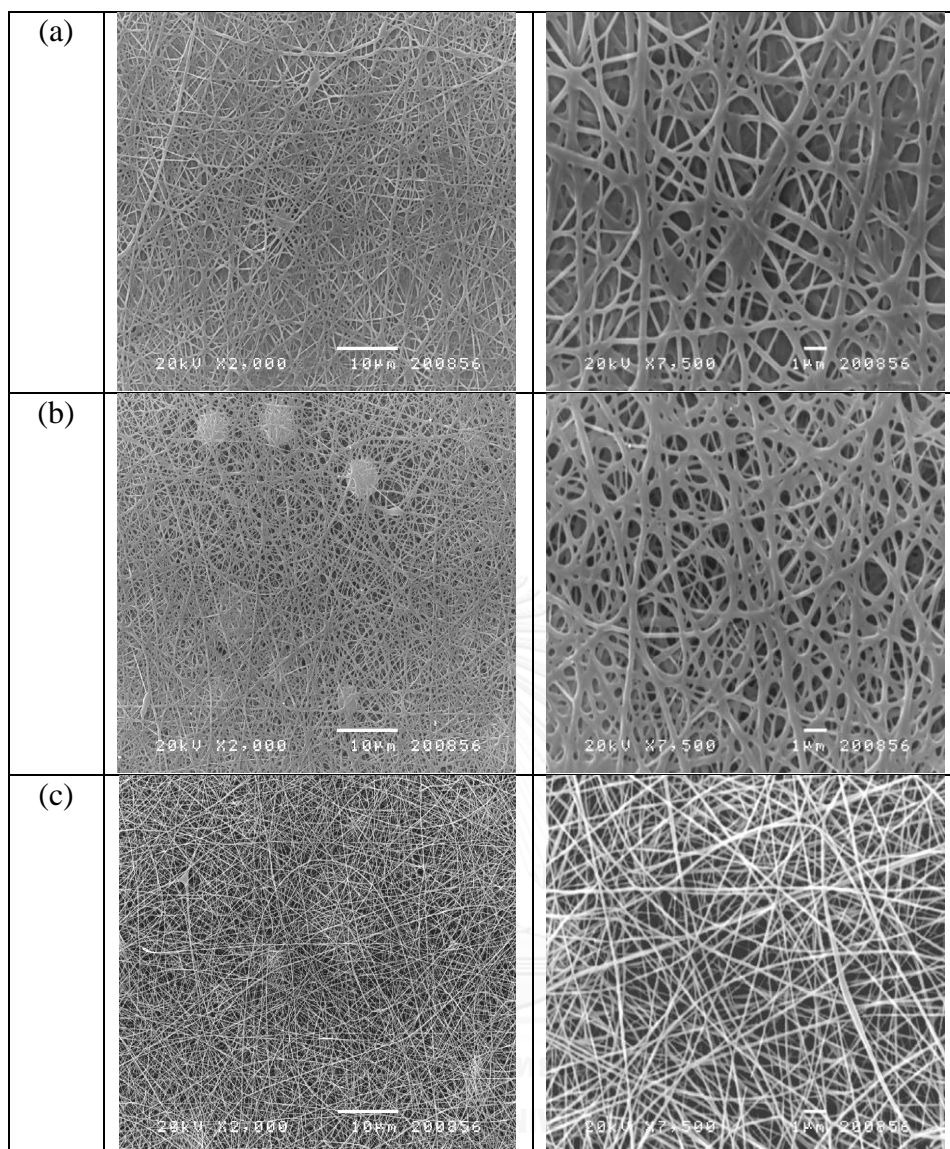


Figure 21 SEM images of electrospun SF: G: C blends (10wt%/20wt%/1wt %) at a spinning distance of 10 cm. and electrical fields of (a) 10 kV. (b) 15 kV. (c) 20 kV. (Magnification X2, 000 and X7, 500)

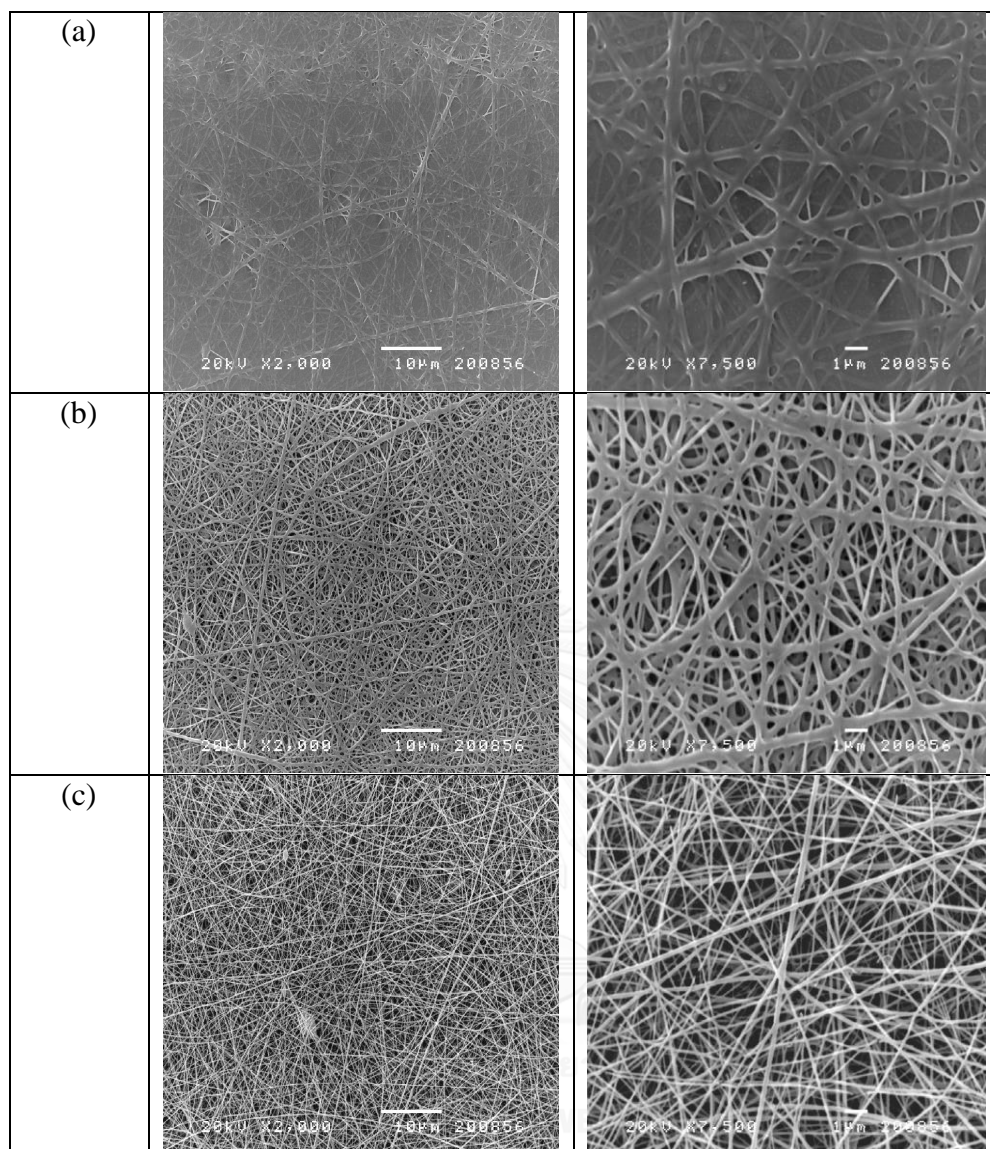


Figure 22 SEM images of electrospun SF: G: C (10wt%/20wt%/1wt%) at a spinning distance of 15 cm and electrical fields of (a) 10 kV. (b) 15 kV. (c) 20 kV. (Magnification x2, 000 and x7, 500)

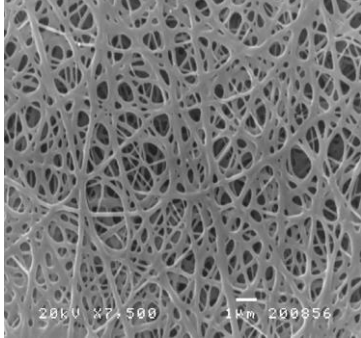
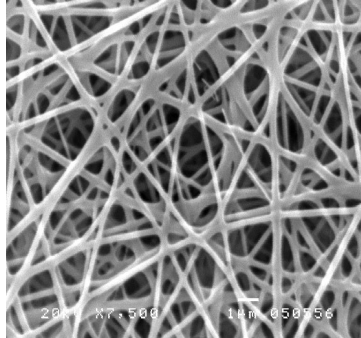
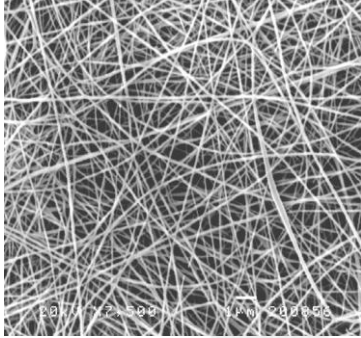
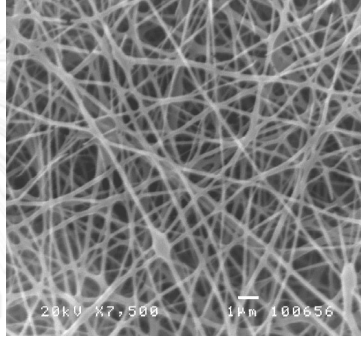
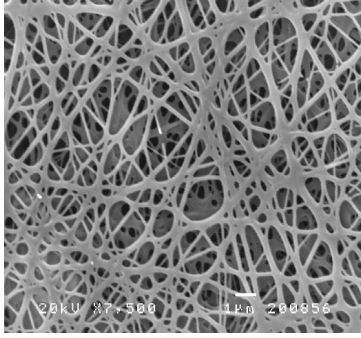
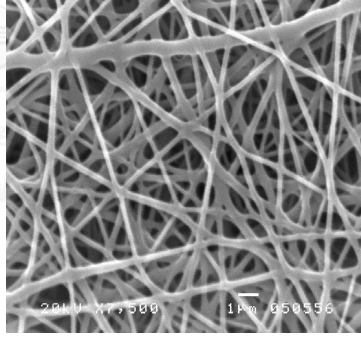
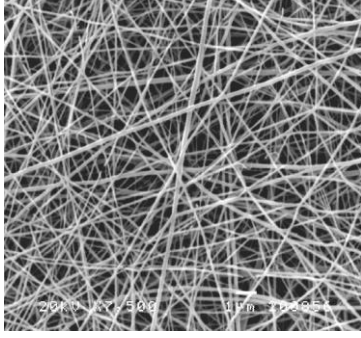
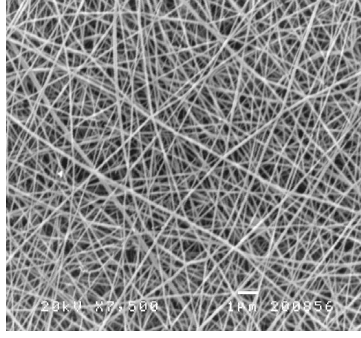
Voltage/Distance (kV/cm)	SF: G: C (wt%:wt%:wt%)	
	10:20:1	20:10:1
15/10		
20/10		
15/15		
20/15		

Figure 23 SEM images of electrospun SF: G: C (10:20:1) and (10:20:1) nanofiber by fixing the spinning distance at 10 and 15 cm and electrical fields at 15 and 20 kV, (Magnification x7, 500)

The morphology of fiber under the electric field of 10 kV at 10 and 15 cm distance showed fused “wet” flat ribbon-like fibers as shown in Figure 21 (a) and (b). Similar appearance also presented at 15 cm distance under the same electric field because the distance from the tip to the collector drum of solvent evaporation might not be appropriated as shown in Figure 22 (a) and (b). In the Figure 23, the composition of SF: G: C changed at 10: 20: 1 to 20: 10:1. The distance at 15 cm and electric 20 kV has uniformity fiber. When voltage and distance increased, fiber may less fused and melded together giving a smaller fiber diameter. An increase in the electric field and spinning distant had an influence on the average diameter of the nanofiber. This could be explained by high electric field induces stretching of the fiber. This condition needs to apply to long distance. According to this the surface area of fiber becomes small. This allows the solvent to evaporate rapidly, resulting in uniformity fiber.

The effects of concentration, solvent, electrical field and spinning distance were factor to fabrication of nanofiber mats from gelatin, chitosan, and silk fibroin by electrospinning technique. In this work, the SF: G: C (20:0:0, 0:24:0, 10:20:1, and 20:10:1) in formic acid of solvent at 20 kV of applied voltage and 15 cm of distance from the tip of needle to collector were obtained smooth and continuous fiber without beads.

Part III: Crosslinking of the barrier membranes

4.5 Morphological appearance of nanofiber mats before and after crosslinking

Method A: ethanol crosslinker

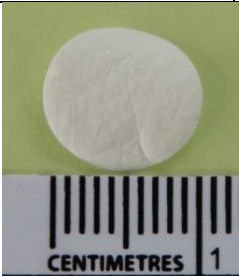











SF: G: C (wt%:wt%:wt%)	Appearance of nanofiber mats		
Concentration	Before ethanol exposure	After exposing in ethanol vapor	After exposing to ethanol and dipping in ethanol
20:0:0			
0:24:0			
10: 20:1			
20:10:1			

Figure 24 Digital photographs of nanofiber mats before and after crosslinking with ethanol

Figure 24 shows the appearance of nanofiber mats before and crosslinked with ethanol. After treatment with ethanol vapor, the appearance of nanofiber mats at various composition of SF: G: C did not change. The component of gelatin in nanofiber mats shrank all directions after dipping in ethanol. Generally gelatin is water soluble and water can immediately destroy nanofiber mats as shown in Figure 25 (a). However, gelatin could form a clear film after crosslinking with ethanol as shown in Figure 25 (b) and (c). The composition of silk fibroin in nanofiber mats became a clear film after dipping in distilled water (b, and c) as shown in Figure 24.



(a) Gelatin nanofiber mats after dipping in water

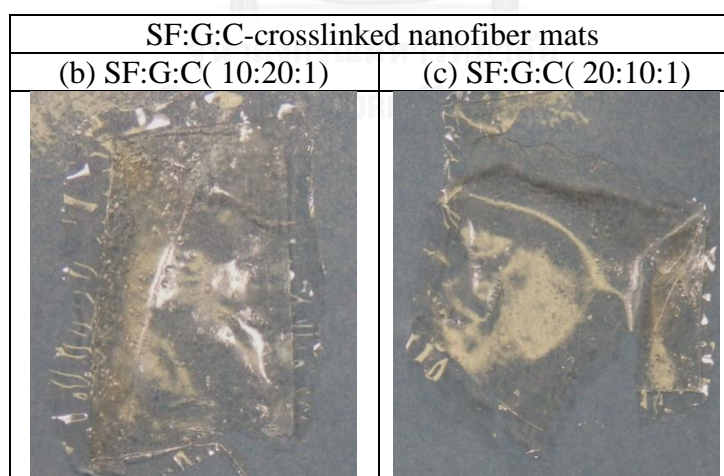


Figure 25 Digital photographs of (a) gelatin nanofiber mats of morphologies after dipping in distilled water, (b) SF: G: C nanofiber mats at (10:20:1), and (c) (20:10:1) after ethanol crosslinking



Figure 26 Weight loss and swelling of SF, G, and SF: G: C at 10:20:1 and 20:10:1 nanofiber mats after crosslinking with ethanol

Figure 26, shows that weight loss (%) of SF, G, and SF: G: C at 10:20:1 and 20:10:1 after crosslinking with ethanol increased with increasing the gelatin composition. It is speculated that during rinsing off the ethanol from the nanofiber mats, parts of gelatin were also removed, leading to high weight loss. The crosslinking method using ethanol vapor and ethanol solution was found to prevent high weight loss of the mats. The ethanol vapor allowed partially crosslinking gelatin molecules and then the ethanol dipping helped crosslinking the residual gelatin molecules. There was no report on weight loss and morphology change of the β - sheet conformation of silk fibroin after rinsing. In this research, it was found that silk fibroin nanofiber mats did not lose weight during rinsing. It might be that the random coil conformation of silk fibroin transforms to β -sheet after crosslinking [73, 83]. The results were consistent with the results that shown in Figure 24. SF: G: C at 10: 20: 1 showed high weight loss more than SF: G: C at 20: 10: 1 because of SF volume.

Method B: GA crosslinker



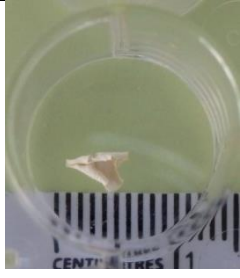


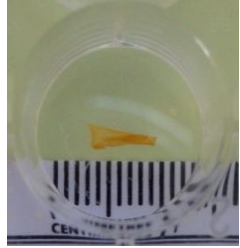

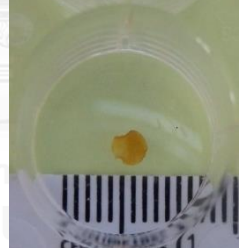
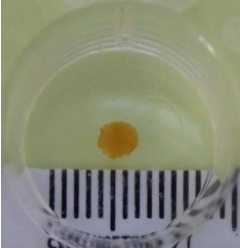



SF: G: C (wt%:wt%:wt%)	Appearance of nanofiber mats		
	Before GA exposure	After exposing in GA vapor	After exposing to GA and dipping in GA
20:0:0			
0:24:0			
10: 20:1			
20:10:1			

Figure 27 Digital photographs of nanofiber mats before and after crosslinking with GA

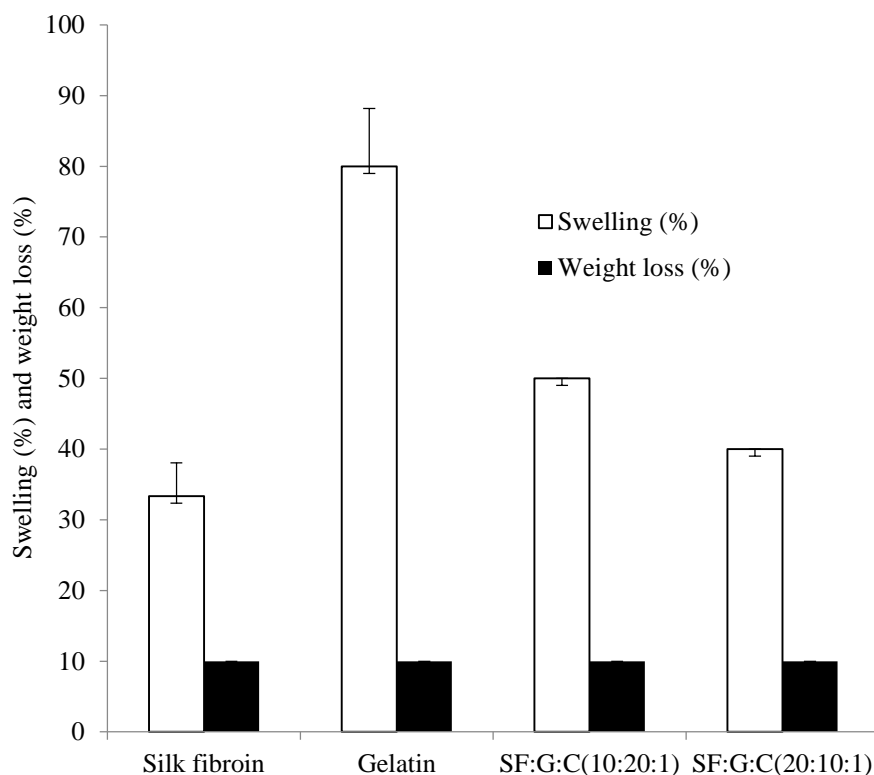


Figure 28 Weight loss and swelling of SF, G, and SF: G: C at 10:20:1 and 20:10:1 nanofiber mats after crosslinking with GA

Figure 27 shows the appearance of original nanofiber mats and the GA crosslinked nanofiber mats. After crosslinking, the color of SF nanofiber mats was opaque white while the G nanofiber mats became transparently yellow. The SF: G: C (10:20:1) was found to be a little darker yellow more than the SF: G: C (20:10:1). Results indicated that the amount of SF in the mats had effect on their color and appearance after the mats were crosslinked with GA. All nanofiber mats shrank all directions after crosslinking with GA. Aldehyde group (-CHO) on GA could react with amino groups of lysine residues of protein to form the $-C\equiv N$ group. The amino groups on gelatin were substituted totally by the quaternary ammonium salt groups and the residual amino groups might react with GA and formed the $-C\equiv N-$ group, a chromophore. Therefore, the color of crosslinked blend mats was discriminated by a slow change in color from white to yellow. The color change occurred because the cross-linkage ($CH\equiv N$) reaction

took place during the cross-linking process [84, 85]. Weight loss and swelling of SF, G, and SF: G: C at 10:20:1 and 20:10:1 after crosslinking with GA shown in Figure 28. It was found that crosslinked gelatin nanofiber mats swelled approximately at about 80% when gelatin content in SF: G: C blend nanofiber mats increased the swelling also increased. It was observe that shrinkage of the nanofiber mats occurred all directions after exposing to GA vapor. The crosslinking of nanofiber mats with GA might be completed during the vapor step. It also showed that all nanofiber mats had similar weight loss after crosslinking with GA.



Method C: EDC/NHS crosslinker



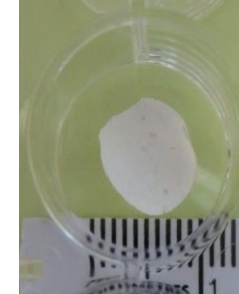

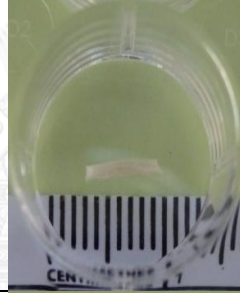

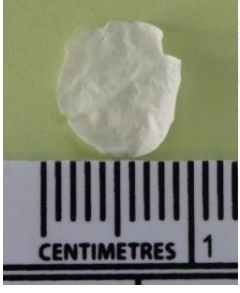





SF: G: C (wt%:wt%:wt%)	Appearance of nanofiber mats		
	Before EDC/NHS exposure	After exposing to EDC/NHS vapor	After exposing to EDC/NHS and dipping in EDC/NHS
20:0:0			
0:24:0			
10: 20:1			
20:10:1			

Figure 29 Digital photographs of the nanofiber mats of morphologies before and after crosslinking with EDC/NHS

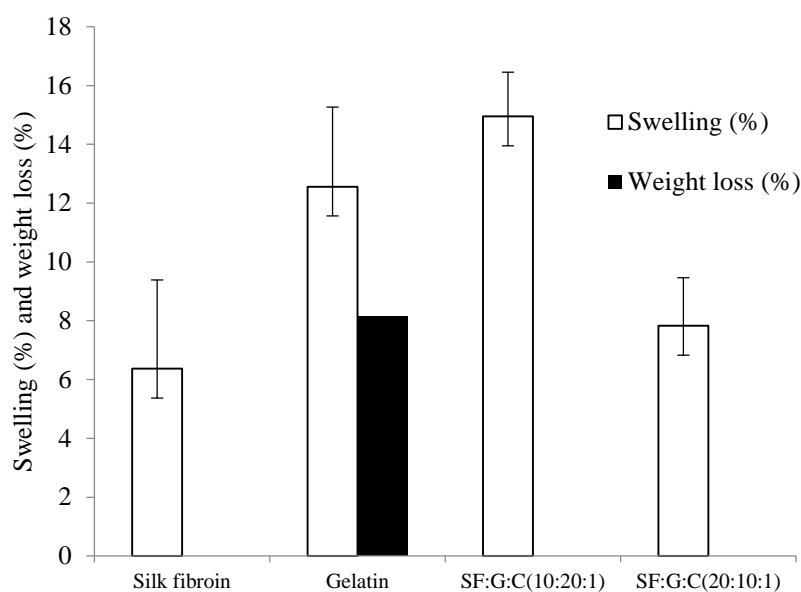


Figure 30 Weight loss and swelling of SF, G, and SF: G: C at 10:20:1 and 20:10:1 nanofiber mats after crosslinking with EDC/NHS

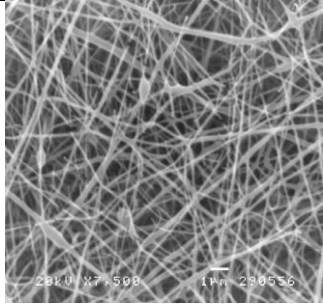
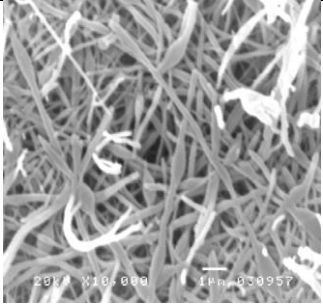
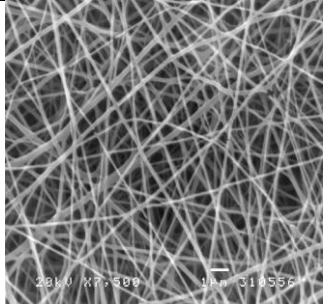
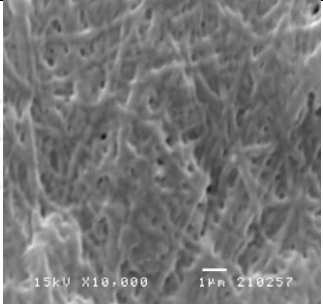
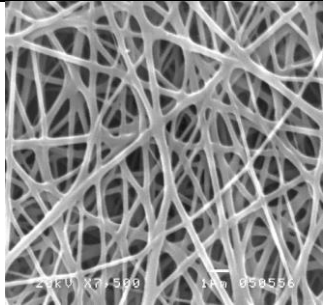
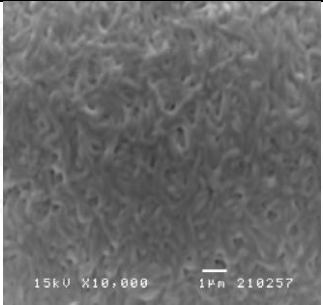
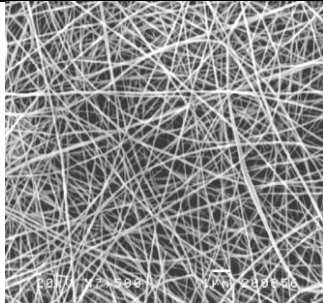
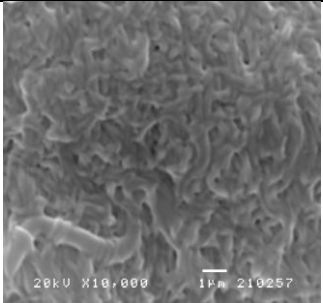
Figure 29 shows the appearance of original nanofiber mats and EDC/NHS-crosslinked nanofiber mats. Gelatin nanofiber mats shrank all directions after dipping in EDC/NHS and washing with water. Color and size of SF, and SF: G: C at 10:20:1 and 20:10:1 nanofiber mats did not change after crosslinking. The swelling of SF: G: C at 10: 20: 1 was higher than SF: G: C at 20: 10: 1 as shown in Figures 29 and 30. Weight loss of gelatin nanofiber mats took place after crosslinking but it was not found in nanofiber mats SF: G: C at 10: 20: 1 and 20: 10: 1. EDC/NHS solution was known as an ideal crosslinking for material containing amino and carboxyl groups due to its well control of crosslinking and low cytotoxicity[65].

EDC/NHS[86] produced optimum crosslinking degree for gelatin nanofiber membrane because carbodiimide could form intramolecular crosslink within a gelatin molecule or intermolecular crosslink between two adjacent gelatin molecules. The reaction between the ϵ -amino group and carboxylic acid groups by carbodiimide could weaken the protonation, so that the water absorption ability of gelatin membrane declined after crosslinking[86]. Then, the higher in the carboxyl groups led to the higher crosslinking degree, especially for the crosslinking with EDC/NHS[69]. In our study,

crosslinking the mats with vapor EDC/NHS solution protected the mats from weight loss. The EDC/NHS vapor onto nanofiber mats allowed the partially crosslinking amino and carboxyl groups and then the dipping in EDC/NHS was to crosslinking the residue amino and carboxyl groups. There was no report on weight loss and morphology change of the β - sheet crystal conformation of silk fibroin. It was found in this result that did not lose weight after crosslinking might be that the random coil conformation transforms to β -sheet after crosslinking.



4.6 Morphology of nanofibers crosslinked with EDC/NHS

SF: G: C (wt%:wt%:wt%)	Magnification	
	Before crosslinking (x7,500)	after crosslinking (x10,000)
20:0:0		
0:24:0		
10:20:0		
10:20:1		

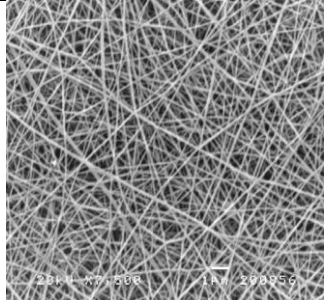
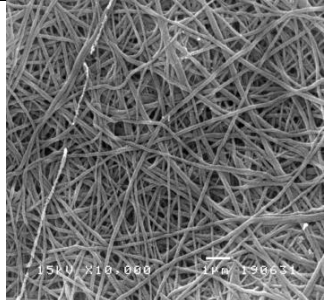
SF: G: C (wt%:wt%:ml)	Magnification	
Concentration	Before crosslinking (x7,500)	after crosslinking (x10,000)
20:10:1		

Figure 31 SEM images of electrospun SF, G, SF: G: C (10:20:1) and (20:10:1) nanofiber mats before crosslinking (Magnification x7,500) and after crosslinking with EDC/NHS (Magnification x10,000)



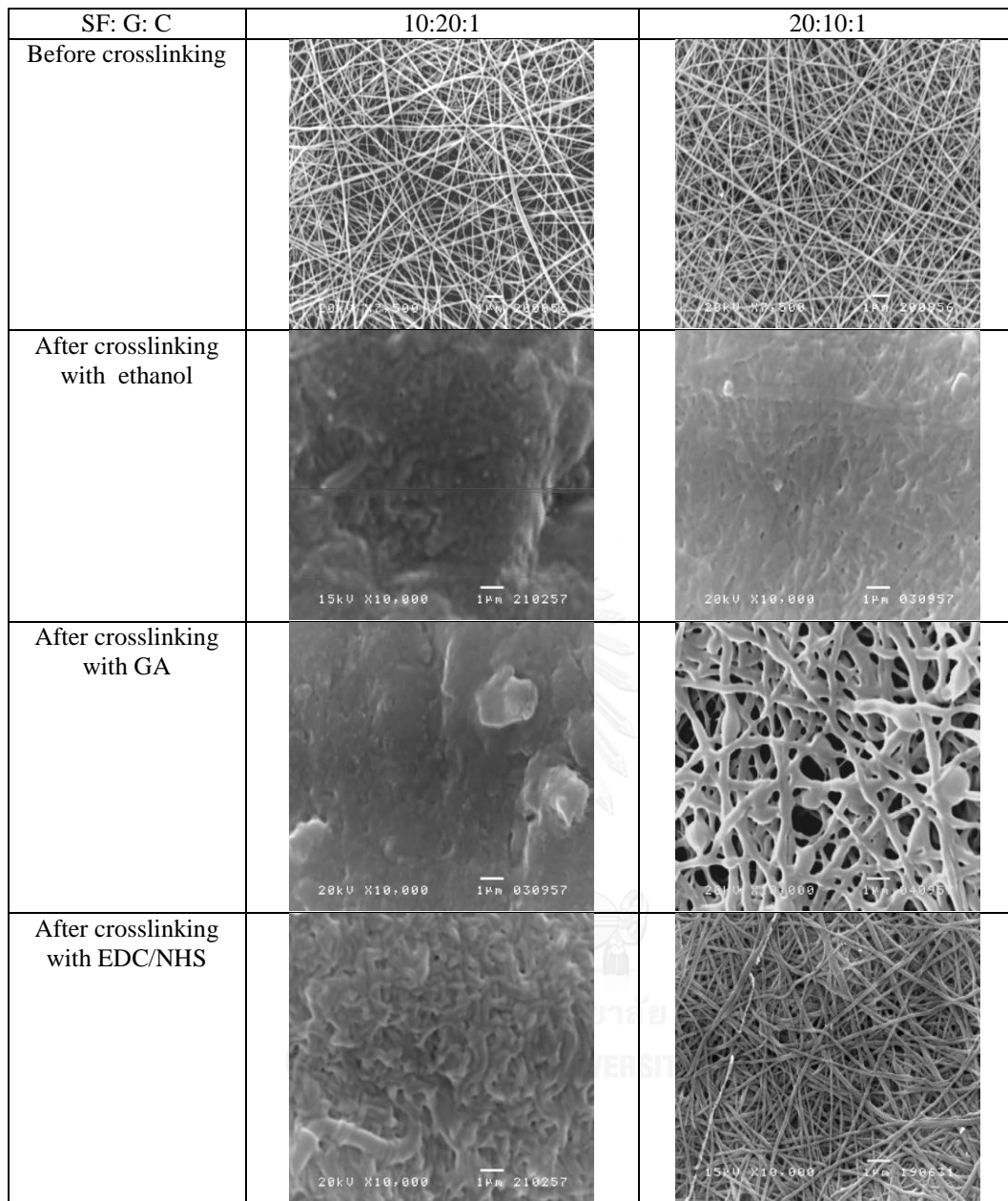


Figure 32 SEM images of nanofiber mats SF: G: C (wt%:wt%:wt%) 10:20:1 and 20:10:1 before and after crosslinking with various crosslinkers

Figure 31 shows morphology of SF: G: C nanofiber mats before and after crosslinking with EDC/NHS. Results indicated that crosslinked SF: G: C (10:20:1) nanofiber mats swelled more than crosslinked SF: G: C (20:10:1). It was obviously noticed that SF: G: C nanofiber mats containing high gelatin content showed fused fibers and less porous structure after crosslinking. The swelling and weight loss of the

SF: G: C (20:10:1) and SF: G: C (10:20:1) nanofiber mats crosslinked with ethanol, GA, and EDC/NHS were shown in Figure 26, 28, and 30. Morphology of SF: G: C (20:10:1) nanofiber mats crosslinked with EDC/NHS was more close to that before crosslinking than other crosslinked mats (Figure 32). Therefore, EDC/NHS-crosslinked SF: G: C (20:10:1) nanofiber mats were selected for further biological testing.

4.7 Air permeability

Air permeability of nanofiber mats was determined using oxygen permeability tester, (Illinois 8000, Germany). Nanofiber mats were cut into a circular shape with 6 mm in diameter and was placed into a sample holder. The test was conducted at 25 °C, 100 %RH. At least 3 samples were tested and averaged results were reported.

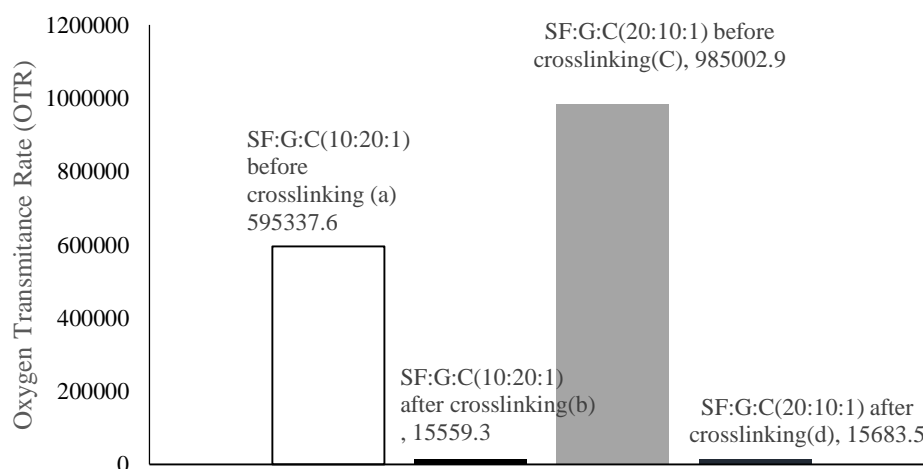


Figure 33 Air permeability of nanofiber mats (a) SF: G: C (10:20:1) before crosslinking, (b) SF: G: C (10:20:1) after crosslinking, (c) SF: G: C (20:10:1) before crosslinking, and (d) SF: G: C (20:10:1) after crosslinking with EDC/NHS

Figure 33 compared oxygen transmittance rates of SF: G: C (10:20:1 and 20:10:1) nanofiber mats before and after crosslinking with EDC/NHS. Before crosslinking, SF: G: C (10:20:1 and 20: 10:1) nanofiber mats had significant higher oxygen transmittance rate more than those after crosslinking. The uncrosslinking nanofiber mats may be caused by laceration during test because the test uses 100% relative humidity. These results indicated that the crosslinking process increased the

network density of nanofiber mats. This could be concluded that the conformation of random coil and α -helix in SF, G and C structure were transformed into β -sheet structure conformation after crosslinking. These results are consistent with the results depicted by X-Ray Diffraction.

4.8 X-Ray Diffraction (XRD) analysis

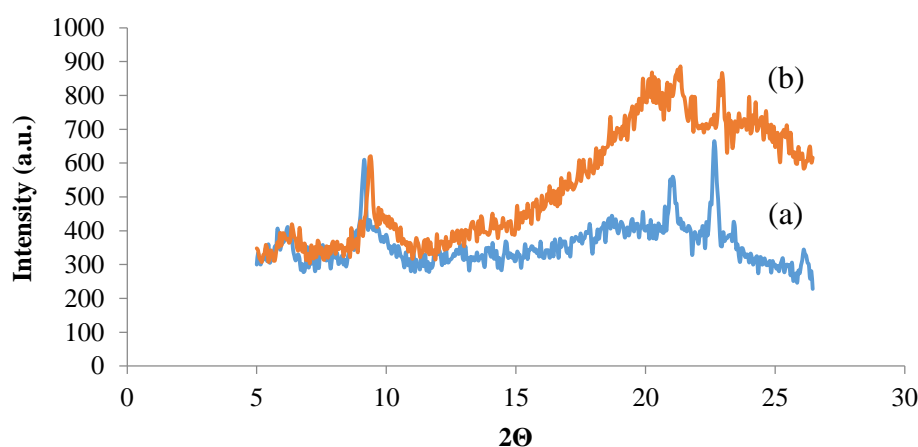


Figure 34 XRD of (a) gelatin nanofiber mats and (b) silk fibroin nanofiber mats

XRD patterns of gelatin and silk fibroin nanofiber mats in Figure 34 showed broad diffraction peaks at $2\theta = 9-10^\circ$ and $20-20.5^\circ$. While in Table 8, their crystalline index of 12% of gelatin nanofiber mats and 36% of silk fibroin nanofiber mats were shown respectively. Results indicated that silk fibroin nanofiber mats could resist to water before and after crosslinking as present at Figure 26, 28, and 30.

Robert, L and co-worker[74] presented the pattern of arrangement of silk fibroin. Glycine- Arginine- Glycine-Tyrosine (GAGT) is amorphous and Glycine- Arginine- Glycine- Arginine- Glycine- Serine- Glycine- Arginine- Glycine- Arginine- Glycine- Serine (GAGAGSGAGAGS) is crystallite in silk fibroin structure. For electrospinning technique, it was found that during a polymer solution was ejected between the needle and the collector, the solvent rapidly evaporated. The strong electric fields forces molecular chain to rearrange structure. The crystalline structures occurred on partial molecular chain.

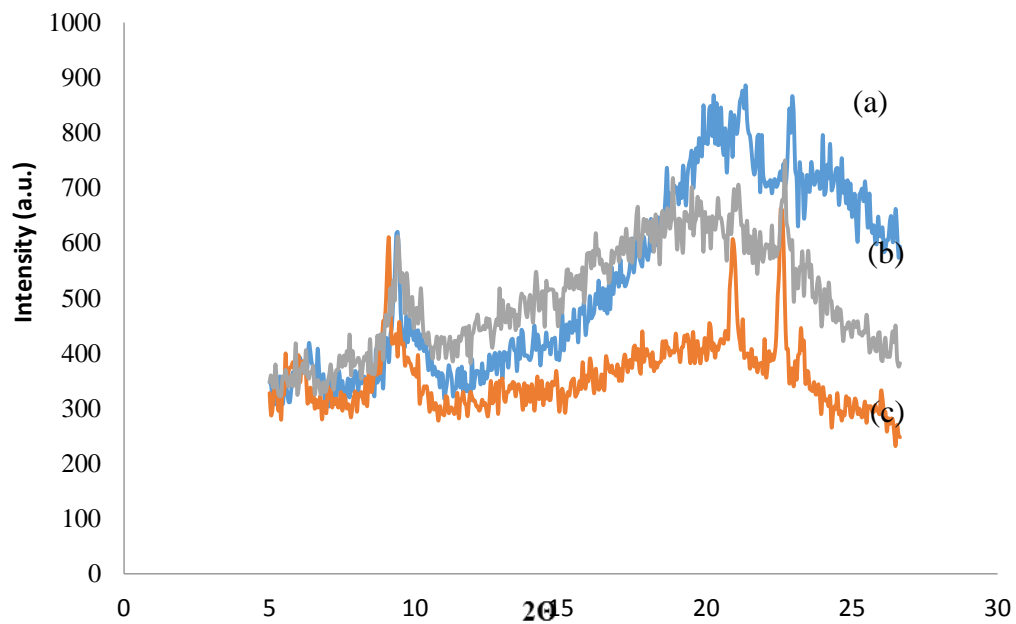


Figure 35 XRD of electrospun nanofiber mats of (a) silk fibroin nanofiber mats, (b) SF: G: C (20:10:1), and (c) SF: G: C (10:20:1) before crosslinking

XRD of (a) silk fibroin nanofiber mats, (b) SF: G: C (20:10:1), and (c) SF: G: C (10:20:1) before crosslinking were confirmed clearly structure. Table 8 present crystalline index at 36% of silk fibroin nanofiber mats, 10% of SF: G: C (20:10:1), and 5% of SF: G: C (10:20:1), respectively. Silk fibroin nanofiber mats have crystalline structures higher than polymer blended nanofiber mats (SF: G: C (20:10:1), and SF: G: C (10:20:1)). Silk fibroin are important of the main of structure of crystalline. In this result, it was cohere with the results of weight loss and swelling (Figure 26, 28, and 30).

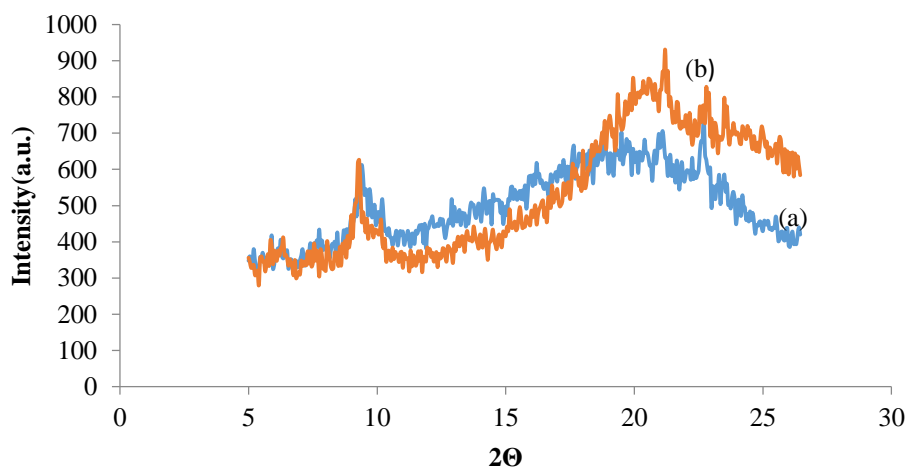


Figure 36 XRD diffraction peaks of SF: G: C of (a) 20:10:1 before crosslinking and (b) after crosslinking with EDC/NHS

Figure 36 shows XRD of SF: G: C of (a) 20:10:1 before crosslinking and (b) after crosslinking with EDC/NHS. Table 8 present crystalline index at 10% of 20:10:1 before crosslinking and 26% of after crosslinking with EDC/NHS, respectively. Results emphasized that the crosslinking process was increased the crystalline in the molecular structure of nanofiber mats.

Table 8 Crystallinity index obtained for SF, G, and SF: G: C nanofiber mats

Sample	$C_r I$ (%)
Gelatin nanofiber mats	12
Silk fibroin nanofiber mats	36
SF: G: C (10:20:1) nanofiber mats uncrosslinking	5
SF: G: C (20:10:1) nanofiber mats uncrosslinking	10
SF: G: C (20:10:1) nanofiber mats crosslinking	26

4.9 Mechanical property analysis

The average tensile strength and elongation at break of the electrospun SF, G and SF: G: C blended nanofiber membranes are shown in Table 9.

Table 9 Tensile strength and elongation at break of the nanofiber electrospun membranes from SF, G and SF: G: C blends solution at different concentrations

Sample	SF (wt %)	G (wt %)	SF: G: C (wt%/wt%/wt%)		
Concentration	20	24	10:20:1.0	20:10:1.0	10:20:1.5
Average tensile strength (MPa)	4.96±1.46	8.60±3.83	5.48±0.72	4.04±1.08	5.23±0.62
Average elongation at break	9.46±4.54	11.46±2.08	13.51±2.22	6.53±2.19	22.71±6.34

The appearances of silk fibroin nanofiber mats were more cracker than gelatin nanofiber mats. As can be seen from Table 9, tensile strength and elongation at break of SF was lower than those of G. The SF: G: C 10:20:1.0 was 13.51±2.22 at elongation at break, but SF content of 20:10:1.0 was increasing by reducing G concentration. The result showed 6.53±2.19 at elongation at break. As the concentration of gelatin have affected the tensile strength and elongation at break of mats increasing. For the sample with a condition SF: G: G of 10:20:1.0 and 10:20:1.5, it found that the tensile strength of both conditions were negligible different. It can also observe that the fiber diameter of 10:20:1.0 was smaller than that from 10:20:1.5. The difference of elongation at break would result from the diameter of the fiber. A small degree of fiber diameter will have a lower ratio of area to volume. According to this, the fiber with finer diameter would be stretched longer. The all component of nanofiber mats became more brittle and crispy than original nanofiber mats after crosslinking with ethanol, GA, and EDC/NHS. There cannot prepare the sample for tensile strength testing. However, the crosslinked samples are being made to weaken causes the water in the biology test before using in part IV.

The results were shown the suitable crosslinking method of SF, G, and SF: G: C nanofiber mats by placing into a desiccator filled with saturated crosslinking agent

vapor, the nanofibers could be reasonable crosslinking. The dipping in crosslinking agent again could be increased crosslinking in molecular structure of nanofiber mats.

The weight loss, swelling, and oxygen permeability of SF, G, and SF: G: C nanofiber mats were decrease after crosslinking.

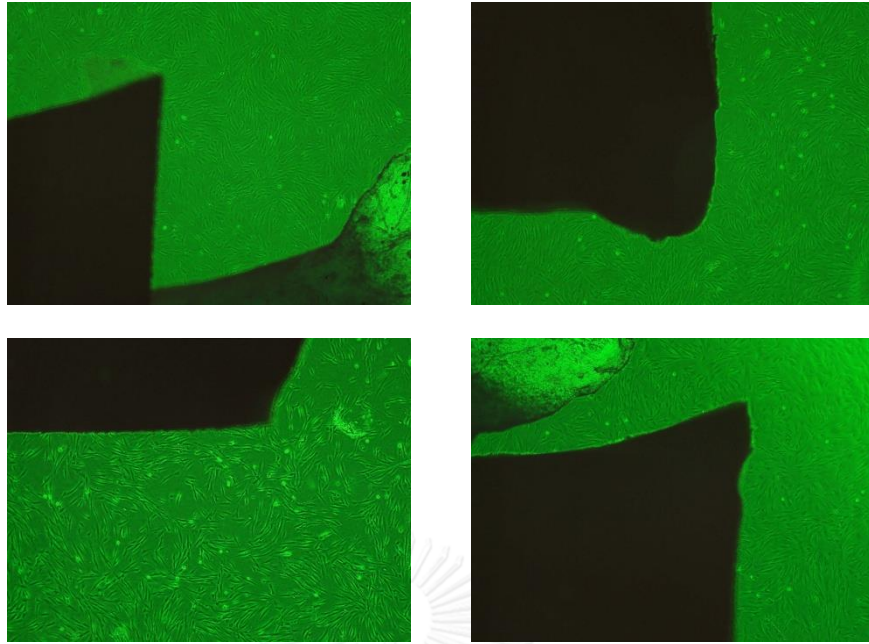
EDC/NHS crosslinking agent was suitable for crosslinking of SF, G, and SF: G: C nanofiber mats. The SF: G: C (20:10:1) nanofiber mats after crosslinking with the EDC/NHS was chosen for biology test in part IV.

Part IV Biological characterization of the membrane

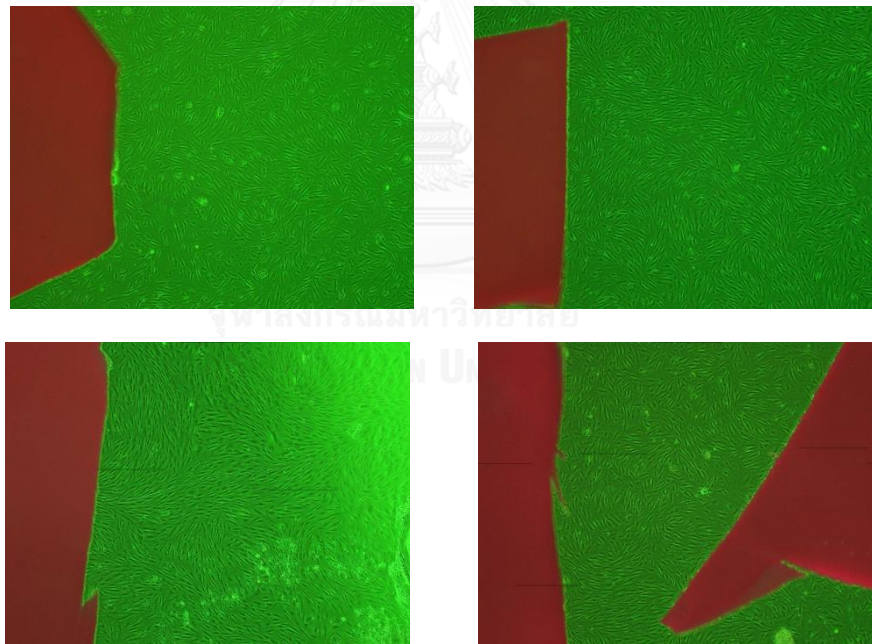
All the samples were cut into a rectangular shape, size 0.7 x 0.5 cm² and soaked in PBS, then immersed in DMEM with 5% antibiotics-antimycotics solution for 1 hour and washed with simple DMEM twice before testing.

4.10 In vitro studies: cellular response to the nanofiber barrier membranes

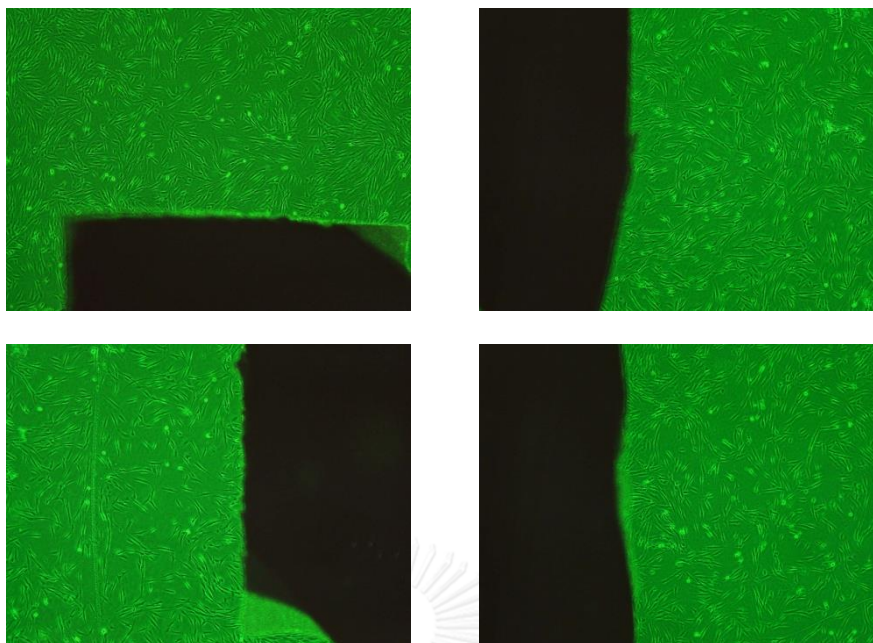
Normal human gingival fibroblasts were prepared from healthy gingival tissues from three patients. The explants were observed under the inverted microscope daily. When the populations of cells reach high density, the subculture was repeated as described above. With this method of selective attachment of the cells, clone of fibroblasts could establish approximately at the 5th passage. In this study, cells from the fifth passage were used in the study the response of fibroblasts to the membrane



The first patient



The second patient



The third patient

Figure 37 Normal human gingival fibroblasts of three patients by the inverted microscope

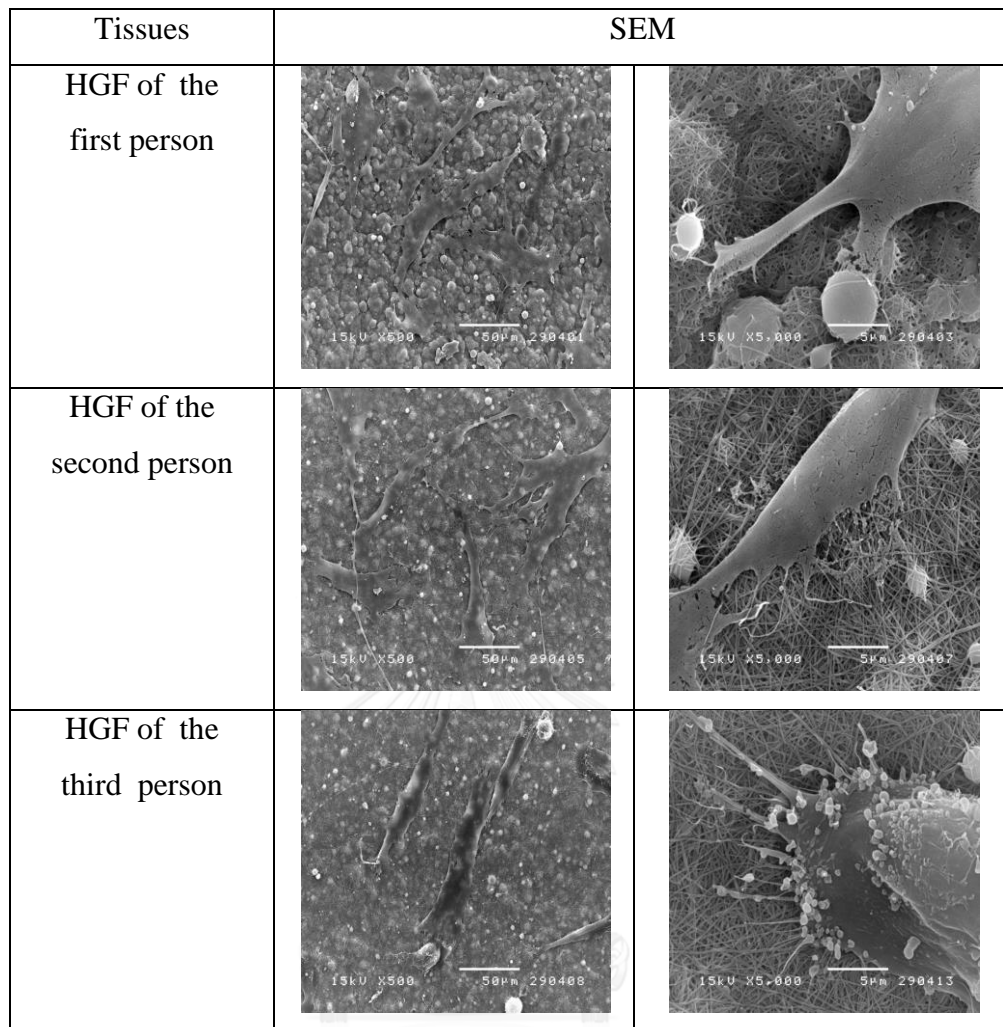


Figure 38 SEM images of HGF on EDC/NHS- crosslinked nanofiber mats at SF: G: C (20:10:1) (Magnification x500 and x5, 000)

The different HGF from three persons was seeded on SF: G: C of 20:10:1 nanofiber mat after 24 hours were investigated with inverted microscope and SEM as shown in Figure 37. HGF from three persons were responded to EDC/NHS- crosslinked nanofiber mats as shown in Figure 38. The migration of cells inside EDC/NHS- crosslinked nanofiber mats obviously shown in SEM. It can be found that cells of the different persons were attached to the surface EDC/NHS- crosslinked nanofiber mats. EDC/NHS- crosslinked nanofiber mats was biocompatible and non-cytotoxic.

4.11 The membrane permeability study

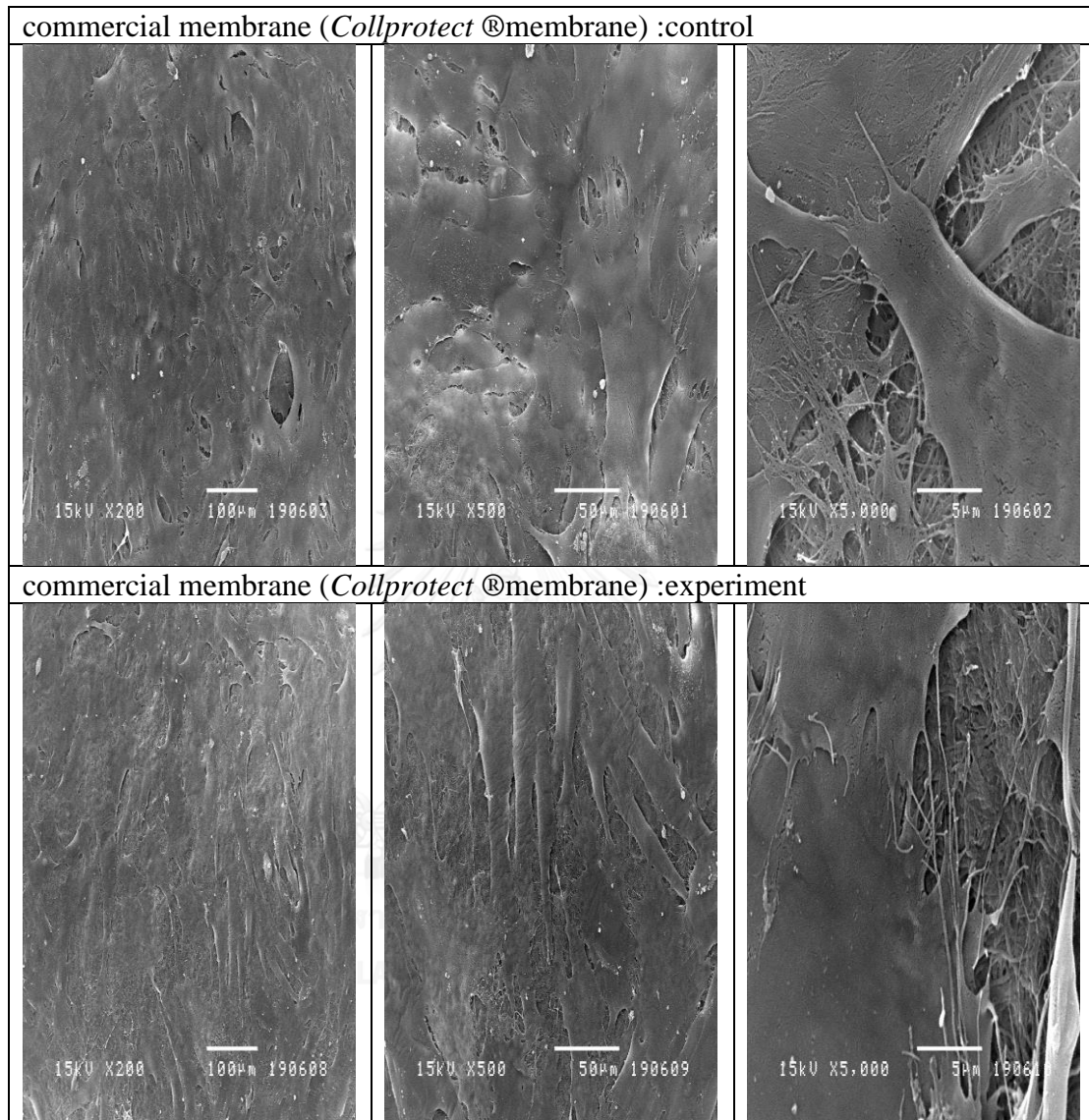
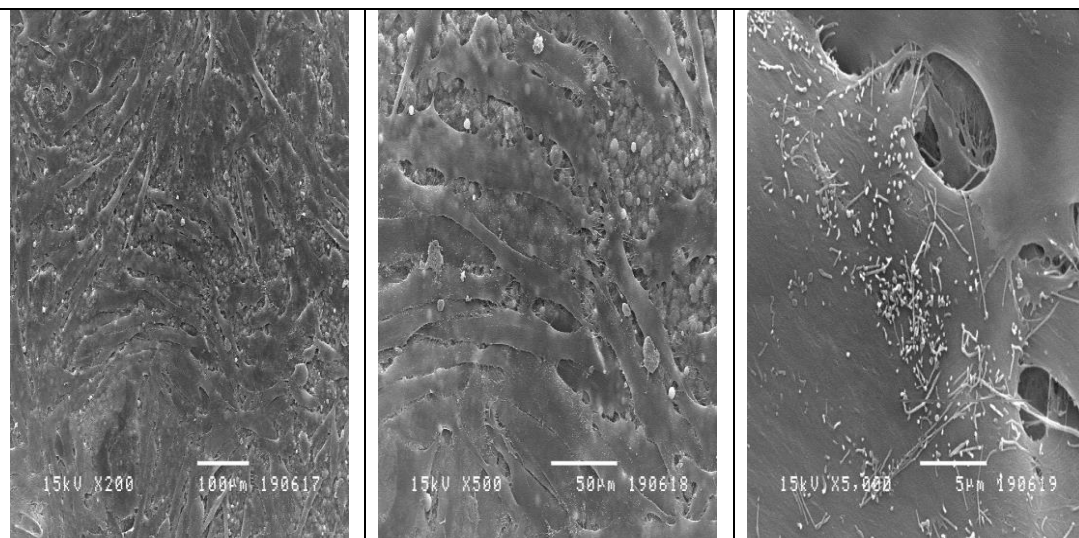
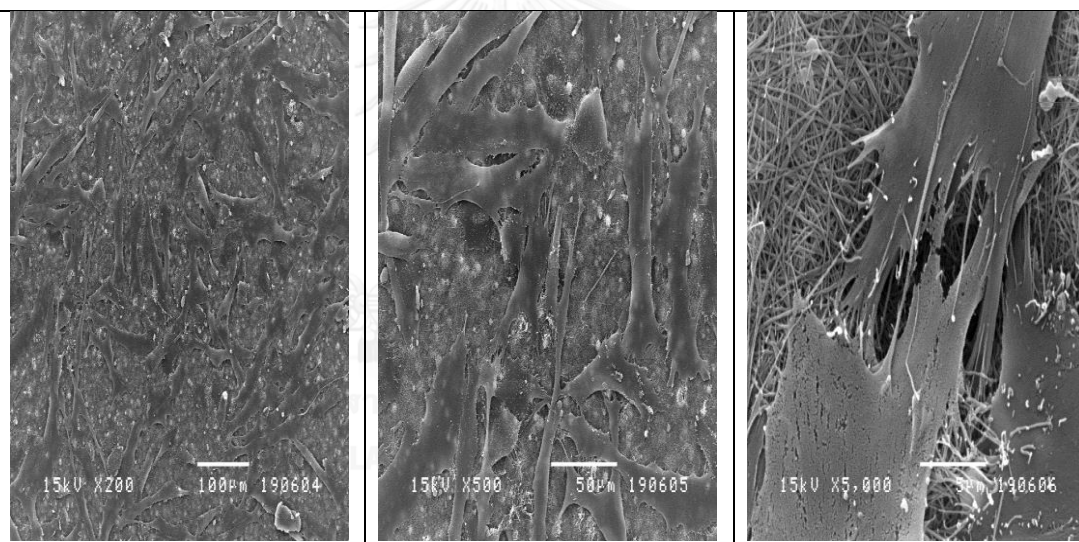


Figure 39 SEM images of HGF on commercial membrane (*Collprotect* ® membrane) (Magnification x200, x500 and x5,000)

EDC/NHS- crosslinked nanofiber mats at SF:G:C(20:10:1): Control

EDC/NHS- crosslinked nanofiber mats at SF:G:C(20:10:1): experiment 1st

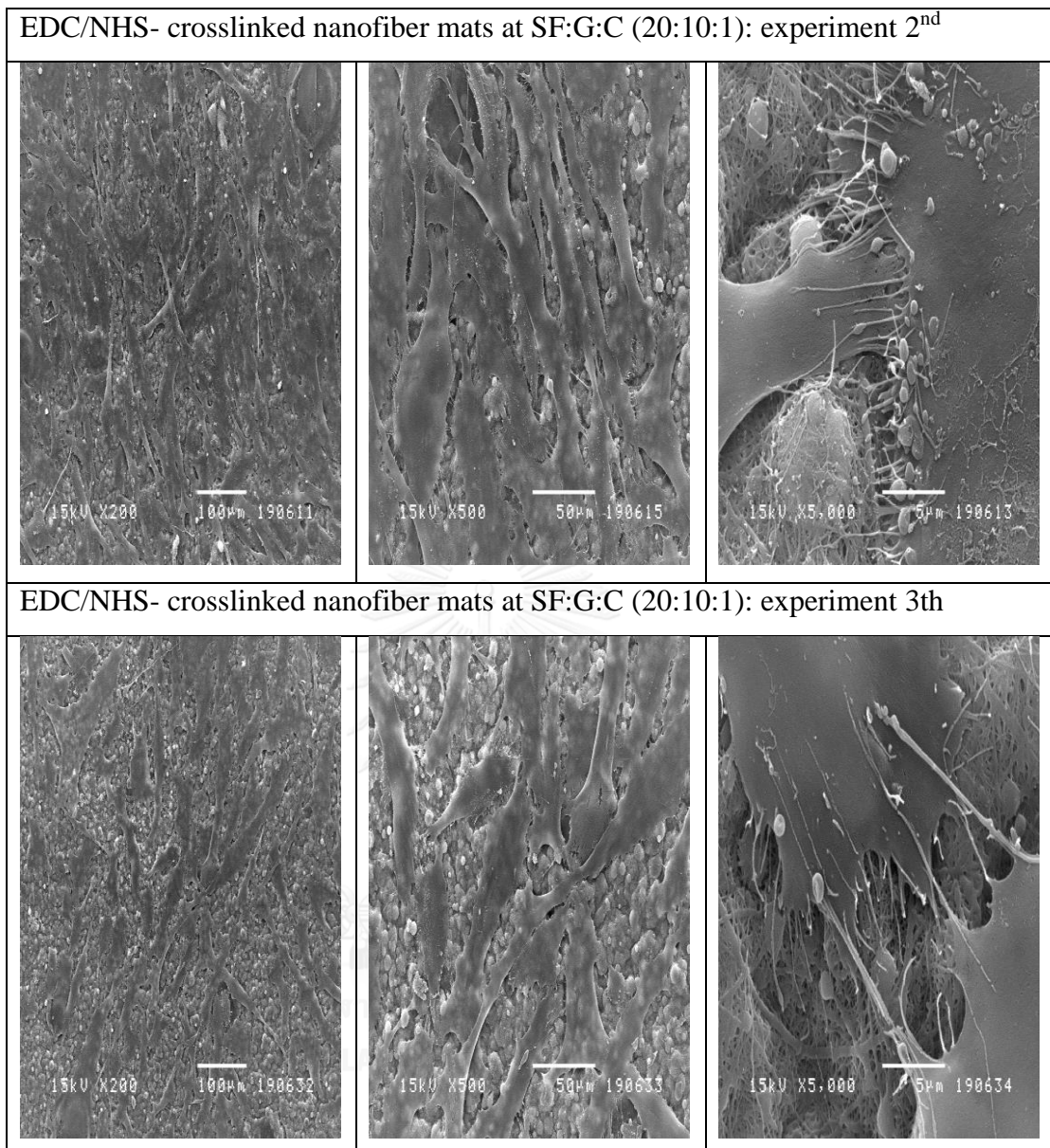


Figure 40 SEM images of HGF 1st, 2nd, and 3th on EDC/NHS- crosslinked nanofiber mats at SF: G: C (20:10:1) (Magnification x 200, x500 and x5,000)

In this study, we wanted to compare EDC/NHS- crosslinked nanofiber mats and the commercial membrane of collagen membrane (*Collprotect*® membrane) by evaluating the development of growth cells. After 72 hours of cell seeding on commercial membrane at control and experiment, the cells were spread on surface more than EDC/NHS- crosslinked nanofiber mats (Figure 39 and 40). However, EDC/NHS- crosslinked nanofiber mats at control and experiment could support the cells spreading

and attach the cell spread on the surface thus indicating that EDC/NHS- crosslinked nanofiber mats have a potential of barrier membrane.

4.12 Cost of materials and membranes

Table 10 Cost of collagen, silk, gelatin, and chitosan

Materials	Approximate cost (per unit)
Silk cocoon	270 baht/kg
Gelatin (lab grade)	2,500 baht/kg
Chitosan	300 baht/kg
Collagen (food grade)	35,000 baht/kg

Collagen as raw material for medical application such as skin substitutes and barrier membrane was widely used. The collagen was more relatively expensive than those materials as comparison in Table 10. For the first aim of this study was to using the natural materials in the Thailand. Our results showed silk fibroin, gelatin, and chitosan properties could be used instead of the collagen without the limiting of cell response. Silk fibroin, gelatin, chitosan could be developed for biomaterial application.

Table 11 Cost of SF, G and C in membrane fabrication by the electrospinning technique (15x20 mm)²

Materials	Cost of SF:G:C (baht/kg)	Cost of EDC/NHS- crosslinked nanofiber mats(200x300 mm) ² (baht/sheet)	Cost of <i>Collprotect</i> ® membrane (15x20 mm) ² (baht/sheet)
SF:G:C(20:10:1) (wt%:wt%:wt%)	88	300 (1.875 baht @ 15x20 mm) ²	
<i>Collprotect</i> ® membrane			3,500

Table 11 illustrated the approximated cost of EDC/NHS- crosslinked nanofiber mats by the electrospinning technique. The cost of commercial membrane, collagen membrane (*Collprotect*® membrane) per sheet (15x20 mm²) was approximated 3,500

baht. The costs of EDC/NHS- crosslinked nanofiber mats were cheaper than the costs of *Collprotect*® membrane at the same size. The EDC/NHS- crosslinked nanofiber mats could be developed for medical application.



CHAPTER V

CONCLUSIONS AND SUGGESTIONS

5.1 Conclusions

According to this study prepared silk fibroin/ gelatin/ chitosan blended nanofiber mats by electrospinning technique. The conclusions were categorized as follows;

Silk fibroin/ gelatin/ chitosan, soluble in formic acid at a ratio of 10:20:0.5, 10:20:1.5, 10:20:2, and 20:10:1 (wt%:wt%:wt%) could spin filament at nanometer size. The fiber sizes were range from 100 to 280 nm and it showed that chitosan content increase the fiber size became small. The size distributions of nanofiber mats were narrow.

For formic acid as the solvent of the silk fibroin/ gelatin/chitosan blends did not destructed the molecular chain on the silk fibroin/ gelatin/chitosan blends. When it spin on the long time, it could also produce the continuously fibers without breaking and beading.

The appropriate condition for produce the silk fibroin/ gelatin/ chitosan blended nanofiber mats ratio at 10:20:1 and 20:10:1 are the electrical field of 20 kV, the injection rate of 0.2 ml per hour and the distance of the needle tip to collector 15 cm for using to produce the nanofiber mats for physical and mechanical and biological testing.

The results of tensile strength and elongation at break of SF: G: C (10:20:1) mats have higher than SF: G: C (20:10:1) nanofiber mats because the concentration of gelatin influenced to flexible on mats. Moreover, the silk fibroin nanofiber mats were very fragile more than the gelatin nanofiber mats. The concentration of chitosan in polymer blend increased 1 to 1.5 wt% .The tensile strength and elongation at break of 10:20:1.5 nanofiber mats increased because of the size of fibers per area increasing.

The SF: G: C nanofiber mats had unstable structure in water and poor mechanical property. Crosslinking is a technique that can be used to improve structures stabilities and mechanical properties of nanofiber mats. Alcohol, GA, and EDC/NHS were used as crosslinking agents with the step of crosslinking, exposing and dipping. A partly interaction between molecular chain occurred before exposing step and

completely crosslinking after dipping step. EDC/NHS selected to crosslinking SF: G: C nanofiber mats because the size of fiber, color of mats, and weight loss and swelling of mats did not changing after crosslinking. The results of XRD emphasized the crosslinking by crystal index increasing.

SF: G: C (20:10:1) EDC/NHS- crosslinked nanofiber mats and commercial membrane (*Collprotect* ® membrane) were used for biological testing. SF: G: C (20:10:1) EDC/NHS- crosslinked nanofiber mats allowed oxygen and culture media permeability. Normal human gingival fibroblasts could spread and attached on the surface of EDC/NHS- crosslinked nanofiber mats.

According to our study, we can fabricated silk fibroin/ gelatin/ chitosan blended nanofiber mats by electrospinning and crosslinking with EDC/NHS. This could be developed as a barrier membrane for GTR.

Silk fibroin, gelatin, chitosan are natural materials commonly available in Thailand which could be developed for medical used. Providing their low cost of these materials and available technology, we hope to improve and expand medical care in the future

5.2 Suggestions

We have accomplished the objectives of this study. However, to further research and development for medical application. It is recommended the following studies are required, such as

1. Degradation of EDC/NHS- crosslinked nanofiber mats for the membrane resorption rate.
2. Anti-bacterial activity of chitosan in SF: G: C blended nanofiber mats.
3. *In vivo* and *in vitro* studies required prior to clinical application.

REFERENCES

- [1] B.K.B. Jack T. Krauser. , Arun K. Garg., Membrane barriers for guided tissue regeneration, in: second (Ed.) Dental Implants The Art and Science, Saunders, Missouri, 2011, pp. 181-215.
- [2] Y. Zhang, X. Zhang, B. Shi, R. Miron, Membranes for guided tissue and bone regeneration, *Oral & Maxillofacial Surgery*, 1 (2013) 10.
- [3] R. Dimitriou, G.I. Mataliotakis, G.M. Calori, P.V. Giannoudis, The role of barrier membranes for guided bone regeneration and restoration of large bone defects: current experimental and clinical evidence, *BMC Med*, 10 (2012) 81.
- [4] M. Mour, D. Das, T. Winkler, E. Hoenig, G. Mielke, M.M. Morlock, A.F. Schilling, Advances in Porous Biomaterials for Dental and Orthopaedic Applications, *Materials*, 3 (2010) 2947-2974.
- [5] A.L. Andrady, Introduction, *Science and Technology of Polymer Nanofibers*, John Wiley & Sons, Inc.2007, pp. 1-26.
- [6] S. Zarkoob, R.K. Eby, D.H. Reneker, S.D. Hudson, D. Ertley, W.W. Adams, Structure and morphology of electrospun silk nanofibers, *Polymer*, 45 (2004) 3973-3977.
- [7] G.H. Altman, F. Diaz, C. Jakuba, T. Calabro, R.L. Horan, J. Chen, H. Lu, J. Richmond, D.L. Kaplan, Silk-based biomaterials, *Biomaterials*, 24 (2003) 401-416.
- [8] C. Vepari, D.L. Kaplan, Silk as a Biomaterial, *Progress in polymer science*, 32 (2007) 991-1007.
- [9] J.A. Matthews, G.E. Wnek, D.G. Simpson, G.L. Bowlin, Electrospinning of collagen nanofibers, *Biomacromolecules*, 3 (2002) 232-238.
- [10] Z.-M. Huang, Y.Z. Zhang, S. Ramakrishna, C.T. Lim, Electrospinning and mechanical characterization of gelatin nanofibers, *Polymer*, 45 (2004) 5361-5368.
- [11] K. Ohkawa, D. Cha, H. Kim, A. Nishida, H. Yamamoto, Electrospinning of Chitosan, *Macromolecular Rapid Communications*, 25 (2004) 1600-1605.
- [12] S.A. Theron, E. Zussman, A.L. Yarin, Experimental investigation of the governing parameters in the electrospinning of polymer solutions, *Polymer*, 45 (2004) 2017-2030.
- [13] B. Gupta, N. Revagade, J. Hilborn, Poly(lactic acid) fiber: An overview, *Progress in Polymer Science*, 32 (2007) 455-482.

- [14] X.M. Mo, C.Y. Xu, M. Kotaki, S. Ramakrishna, Electrospun P(LLA-CL) nanofiber: a biomimetic extracellular matrix for smooth muscle cell and endothelial cell proliferation, *Biomaterials*, 25 (2004) 1883-1890.
- [15] K.-H. Kim, L. Jeong, H.-N. Park, S.-Y. Shin, W.-H. Park, S.-C. Lee, T.-I. Kim, Y.-J. Park, Y.-J. Seol, Y.-M. Lee, Y. Ku, I.-C. Rhyu, S.-B. Han, C.-P. Chung, Biological efficacy of silk fibroin nanofiber membranes for guided bone regeneration, *Journal of Biotechnology*, 120 (2005) 327-339.
- [16] X. Liu, P.X. Ma, Phase separation, pore structure, and properties of nanofibrous gelatin scaffolds, *Biomaterials*, 30 (2009) 4094-4103.
- [17] R. Jayakumar, M. Prabakaran, P.T. Sudheesh Kumar, S.V. Nair, H. Tamura, Biomaterials based on chitin and chitosan in wound dressing applications, *Biotechnol Adv*, 29 (2011) 322-337.
- [18] U.-J. Kim, J. Park, H. Joo Kim, M. Wada, D.L. Kaplan, Three-dimensional aqueous-derived biomaterial scaffolds from silk fibroin, *Biomaterials*, 26 (2005) 2775-2785.
- [19] B.B. Mandal, J.K. Mann, S.C. Kundu, Silk fibroin/gelatin multilayered films as a model system for controlled drug release, *Eur J Pharm Sci*, 37 (2009) 160-171.
- [20] M.-H. Ho, C.-C. Hsieh, S.-W. Hsiao, D. Van Hong Thien, Fabrication of asymmetric chitosan GTR membranes for the treatment of periodontal disease, *Carbohydrate Polymers*, 79 (2010) 955-963.
- [21] F. Croisier, C. Jérôme, Chitosan-based biomaterials for tissue engineering, *European Polymer Journal*, 49 (2013) 780-792.
- [22] C. Huang, R. Chen, Q. Ke, Y. Morsi, K. Zhang, X. Mo, Electrospun collagen–chitosan–TPU nanofibrous scaffolds for tissue engineered tubular grafts, *Colloids and Surfaces B: Biointerfaces*, 82 (2011) 307-315.
- [23] K.E. Park, S.Y. Jung, S.J. Lee, B.-M. Min, W.H. Park, Biomimetic nanofibrous scaffolds: Preparation and characterization of chitin/silk fibroin blend nanofibers, *International Journal of Biological Macromolecules*, 38 (2006) 165-173.
- [24] C. Meechaisue, P. Wutticharoenmongkol, R. Waraput, T. Huangjing, N. Ketbumrung, P. Pavasant, P. Supaphol, Preparation of electrospun silk fibroin fiber mats as bone scaffolds: a preliminary study, *Biomed Mater*, 2 (2007) 181-188.

- [25] S. Wang, G. Zhao, Quantitative characterization of the electrospun gelatin–chitosan nanofibers by coupling scanning electron microscopy and atomic force microscopy, *Materials Letters*, 79 (2012) 14-17.
- [26] M.Z. Elsabee, H.F. Naguib, R.E. Morsi, Chitosan based nanofibers, review, *Materials Science and Engineering: C*, 32 (2012) 1711-1726.
- [27] Y. Zhou, D. Yang, X. Chen, Q. Xu, F. Lu, J. Nie, Electrospun Water-Soluble Carboxyethyl Chitosan/Poly(vinyl alcohol) Nanofibrous Membrane as Potential Wound Dressing for Skin Regeneration, *Biomacromolecules*, 9 (2008) 349-354.
- [28] N. Amiralijan, M. Nouri, M. Haghghat Kish, Structural characterization and mechanical properties of electrospun silk fibroin nanofiber mats, *Polymer Science Series A*, 52 (2010) 407-412.
- [29] B.M. Min, G. Lee, S.H. Kim, Y.S. Nam, T.S. Lee, W.H. Park, Electrospinning of silk fibroin nanofibers and its effect on the adhesion and spreading of normal human keratinocytes and fibroblasts in vitro, *Biomaterials*, 25 (2004) 1289-1297.
- [30] Y.Z. Zhang, J. Venugopal, Z.M. Huang, C.T. Lim, S. Ramakrishna, Crosslinking of the electrospun gelatin nanofibers, *Polymer*, 47 (2006) 2911-2917.
- [31] C.S. Ki, D.H. Baek, K.D. Gang, K.H. Lee, I.C. Um, Y.H. Park, Characterization of gelatin nanofiber prepared from gelatin–formic acid solution, *Polymer*, 46 (2005) 5094-5102.
- [32] Y.S. Choi, S.R. Hong, Y.M. Lee, K.W. Song, M.H. Park, Y.S. Nam, Study on gelatin-containing artificial skin: I. Preparation and characteristics of novel gelatin-alginate sponge, *Biomaterials*, 20 (1999) 409-417.
- [33] J. Xu, J. Yan, Q. Gu, J. Li, H. Wang, Preparation of fluoride-containing gelatin nanofiber scaffold, *Materials Letters*, 65 (2011) 2404-2406.
- [34] L. Ghasemi-Mobarakeh, M.P. Prabhakaran, M. Morshed, M.H. Nasr-Esfahani, S. Ramakrishna, Electrospun poly(epsilon-caprolactone)/gelatin nanofibrous scaffolds for nerve tissue engineering, *Biomaterials*, 29 (2008) 4532-4539.
- [35] K.T. Shalumon, K.H. Anulekha, K.P. Chennazhi, H. Tamura, S.V. Nair, R. Jayakumar, Fabrication of chitosan/poly(caprolactone) nanofibrous scaffold for bone and skin tissue engineering, *International Journal of Biological Macromolecules*, 48 (2011) 571-576.

- [36] H. Homayoni, S.A.H. Ravandi, M. Valizadeh, Electrospinning of chitosan nanofibers: Processing optimization, *Carbohydrate Polymers*, 77 (2009) 656-661.
- [37] V. Sencadas, D.M. Correia, C. Ribeiro, S. Moreira, G. Botelho, J.L. Gómez Ribelles, S. Lanceros-Mendez, Physical-chemical properties of cross-linked chitosan electrospun fiber mats, *Polymer Testing*, 31 (2012) 1062-1069.
- [38] W.H. Park, L. Jeong, D.I. Yoo, S. Hudson, Effect of chitosan on morphology and conformation of electrospun silk fibroin nanofibers, *Polymer*, 45 (2004) 7151-7157.
- [39] Crosslinking-Reagents-Handbook, in: T. scientific (Ed.), Thermo scientific, 2015.
- [40] M.G. Haugh, M.J. Jaasma, F.J. O'Brien, The effect of dehydrothermal treatment on the mechanical and structural properties of collagen-GAG scaffolds, *J Biomed Mater Res A*, 89 (2009) 363-369.
- [41] L.A. Chodosh, UV crosslinking of proteins to nucleic acids, *Curr Protoc Mol Biol*, Chapter 12 (2001) Unit 12 15.
- [42] D.J. Dijkstra, W. Hoogsteen, A.J. Pennings, Cross-linking of ultra-high molecular weight polyethylene in the melt by means of electron beam irradiation, *Polymer*, 30 (1989) 866-873.
- [43] P. Jetbumpenkul, P. Amornsudthiwat, S. Kanokpanont, S. Damrongsakkul, Balanced electrostatic blending approach – An alternative to chemical crosslinking of Thai silk fibroin/gelatin scaffold, *International Journal of Biological Macromolecules*, 50 (2012) 7-13.
- [44] A. Bigi, G. Cojazzi, S. Panzavolta, N. Roveri, K. Rubini, Stabilization of gelatin films by crosslinking with genipin, *Biomaterials*, 23 (2002) 4827-4832.
- [45] J. Wang, L. Wang, Z. Zhou, H. Lai, P. Xu, L. Liao, J. Wei, Biodegradable Polymer Membranes Applied in Guided Bone/Tissue Regeneration: A Review, *Polymers*, 8 (2016) 115.
- [46] H. Tal, O. Moses, A. Kozlovsky, C. Nemcovsky, Bioresorbable Collagen Membranes for Guided Bone Regeneration.
- [47] I. Darby, Periodontal materials, *Aust Dent J*, 56 Suppl 1 (2011) 107-118.
- [48] M. Simion, M. Baldoni, P. Rossi, D. Zaffe, A comparative study of the effectiveness of e-PTFE membranes with and without early exposure during the healing period, *Int J Periodontics Restorative Dent*, 14 (1994) 166-180.

- [49] V. Zargar, M. Asghari, A. Dashti, A Review on Chitin and Chitosan Polymers: Structure, Chemistry, Solubility, Derivatives, and Applications, *ChemBioEng Reviews*, 2 (2015) 204-226.
- [50] G. Decher, Fuzzy Nanoassemblies: Toward Layered Polymeric Multicomposites, *Science*, 277 (1997) 1232-1237.
- [51] X. Liu, K.-Q. Zhang, *Silk Fiber — Molecular Formation Mechanism, Structure-Property Relationship and Advanced Applications*, (2014).
- [52] J. Ayutsede, M. Gandhi, S. Sukigara, H. Ye, C.M. Hsu, Y. Gogotsi, F. Ko, Carbon nanotube reinforced Bombyx mori silk nanofibers by the electrospinning process, *Biomacromolecules*, 7 (2006) 208-214.
- [53] <http://www1.lsbu.ac.uk/water/gelatin.html>, Gelatin, 2016.
- [54] O.M.R. Institute, Gelatin, Processing OMRI, National Organic Standards Board Technical Advisory Panel 2002, pp. 1.
- [55] A.A. Karim, R. Bhat, Fish gelatin: properties, challenges, and prospects as an alternative to mammalian gelatins, *Food Hydrocolloids*, 23 (2009) 563-576.
- [56] W.-J. Li, R.M. Shanti, R.S. Tuan, *Electrospinning Technology for Nanofibrous Scaffolds in Tissue Engineering*, *Nanotechnologies for the Life Sciences*, Wiley-VCH Verlag GmbH & Co. KGaA2007.
- [57] A. Martins, J.V. Araujo, R.L. Reis, N.M. Neves, Electrospun nanostructured scaffolds for tissue engineering applications, *Nanomedicine (Lond)*, 2 (2007) 929-942.
- [58] L. Wannatong, A. Sirivat, P. Supaphol, Effects of solvents on electrospun polymeric fibers: preliminary study on polystyrene, *Polymer International*, 53 (2004) 1851-1859.
- [59] B. Sun, Y.Z. Long, H.D. Zhang, M.M. Li, J.L. Duvail, X.Y. Jiang, H.L. Yin, Advances in three-dimensional nanofibrous macrostructures via electrospinning, *Progress in Polymer Science*, 39 (2014) 862-890.
- [60] C.K.S. Pillai, W. Paul, C.P. Sharma, Chitin and chitosan polymers: Chemistry, solubility and fiber formation, *Progress in Polymer Science*, 34 (2009) 641-678.
- [61] A. Cooper, R. Oldinski, H. Ma, J.D. Bryers, M. Zhang, Chitosan-based nanofibrous membranes for antibacterial filter applications, *Carbohydrate polymers*, 92 (2013) 254-259.

- [62] M. Okhawilai, R. Rangkupan, S. Kanokpanont, S. Damrongsakkul, Preparation of Thai silk fibroin/gelatin electrospun fiber mats for controlled release applications, *Int J Biol Macromol*, 46 (2010) 544-550.
- [63] C.M. Vaz, S. van Tuijl, C.V.C. Bouten, F.P.T. Baaijens, Design of scaffolds for blood vessel tissue engineering using a multi-layering electrospinning technique, *Acta Biomaterialia*, 1 (2005) 575-582.
- [64] S. Putthanarat, S. Zarkoob, J. Magoshi, J.A. Chen, R.K. Eby, M. Stone, W.W. Adams, Effect of processing temperature on the morphology of silk membranes, *Polymer*, 43 (2002) 3405-3413.
- [65] Z. She, B. Zhang, C. Jin, Q. Feng, Y. Xu, Preparation and in vitro degradation of porous three-dimensional silk fibroin/chitosan scaffold, *Polymer Degradation and Stability*, 93 (2008) 1316-1322.
- [66] B.B. Mandal, S.C. Kundu, Non-Bioengineered Silk Fibroin Protein 3D Scaffolds for Potential Biotechnological and Tissue Engineering Applications, *Macromolecular Bioscience*, 8 (2008) 807-818.
- [67] J.Y. Song, S.G. Kim, J.W. Lee, W.S. Chae, H. Kweon, Y.Y. Jo, K.G. Lee, Y.C. Lee, J.Y. Choi, J.Y. Kim, Accelerated healing with the use of a silk fibroin membrane for the guided bone regeneration technique, *Oral Surg Oral Med Oral Pathol Oral Radiol Endod*, 112 (2011) e26-33.
- [68] A. Sionkowska, A. Płancka, Preparation and characterization of silk fibroin/chitosan composite sponges for tissue engineering, *Journal of Molecular Liquids*, 178 (2013) 5-14.
- [69] J. Ratanavaraporn, R. Rangkupan, H. Jeeratawatchai, S. Kanokpanont, S. Damrongsakkul, Influences of physical and chemical crosslinking techniques on electrospun type A and B gelatin fiber mats, *International Journal of Biological Macromolecules*, 47 (2010) 431-438.
- [70] E. Marin, J. Rojas, Y. Ciro, A review of polyvinyl alcohol derivatives: Promising materials for pharmaceutical and biomedical applications, *African Journal of Pharmacy and Pharmacology*, 8 (2014) 674-684.
- [71] S. Jeong, E.J. Yoon, H.G. Lim, S.C. Sung, Y.J. Kim, The Effect of Space Fillers in the Cross-Linking Processes of Bioprosthesis, *BioResearch Open Access*, 2 (2013) 98-106.

- [72] J.M. Lee, H.H.L. Edwards, C.A. Pereira, S.I. Samii, Crosslinking of tissue-derived biomaterials in 1-ethyl-3-(3-dimethylaminopropyl)-carbodiimide (EDC), *J Mater Sci: Mater Med*, 7 (1996) 531-541.
- [73] R. Liu, J. Ming, H. Zhang, B. Zuo, EDC/NHS crosslinked electrospun regenerated tussah silk fibroin nanofiber mats, *Fibers and Polymers*, 13 (2012) 613-617.
- [74] R.L. Klein, J. Edwin H. Shaw, X-ray diffraction studied of the cryatalline structure of silk fibroin, *Proc. S.D.Acad.Sci.*, XXXII (1953) 52-56.
- [75] S. Rungsiyanont, N. Dhanesuan, S. Swasdison, S. Kasugai, Evaluation of biomimetic scaffold of gelatin-hydroxyapatite crosslink as a novel scaffold for tissue engineering: biocompatibility evaluation with human PDL fibroblasts, human mesenchymal stromal cells, and primary bone cells, *J Biomater Appl*, 27 (2012) 47-54.
- [76] M.A.d. Moraes, G.M. Nogueira, R.F. Weska, M.M. Beppu, Preparation and Characterization of Insoluble Silk Fibroin/Chitosan Blend Films, *Polymers*, 2 (2010) 719.
- [77] <AliAlmansor-Chap 1-2.pdf>.
- [78] S. Kim, M.E. Nimni, Z. Yang, B. Han, Chitosan/gelatin-based films crosslinked by proanthocyanidin, *Journal of biomedical materials research. Part B, Applied biomaterials*, 75 (2005) 442-450.
- [79] J.P. Chen, S.H. Chen, G.J. Lai, Preparation and characterization of biomimetic silk fibroin/chitosan composite nanofibers by electrospinning for osteoblasts culture, *Nanoscale research letters*, 7 (2012) 170.
- [80] H. Nagahama, H. Maeda, T. Kashiki, R. Jayakumar, T. Furuike, H. Tamura, Preparation and characterization of novel chitosan/gelatin membranes using chitosan hydrogel, *Carbohydrate Polymers*, 76 (2009) 255-260.
- [81] M.A.d. Moraes, G.M. Nogueira, R.F. Weska, M.M. Beppu, Preparation and Characterization of Insoluble Silk Fibroin/Chitosan Blend Films, *Polymers*, 2 (2010) 719-727.
- [82] Y. Zhou, H. Yang, X. Liu, J. Mao, S. Gu, W. Xu, Electrospinning of carboxyethyl chitosan/poly(vinyl alcohol)/silk fibroin nanoparticles for wound dressings, *International journal of biological macromolecules*, 53 (2013) 88-92.

- [83] E.S. Gil, D.J. Frankowski, S.M. Hudson, R.J. Spontak, Silk fibroin membranes from solvent-crystallized silk fibroin/gelatin blends: Effects of blend and solvent composition, *Materials Science and Engineering: C*, 27 (2007) 426-431.
- [84] Q. Yu, Y. Song, X. Shi, C. Xu, Y. Bin, Preparation and properties of chitosan derivative/poly(vinyl alcohol) blend film crosslinked with glutaraldehyde, *Carbohydrate Polymers*, 84 (2011) 465-470.
- [85] T.-H. Nguyen, B.-T. Lee, Fabrication and characterization of cross-linked gelatin electro-spun nano-fibers, *Journal of Biomedical Science and Engineering*, 03 (2010) 1117-1124.
- [86] S. Zhang, Y. Huang, X. Yang, F. Mei, Q. Ma, G. Chen, S. Ryu, X. Deng, Gelatin nanofibrous membrane fabricated by electrospinning of aqueous gelatin solution for guided tissue regeneration, *Journal of Biomedical Materials Research Part A*, 90A (2009) 671-679.



APPENDIXS



Appendix A

Table A-1: Swelling and weight loss (%) of SF, G, SF: G: C (10:20:1) and SF: G: C (20:10:1) nanofiber mats with EDC/NHS

Weight (mg)	Silk fibroin				Gelatin				SF: G: C (10:20:1)				SF: G: C (20:10:1)			
	1	2	3	4	1	2	3	4	1	2	3	4	1	2	3	4
Initial weight	1.70	4.10	5.50	5.10	2.60	3.20	3.80	2.80	2.10	3.00	3.60	3.20	3.60	4.40	4.20	3.20
Vapor weight	1.70	4.10	5.50	5.10	2.60	3.20	3.80	2.80	2.10	3.00	3.60	3.20	3.60	4.40	4.20	3.20
Wet weight	2.00	4.50	5.70	5.10	2.90	3.70	4.20	3.30	2.40	3.50	4.10	3.50	3.9-	4.50	4.60	3.40
Final weight	1.70	4.10	5.50	1.50	2.20	2.90	3.50	2.60	2.10	3.00	3.60	3.20	3.60	4.40	4.20	3.20
Weight loss	-	-	-	-	0.40	0.30	0.30	0.20	-	-	-	-	-	-	-	-
Weight loss (%)	-	-	-	-	15.38	9.38	7.90	7.14	-	-	-	-	-	-	-	-
Swelling & weight	0.30	0.40	0.30	0.20	0.30	0.50	0.40	0.50	0.30	0.50	0.50	0.30	0.30	0.10	0.40	0.20
Swelling g(%)	17.65	9.75	5.45	3.92	11.53	15.63	10.53	17.86	14.29	16.67	13.89	9.38	7.72	2.27	9.52	6.25

Table A-2: Swelling and weight loss (%) of SF, G, SF: G: C (10:20:1) and SF: G: C (20:10:1) nanofiber mats with ethanol

Weight (mg)	Silk fibroin				Gelatin				SF: G: C (10:20:1)				SF: G: C (20:10:1)			
	1	2	3	4	1	2	3	4	1	2	3	4	1	2	3	4
Initial weight	1.70	4.10	5.50	5.10	2.60	3.20	3.80	2.80	2.10	3.00	3.60	3.20	3.60	4.40	4.20	3.20
Vapor weight	1.70	4.10	5.50	5.10	2.60	3.20	3.80	2.80	2.10	3.00	3.60	3.20	3.60	4.40	4.20	3.20
Wet weight	2.00	4.50	5.70	5.10	2.90	3.70	4.20	3.30	2.40	3.50	4.10	3.50	3.9-	4.50	4.60	3.40
Final weight	1.70	4.10	5.50	1.50	2.20	2.90	3.50	2.60	2.10	3.00	3.60	3.20	3.60	4.40	4.20	3.20
Weight loss	-	-	-	-	0.40	0.30	0.30	0.20	-	-	-	-	-	-	-	-
Weight loss (%)	-	-	-	-	15.38	9.38	7.90	7.14	-	-	-	-	-	-	-	-
Swelling weight	0.30	0.40	0.30	0.20	0.30	0.50	0.40	0.50	0.30	0.50	0.50	0.30	0.30	0.10	0.40	0.20
Swelling g (%)	17.65	9.75	5.45	3.92	11.53	15.63	10.53	17.86	14.29	16.67	13.89	9.38	7.72	2.27	9.52	6.25

Table A-3: Swelling and weight loss (%) of SF, G, SF: G: C (10:20:1) and SF: G: C (20:10:1) nanofiber mats with GA

Weight (mg)	Silk fibroin				Gelatin				SF: G: C (10:20:1)				SF: G: C (20:10:1)			
	1	2	3	4	1	2	3	4	1	2	3	4	1	2	3	4
Initial weight	2.4	2.4	2.4	2.1	6.0	2.3	2.2	2.9	3.5	3.9	3.0	1.2	3.2	4.7	4.6	2.4
Vapor weight	2.4	2.4	2.4	2.2	5.9	2.3	2.2	2.9	3.5	3.9	3.0	2.2	3.3	4.6	4.5	2.4
Wet weight	2.7	2.8	2.6	2.5	6.8	2.9	3.0	3.8	3.8	4.4	3.5	1.7	3.7	5.0	5.0	2.7
Final weight	2.3	2.3	2.3	2	6.1	2.4	2.1	3.0	3.4	3.8	3.1	1.1	3.3	4.6	4.5	2.3
Weight loss	0.1	0.1	0.1	0.1	-0.1	-0.1-	0.1	-0.1	0.1	0.1	-0.1	0.1	-0.1	0.1	0.1	0.1
Weight loss (%)	10	10	10	10	10	10	10	10	10	10	10	10	10	10	10	10
Swelling g	0.3	0.4	0.2	0.3	0.8	0.7	0.8	0.9	0.3	0.5	0.5	0.5	0.4	0.3	0.4	0.3
Swelling g (%)	30	40	20	30	80	70	80	90	30	50	50	50	40	30	40	30

Appendix B

Table B Air permeability

	SF:G:C(10:20:1)	SF:G:C(10:20:1)	SF:G:C(20:10:1)	SF:G:C(20:10:1)	SF:G:C(10:20:1)	SF:G:C(20:10:1)
	612084	595765	984462	952270	15568	15650
	611644	595545	984270	952436	15571	15670
	611247	594990	984447	952555	15569	15881
	611302	594983	984580	952600	15553	15606
	611221	595160	984224	952487	15564	15606
	611403	595359	985547	952419	15551	15708
	611577	595149	985584	952724	15554	15715
	611283	595500	985848	952517	15543	15658
	611340	595252	985425	952782	15558	15647
	611442	595673	985642	952934	15562	15694
Average	611454.3	595337.6	985002.9	952572.4	15559.3	15683.5
SD	188.42	230.80	606.30	150.08	7.50	52.8

VITA

Pornpen Siridamrong was born 23 December 1970 in Sakhon nakorn. She is a daughter of Mr. Phayung and Ms. Wanpen Siridamrong. In 1995. She graduated from Ramkhamhang University on Bachelor's degree of Science, the major of material science and from Chulalongkorn University on Master's degree of Science, the major of applied polymer science and textile technology in 2005. Finally, she graduated Doctor of Philosophy program in Dental Biomaterials science (Interdisciplinary program) in academic year 2015.

